الجمهورية الجزائرية الديمقراطية الشعبية
وزارة التعليم العالي والبحث العلمي

Université Ferhat Abbas
Sétif 1
Faculté des sciences
De la Nature et de la Vie

جامعة فرحات عباس
سطيف 1
كلية علوم الطبيعة والحياة

Université Ferhat Abbas Sétif 1

DEPARTEMENT OF BIOCHEMISTRY

N°……/SNV/**2022**

THESIS

Presented by

Abed Lina

For the fulfillment of the requirements for the degree of

DOCTORATE 3rd Cycle IN BIOLOGY
Special filed: **BIOCHEMISTRY**

TOPIC

Adsorption capacity of *Punica granatum* L. peels towards lead Pb(II) and antioxidant activities of its extracts

Presented publically in: **22/12/2022**

JURY:

Supervisor:	**Dr. Belattar Noureddine**	**Pr., FSNV, UFA Sétif 1**
President:	**Dr. Bouriche Hamama**	**Pr., FSNV, UFA Sétif 1**
Exiaminators:	**Dr. Bougattoucha Abdallah**	**Pr., FT, UFA Sétif 1**
	Dr. Benchikh Fatima	**MCA., FSNV, UFA Sétif 1**
	Dr. Mekhalif Tahar	**MCA., FS, UNIV BBA**

Laboratory of Applied Biochemistry

Acknowledgements

First and foremost, I would like to praise Allah the Almighty, the Most Gracious, and the Most Merciful for His blessing given to me during my study and in completing this thesis. May Allah's blessings go to His final Prophet Muhammad (peace be up on him), his family and his companions.

I would like to say a special thank you to my supervisor, Pr. Belattar Noureddine, His support, guidance and overall insights in this field have made this an inspiring experience for me. Without his succinct directions and insightful comments on all aspects of this dissertation, this research wouldn’t have been possible.

I would like to deeply thank the ENPEC (National Company of Electrochemical Products) of Setif (Algeria) for their availability and fruitful cooperation. Particular gratitude is addressed to the managers of the analysis laboratory for their friendliness and helpfulness during the performance of the work by atomic absorption.

My gratitude and my respect also go to Pr. Bouriche Hamama for doing me the honor of presiding my jury and agreeing to evaluate this work and for all her encouargments.

My deep appreciation for all the members of the jury Dr. Benchikh Fatima, Dr. Meikhalif Tahar and Pr. Bougattoucha Abdallah for their presence and for accepting to examine and evaluate my work.

Finally, I wish to express my sincere gratitude and appreciation to my family, friends and everyone who assisted and supported me throughout the course of this work.

Dedication

- I dedicate this work to my source of love, my parents Dr. Abed Abdelouahab and Hamouda Sonia; No amount of words is enough to describe my love and my gratitude, I wouldn't be able to take a step forward without your encouragement and affection. I am truly thankful and proud to have you as my parents you have been idols for me from the beginning to the end.

- I also dedicate this work for my little brother Taha Al Amin and my lovely sisters Nadine and Alaa Al Rahman; thank you for being there for me and supporting me uncondiontally, i love you all so much.

- I dedicate this work to my fiance Hicham, a special thank you for supporting me and beliving in me.

- I would like to thank my second family Laazazga and Bara, my Grandmother Aicha, Wissem, my second mother Hada, my dearest Hicham and Liza and her little Angles Alaa, Amira and Aya and to the whole family for their support.

- I would like to sincerely thank my best friend and my sister Boumarfeg Meriem for her faith in me and her encouragements throughtout the way, and for always being ther for me.

- A special dedication to my uncle Abed Zaidi for his caring, encouragement and support, you have been like a second father to me.

- I also would to deeply thank my friends Dr, Gheraibia Sara for their help and support thought this journey.

- I also have a special thank you to all my friends follow PhD students and future doctors; Keffous Besma Safa, Bouaoud Laldja, Rahmani Amira, Amira Hind, Gharzouli Asma, Regaz Katia, Dichi Meriem, Laouri Haifa, Boudechicha Amel, Lamouri Amina and Derguine Rania

- Finally, a special gratitude is dedicated to my friend and the excellent chemist Khelalfa Roumaissa for her big help during this work, and her encouragement throughout this period.

Lina

List of publications

1. **Abed, L.,** Belattar, N. (2021). THE ANTIOXIDANT ACTIVITIES OF TWO POMEGRANATE CULTIVARS JUICES. *International journal of human settlements*, *5*(2), 815–822.

2. **Abed, L.,** Belattar, N. (2022). Polyphenols Content, Chelating Properties and Adsorption Isotherms and Kinetics of Red and Yellow Pomegranate Peels (*Punica granatum* L.) Towards Lead (II). *Polish Journal of Environmental Studies*, *31*(6), 1–15.

List of communications

1. **Abed, L.,** Belattar, N. Biochemical profile and polyphenolic content of two pomegranate cultivars juices and their antioxidant activities. Oral communication. Séminaire international sur les sciences naturelles et de la vie (webinaire), international journal of human settlements, le 19 et 20 février 2021.

2. **Abed, L.,** Belattar, N. The antioxidant activity of the aqueous extract of the yellow *Punica granatum* peel against the DPPH radical. Poster. Journé national de l'agro-éco-biotechnologie (JNAEB 2021), Laboratoire de Biotechnologie des Productions Végétales (LBPV), Faculté des Sciences de la Nature et de la Vie (Blida1), le 15 et 16 Octobre 2021.

3. **Abed, L.,** Belattar, N. The antioxicant activity of the aqueous extract of the red *Punica granatum* peel against the DPPH radical. Poster. La 1ère Journée scientifique sur La Blochimie fonctionnelle et la physiopathologle cellulaire (JSBFPC), Université Alger 1, Benyoucel Benkhedda , le 06 novembre 2021.

4. **Abed, L.,** Belattar, N. The antioxidant activity of the methanolic extract of the red *Punica granatum* peel against the DPPH radical. Poster. Le 1er Séminaire National sur La Valorisation des Ressources Naturelles et de l'Environnement (VRNE 2022) Université Ferhat Abbas Sétif 1, le 30 mars 2022.

5. **Abed, L.,** Belattar, N. Antiradical and iron chelating activities of the yellow *Punica granatum* methanolic peel extract. Oral communication. Webinaire International sur les Biotechnologies au Service de l'Agriculture Durable (WIBSAD-2022) organisé par le Laboratoire de Recherche en Biotechnologie des Productions Végétales (Faculté S.N.V– Université Blida 1), les 25 et 26 et Juin 2022.

ملخص

أصبحت المعادن الثقيلة التي تنتجها مياه الصرف الصناعي مشكلة عالمية بسبب آثارها السلبية على البيئة وعلى صحة الإنسان لأنها تسبب الإجهاد التأكسدي المرتبط بالعديد من الأمراض (القلب والأوعية الدموية ، التنكس العصبي ، الالتهابات ، السرطان وغيرها). تشتهر فاكهة الرمان *Punica granatum* L. و أجزائها المختلفة بفوائدها الصحية وقد استخدمو منذ القدم في التغذية والطب التقليدي. يهدف الجزء الأول من هذه الدراسة إلى توصيف مسحوق قشر الرمان من الصنفين عن طريق التحليل بواسطة FT-IR ونقطة الشحن صفر والمجموعات الوظيفية السطحية وتقييم قدرات الادمصاص لهذه الكتل الحيوية مقابل أيونات الرصاص باستخدام طريقة الدُفعات وإمكانية استخدامها في معالجة مياه الصرف الصناعي الملوثة بالرصاص. تمت دراسة تأثير بعض المتغيرات التجريبية على قدرات الادمصاص. تمت أيضا دراسة حرارة وحركية الادمصاص ومعالجتها بنماذج رياضية مختلفة. كما تم تقييم تجديد مسحوق قشر الرمان الأحمر والأصفر بعد الادمصاص. يهدف الجزء الثاني من هذا العمل إلى تحديد محتوى البوليفينول الكلي والفلافونويد والعفص المكثف والأنثوسيانين في المستخلصات المائية والميثانولية والإيثانولية لقشرة الأصناف الحمراء والصفراء من *Punica granatum* L. وتقييم نشاطها المضاد للأكسدة في المختبر. أظهرت النتائج ثراء الكتلتين الحيويتين بالمجموعات الوظيفية الحمضية السطحية. أظهرت دراسة العوامل المختلفة على عملية الادمصاص أن قدرة الادمصاص تزداد مع الأس الهيدروجيني حتى الرقم الهيدروجيني 6 ووقت التجربة وتركيز المعدن الأولي وتتناقص مع زيادة جرعة المدمص الحيوي. بالنسبة لحرارة ادمصاص الرصاص على مسحوق قشر الرمان الأحمر والأصفر ، كان نموذج Langmuir أكثر ملائمة مع قدرة ادمصاص (Q_{max}) تبلغ 90 و 89.25 مجم / جرام على التوالي. تلائم البيانات الحركية نموذج الدرجة الثانية بشكل أفضل. كان اندصاص الرصاص الحمضي فعالاً مع نسبة عالية من الاسترجاع. تشير النتائج إلى أنه يمكن استخدام هذه الكتل الحيوية كمواد مدمصة حيوية لإزالة الرصاص من المحاليل المائية مع إمكانية إعادة استخدامها. أظهرت النتائج ايضا أن مستخلصات القشور الميثانولية والإيثانولية للأصناف الحمراء والصفراء أكثر ثراءً في البوليفينول والفلافونويد والعفص المكثف والأنثوسيانين من المستخلصات المائية. أظهرت جميع المستخلصات التي تم اختبارها أنشطة استخلاب قوية للجذور الحرة DPPH و ABTS وتأثير مضاد للأكسدة مع اختبار ارجاع الطاقة ، واستخلاب الحديد واختبارات بيتا كاروتين.

الكلمات المفتاحية: *Punica granatum* L. ، قشر الرمان ، مركبات الفينول ، نشاط مضاد الأكسدة ، الادمصاص الحيوي ، حرارة الادمصاص ، حركيات الادمصاص ، معالجة مياه الصرف الصحي الصناعية ، المعادن الثقيلة ، الرصاص.

Abstract

Heavy metals produced by industrial wastewaters have become a global problem due to their negative effects on the environment and on human health as they induce oxidative stress which has been linked to several diseases (cardiovascular, neurodegenerative, inflammatory, cancer and others). Pomegranate fruit *Punica granatum* L. and its diffrent parts are known for their health benefits and have been used since ancient times in nutrition and in traditional medicine. The first part of this study aimed to characterize the pomegranate peels powder of both varieties via FT-IR, point of zero charge and surface functional groups analysis and to evaluate the adsorption capacities of these biomasses towards leads ions using batch method and the potential of using them for the treatment of industrial wastewater polluted with lead. The effect of some experimental parameters on the adsorption capacities was studied. Isotherms and adsorption kinetics have also been studied and treated with different mathematical models. The regeneration of the red and yellow pomegranate peels powder after adsorption was also assessed. The second part of this work aimed to determine the total polyphenols, flavonoids, condensed tannins and anthocyanins content in the aqueous, methanolic and ethanolic peels extracts of the red and yellow *Punica granatum* L. varieties and to evaluate their antioxidant activity *in vitro*. Results showed the richness of both biomasses with acidic functional surface groups. The study of different factors on the adsorption process showed that the adsorption capacity increases with pH until pH 6, contact time and initial metal concentration and it decreases with increasing the biosorbent dose. For the adsorption isotherms of lead onto the red and yellow pomegranate peels powder, the Langmuir model was more fitting with an adsorption capacity (Q_{max}) of 90 and 89.25 $mg.g^{-1}$, respectively. The kinetic data suited better with the pseudo-second order model. Lead acidic desorption was efficient, with a high percentage of recovery. The findings indicate that these biomasses can be utilized as biosorbents for lead removal from aqueous solutions with the possibility of their reuse. The results also showed that the methanolic and ethanolic peels extracts of red and yellow varieties are richer in polyphenols, flavonoids, condensed tannins and anthocyanins than the aqueous ones. All the tested extracts have shown powerful scavenging activities towards DPPH and ABTS radicals and an appreciable antioxidant inhibiting effects with the reducing power, iron chelation and β-carotene tests.

Keywords: *Punica granatum* L., Pomegranate peels, Phenolic compounds, Antioxidant activity, Biosorption, Adsorption isotherms, Adsorption kinetics, Wastewater treatment, Heavy metals, Lead.

Résumé

Les métaux lourds produits par les eaux usées industrielles sont devenus un problème mondial à cause de leurs effets négatifs sur l'environnement et sur la santé humaine car ils induisent le stress oxydant qui a été lié avec plusieurs maladies (cardiovasculaires, neurodégénératives, inflammatoires, cancéreuses et autres). Le fruit de la grenade *Punica granatum* L. et ses différentes parties sont connues pour leurs bienfaits pour la santé et sont utilisées depuis l'Antiquité en nutrition et en médecine traditionnelle. La première partie de cette étude visait à caractériser la poudre des écorces de grenade des deux variétés via l'analyse par IR-TF, point de charge nulle et des groupes fonctionnels de surface et à évaluer les capacités d'adsorption de ces biomasses vis-à-vis des ions plomb en utilisant la méthode batch et le potentiel de leur utilisation pour le traitement des eaux usées industrielles polluées par le plomb. L'effet de certains paramètres expérimentaux sur les capacités d'adsorption a été étudié. Les isothermes et la cinétique d'adsorption ont également été étudiées et traitées avec différents modèles mathématiques. La régénération de la poudre des écorces de grenade rouge et jaune après adsorption a également été évaluée. La deuxième partie de ce travail visait à déterminer la teneur en polyphénols totaux, flavonoïdes, tanins condensés et anthocyanes dans les extraits aqueux, méthanoliques et éthanoliques des écorces des variétés rouges et jaunes de *Punica granatum* L. et à évaluer leur activité antioxydante *in vitro*. Les résultats ont montré la richesse du deux biomasses en groupements fonctionnels acides de surface. L'étude de différents facteurs sur le processus d'adsorption a montré que la capacité d'adsorption augmente avec le pH jusqu'à pH 6, le temps de contact et la concentration initiale en métal et qu'elle diminue avec l'augmentation de la dose de biosorbant. Pour les isothermes d'adsorption du plomb sur la poudre des écorces de grenade rouge et jaune, le modèle de Langmuir était plus adapté avec une capacité d'adsorption (Q_{max}) de 90 et 89,25 $mg.g^{-1}$, respectivement. Les données cinétiques convenaient mieux au modèle de pseudo-second ordre. La désorption acide du plomb a été efficace, avec un pourcentage élevé de récupération. Les résultats indiquent que ces biomasses peuvent être utilisées comme biosorbants pour l'élimination du plomb des solutions aqueuses avec la possibilité de leur réutilisation. Les résultats ont également montré que les extraits méthanoliques et éthanoliques des écorces des variétés rouges et jaunes sont plus riches en polyphénols, flavonoïdes, tanins condensés et anthocyanes que les extraits aqueux. Tous les extraits testés ont montré de puissantes activités de piégeage des radicaux DPPH et ABTS et un effet antioxydant appréciable avec les tests de pouvoir réducteur, chélation du fer et β-carotène.

Mots-clés : *Punica granatum* L., Ecorces de grenade, Composés phénoliques, Activité antioxydante, Biosorption, Isothermes d'adsorption, Cinétique d'adsorption, Traitement des eaux usées, Métaux lourds, Plomb.

List of tables

List of figures

List of abbreviations

$^{\bullet}$OH: Hydroxyl

4-HNE: 4-Hydroxynonenal

8-oxoG: 8-Oxo-7,8-dihydroguanine

$A_{0.5}$: The absorbance corresponding to 50 % of inhibition

AAS: Atomic absorption spectrophotometer

ABTS: 2,2′- Azinobis-3- ethylbenzothiazoline-6- sulfonic acid

AC: Anthocyanins content

ACE: Angiotensin converting enzyme

AEM: Anion exchange membrane

Al: Aluminium

AOX: Alternative oxidase

AP: Abasic apurinic/apyrimidinic sites

APX: Ascorbate peroxidase

ATP: Adenosine triphosphate

BDD: Boron doped diamond

BHT: Butylated hydroxytoluene

C Aq: Aqueous control

C Met: Methanolic control

C: The thickness of boundary layer

C_0: The initial adsorbate concentration ($mg.L^{-1}$)

C3GE: Cyanidin-3-glucoside equivalent

Ca: Calcium

CAT: Catalase

Cd: Cadmium

CE: Catechin equivalent

C_e: The equilibrium concentration of the adsorbate ($mg.L^{-1}$)

CEM: Cation exchange membrane

Co: Cobalt

Cr: Chromium

CTC: Condensed tannins content

Cu: Copper

CVDs: Cardiovascular diseases

DF: Dilution factor

DNA: Deoxyribonucleic acid

DPPH: 2,2-Diphenyl-1-picrylhydrazyl

DSA: Dimensional stable anode

DSBs: Double-strand breaks

DW: Dry weight

ED: Electrodialysis

ENPEC: National Company of Electrochemical Products

EPA: Environmental protection agency

ER: Estrogen receptor

FAD: Flavin adenine dinucleotide

Fe: Iron

FT-IR: Fourier transform infrared

GAE: Gallic acid equivalent

GAL: L-Galactono-gama-lactone dehydrogenase

GPx: Glutathione peroxidase

GSH: Glutathione

GSH-Px: Glutathione peroxydase

GSSG: Glutathione disulfide

H_2O_2: Hydrogen peroxide

Hg: Mercury

HL-60: Human leukemia cell

HOBr: Hypobromous acid

HOCl: Hypochloride

HOCl: Hypochlorous acid

HONOO: Peroxynitrous acid

IARC: The international agency for research on cancer

IC_{50}: The concentration corresponding to 50 % of inhibition

K: Potassium

K_1: The first-order model constant (min^{-1})

K_2: The second-order model constant ($g.mg^{-1}.min^{-1}$)

K_f: The Freundlich constant ($mg.g^{-1}(L.mg^{-1})^{1/n}$)

K_{IPD}: The intra-particle diffusion constant ($mg.g^{-1}.min^{1/2}$)

K_L: The Langmuir constant ($L.mg^{-1}$)

K_s: Sips constant ($L.mg^{-1}$)

LDL: Low-density lipoprotein

MAC: The molar absorption coefficient of cyanidin-3-glucoside

MC3T3-E1: Clonal murine cell line of immature osteoblasts

MDA: Malondialdehyde

MDCK: Madin-Darby canine kidney

MF: Microfiltration

Mg: Magnesium

Mn: Manganese

MPO: *Myeloperoxidase*

MW: Molecular weight

Na: Sodium

Na_2EDT: Ethylenediaminetetraacetic Acid, Disodium Salt
NAD: Nicotinamide adenine dinucleotide

NADPH: Nicotinamide adenine dinucleotide phosphate hydrogen

n_f : Freundlich constant

Ni: Nickel

$NO^{\bullet}$: Nitric oxide

$NO_2^{\bullet}$: Nitrogen dioxide

NOS: Nitric oxide synthase

NOX: NADPH oxidases

n_s: Sips constant

$O2^{\bullet-}$: Superoxide anion

$ONOO^-$: Peroxynitrite

P: Phosphorus

Pb: Lead

PbRPP: Red peels powder after lead adsorption

PbYPP: Yellow peels powder after lead adsorption

PUFAs: Particularly polyunsaturated fatty acids

PZC: Point of zero charge

Q_e: The amount adsorbed at equilibrium ($mg.g^{-1}$)

Q_m: The theoretical maximum adsorption capacity ($mg.g^{-1}$)

Q_t: The concentration of the adsorbate at time t ($mg.g^{-1}$)

R Aq: Red aqueous extract

R Et: Red ethanol extract

R Met: Red methanol extract

R%: Removal efficiency of the adsorbent

R: Pearson coefficient

r^2: Coefficient of correlation and regression

RE: Rutin equivalent

R_L: Dimensionless constant separation factor

RNA: Ribonucleic acid

RNS: Reactive nitrogen species

RO: Reverse osmosis

$RO^{\bullet}$: Alkoxyl

$ROO^{\bullet}$: Peroxyl

ROOH: Organic hydroperoxides

ROS: Reactive oxygen species

Rpm: Revolutions per minute

RPP: Red peels powder

Se: Selenium

SE: Standard error

SOD: Superoxide dismutase

SSBs: Single-strand breaks

TCA: Trichloroacetic acid

TFC: Total flavonoids content

TGF- β: Transforming growth factor beta

TMs: Trace minerals

TPC: Total polyphenols content

UA: Uric acid

UF: Ultrafiltration

UV-Vis: Ultraviolet-visible

WHO: World health organization

Wnt: Wingless-related integration site

Y Aq: Yellow aqueous extract

Y Et: Yellow ethanol extract

Y Met: Yellow methanol extract

YPP: Yellow peels powder

Zn: Zinc

β-catenin: Beta-catenin is a dual function protein, involved in regulation and coordination of cell–cell adhesion and gene transcription.

Table of content

Introduction

Review of literature

Material and Methods

Results and Discussion

Introduction

Environmental pollution is a global issue that has the potential to degrade the earth's ecosystems. It is therefore urgent nowadays more than ever to limit the deterioration of the abiotic sphere (air, water and soil) and the biotic sphere (plants, animals and microbes), which interact in cycles and any harm done to one of them affects the other one (Pratiksha *et al*., 2020). Indeed, intensive agriculture, industrialization and globalization have changed the ecological system's equilibrium by introducing organic and metal compounds that are extremely harmful to environment and the lives of humans and animals. Numerous contaminants have polluted the environment, including inorganic ions, organic pollutants, radioactive elements, gaseous pollutants and nanoparticles (Briffa *et al*., 2020).

Heavy metals have a negative influence on the environment and can cause catastrophic repercussions for human health due to their high toxicity and adverse effects, especially arsenic, cadmium, chromium, lead and mercury (Dökmeci, 2020). The exposure of people to these metals has been significantly enhanced by industrial development related to the demands of various technologies (Hubeny *et al*., 2021). Lead is found in the earth's crust and all compartments of the abiotic sphere (Egendorf *et al*., 2020). It is one of the most commonly used metals in the production of batteries and accumulators, as well as metal extraction and finishing operations. Many employees mainly in the developing countries are exposed to the hazardous effects of lead due to a lack of occupational safety standards (Majumder *et al*., 2021). Humans are mainly subjected to lead with the direct ingestion of polluted aliments or water or indirectly through polluted soil and inhalation of lead in the form of micro particles. The children are more vulnerable than adults towards lead toxicity (Abdulla, 2020; Markowitz, 2021).

Different sensitive organs can be affected after lead absorption due to the buildup of its toxicity such as, the cardiovascular, neurological, hematological, immunological, renal, hepatic and reproductive systems. Furthermore, due to its systemic toxicity, lead has been identified as a probable human carcinogen (Luz *et al*., 2018; Wang *et al*., 2021). The key mechanism involved in heavy metal toxicity and carcinogenicity is oxidative stress, which is defined as an imbalance between antioxidants and oxidants that creates damaging reactive oxygen species (ROS) (Killian *et al*., 2020). Lead, in effect, has the ability to deregulate the antioxidant defensive barriers, including the antioxidant enzymes, affecting cellular integrity and the metabolism of the cells components (Wu *et al*., 2019).

Given the highly harmful environmental impacts of metal pollution, as well as its influence on ecological balance and human health in particular, it is critical to clean up the industrial sources of these contaminated effluents before releasing them into the environment.

Various treatment procedures have been tested and assessed for this purpose, including precipitation, Reverse osmosis, membrane filtration, electrochemical techniques and adsorption (Qasem *et al.*, 2021). Adsorption is considered a viable alternative to these technologies for eliminating metal contaminants due to its high efficiency, low operating costs and ease of use (Younas *et al.*, 2021).

Annually, agricultural and agro-food activities emit massive amounts of byproducts, which represent a major source of plant biomasses to solve the problem of heavy metal pollution due to their abundance, cost-effectiveness and high efficiency in removing pollutants while having no negative environmental consequences (Kwikima *et al.*, 2021). Furthermore, various plant based adsorbents have been used efficiently in the adsorption of different metals such as lead such as potato peels, banana peels and *Nigella sativa* L. seeds (Addala *et al.*, 2018; Afolabi *et al.*, 2020; Ashfaq *et al.*, 2021).

Pomegranate (*Punica granatum* L.) is a long-cultivated fruit all over the world. Because of its health advantages, its intake has grown, either as it is or as a juice. As a result, its production and processing were boosted concurrently, resulting in vast quantities of peels as a primary byproduct (Kandylis and Kokkinomagoulos, 2020; Yan-hui *et al.*, 2022). Pomegranate peels contain a high concentration of bioactive substances belonging to their polyphenolic secondary metabolites, such as phenolic acids, flavonoids and tannins, which have a variety of biological activities, including antioxidant and chelating characteristics (Benchagra *et al.*, 2021). These secondary metabolites are known to be a powerful metal chelating bio-molecules due to the presence of phenolic group in their structure (Hider *et al.*, 2001; Kruk *et al.*, 2022). The metal chelation potential of polyphenols is highly influenced by catechol moieties and hydroxyl and carbonyl group combinations (Lakey-Beitia *et al.*, 2021).

On this context the objectives of this study are:

- → Characterization of the peels powder of both red and yellow *Punica granatum* L. varieties (The equilibrium pH, Point of zero charge (pH_{pzc}), Surface functional groups and FT-IR analysis).
- → Evaluating the peels powder of both red and yellow *Punica granatum* L. varieties as adsorbents towards Pb(II) ions and assess the effects of different factors on the adsorption capacity of the two adsorbents (pH, contact time, biosorbent dose and initial metal concentration).
- → Modeling the adsorption isotherms and determination of the maximum adsorption capacity of the peels powder of both red and yellow *Punica granatum* L. varieties.
- → Modeling the adsorption kinetics of the peels powder of both red and yellow *Punica granatum* L. varieties.

→ Evaluating the possibility of regeneration of the peels powder of both red and yellow *Punica granatum* L. varieties after adsorption using acidic desorption.

→ Extraction of the polyphenols of the two varieties of *Punica granatum* L. using different extraction solvents.

→ Determination of polyphenols, flavonoids, condensed tannins and anthocyanins contents of *Punica granatum* L. extracts.

→ Evaluation of the in vitro antioxidant activity of *Punica granatum* L. extracts using different assays (DPPH, ABTS, reducing power, iron chelation and β-carotene bleaching).

1. Pollution

The term pollution is defined as the direct or indirect introduction of harmful substances into the environment either naturally or anthropogenically, which affects negatively the living organisms (humans, animals, plants and microorganisms) and the environment (Al-Dulaimi and Al-Taai, 2021). The pollution is also described as any unfavorable change in the physical, chemical or biological properties of air, water or soil that may or will have a harmful effect on the human existence and on the ecosystem. The three primary types of environmental pollution are air pollution, water pollution and land contamination. Pollution can also refer to an excessive human activity, such as noise pollution or particular pollutants, such as plastic (Ajibade *et al*., 2021).

1.1. Water pollution

Water is a valuable natural resource that is important to the survival and the growth of the mankind, either for its consumption or its use in different industries and in agriculture. It is therefore essential to preserve its quality and use it responsibly. Water pollution is the alteration of the quality of water by introducing external elements, substances and/or organism into groundwater or surface water, which changes its biological, physical and chemical proprieties as a result of natural or anthropogenic causes, leading to the disruption of the aquatic ecosystem (Akhtar *et al*., 2018).

Water pollution can come from two different sources;

Point sources, such as industrial, hospital and sewage treatment effluents, release pollutants directly into diverse waterways (rivers, streams, lakes, etc) at discrete identifiable places where emissions may be readily measured.

Non-point sources, on the other hand, are difficult to pinpoint since they originate at such large geographical scales. Nonpoint source pollution is often caused by runoff, such as agricultural runoff, rainfall and snowmelt runoff, which transport contaminants to water bodies (Ravikumar *et al*., 2022).

1.2. Pollution origins

Pollution can originate from different sources either naturally or by humans intervention whether it was direct or indirect.

1.2.1. Natural pollution

Natural pollution modifies the properties of water in an undesirable way naturally and not with human intervention. The natural causes are the same in the urban and rural areas;

geology of rocks, climate change, natural disasters (floods, droughts, earthquakes etc.), atmospheric deposition and weathering of rocks (Khatri and Tyagi, 2015).

1.2.2. Domestic pollution

Aquatic ecosystems, such as streams, lakes, rivers and underground waters, are crucial for human health and survival because they supply essential drinking water and protein supplies. Because humans live close to these ecosystems and frequently utilize them for daily household activities and for waste disposal, freshwater systems are especially vulnerable to sewage contamination. The germs and bacteria present in that wastewater produce illness and are thus a source of health problems in humans and animals (Wear *et al*., 2021).

1.2.3. Urban pollution

Urbanization is linked to population expansion as well as agricultural and industrial development. As a result, there has been a significant increase in sewage water and a decrease in groundwater infiltration, with less and less space accessible for groundwater recharge. Thus, one of the biggest difficulties of urbanization has been groundwater reduction. Surface water bodies are significantly polluted by untreated sewage and contaminated urban runoff, leaving them unable to furnish fresh water to urban needs (Estrada-Rivera *et al*., 2022).

1.2.4. Agriculture pollution

The population in rural regions is lower; it includes more pesticides, fertilizers and more erosion of soil. After rain and flooding, these contaminants reach water bodies via runoff. In fact, the eutrophication phenomenon is caused by this agricultural runoff. The primary cause of eutrophication is phosphate, because its high concentration encourages Cyanobacteria and Algae growth which release toxins into water, thus affect the food chain as well as lowering the dissolved oxygen in water. The oceanic life is also affected by the deficiency of dissolved oxygen in lakes and rivers due to fertilizers that are rich in nitrogen, which have high water solubility, resulting in ground water contamination. Likewise, pesticides used in agriculture leaches groundwater hence, polluting it (Chaudhry and Malik, 2017).

1.2.5. Industrial pollution

Industrial wastewater is the water containing dissolved and suspended pollutants discharged from various industrial operations, such as mining, steel production, oil refineries, metal finishing, batteries manufacturing and the food industry. These diverse industrial sectors release many harmful contaminants in their effluents that are detrimental to human and aquatic life like textile, chemicals, silt, oils, phenolic compounds, pesticides, medicines,

heavy metals and other industrial by-products. These pollutants are harmful to animals, people and plants in both direct and indirect ways. When heavy metals or chemicals from businesses reach a critical level, they can impair the entire ecological system and render water poisonous and unsafe to drink (Ahmed *et al*., 2021).

1.3. Effects of pollution

Pollution can affect both the environment and human health

1.3.1. Effect of pollution on the environment

Water pollution can affect all kinds of water bodies such as seas, lakes, oceans, rivers and groundwater and modify their physical, chemical and biological qualities which change their natural proprieties, harming the aquatic plants and animals. Plants development is hampered as a result of rising water pollution; the minerals required for photosynthesis cannot be acquired therefore, the forest cover cannot grow. Algae growth hinders fish and other marine animals from absorbing oxygen, significantly impacting the environment. The unrestricted flow of hazardous streams in nature damages the soil and in particular, pollutes groundwater (Kılıç, 2021).

Plant nutrients like phosphate, nitrogen and other elements that promote the growth of aquatic plant if presented in excess, results in algal blooming and excessive weed growth. This adds odor, flavor and occasionally color to the water. Nitrogen oxides and sulfur dioxide generate acid rain, which makes the soil's pH low, while carbon dioxide CO_2 emissions cause ocean acidification (Owa, 2014).

1.3.2. Effect of pollution on human health

Polluted water has serious consequences on human health. According to the UNESCO 2021 World Water Development Report, approximately 829,000 people die each year from diarrhea caused by contaminated drinking water, poor sanitation and poor hand hygiene. Diseases such as cholera, trachoma, schistosomiasis and helminthiasis are also on the rise as a result of a lack of water and sanitation services. Risky drinking water and poor environmental cleanliness can cause gastrointestinal illness, impairing nutritional absorption and leading to malnutrition. These effects are especially noticeable in children (Lin *et al*., 2022).

The excessive presence of heavy metals such as fluoride, arsenic, lead, cadmium, mercury and others in the water is hazardous to human health. As an example, concentrations of fluoride below 0.5 $mg.L^{-1}$ induce dental cavities and mottling of teeth. Toxic elements such as arsenic and cadmium are extremely dangerous to human health and if presented in high doses, they can cause respiratory cancer and skin lesions. Long-term exposure to these

carcinogenic elements causes bladder and lung cancer. Pipes and domestic plumbing systems can also contribute to lead pollution in drinking water, which affects the blood, kidneys and the central nervous system of humans, which can lead children and pregnant women to death (Negi *et al.*, 2021).

Water-borne illnesses such as typhoid fever, diarrhea, cholera, ulcers, arsenicosis, dracunculiasis, hepatitis, respiratory tract infection, kidney and endocrine damage are extremely dangerous and can threat the human lives. These diseases are mostly caused by drinking water contamination owing to the existence of many hazardous bacteria and germs (Fazal-ur-Rehman, 2019).

1.4. Types of water pollution

According to the nature of pollutants, water pollution can be divided to several types.

1.4.1. Physical pollution

Physical pollution is caused by the organic and inorganic materials suspended in water. These contaminants alter the color, taste and odor of water. One of the forms of physical pollution is the thermal pollution as a result of pouring the cold water of factories into water which decreases in the amount of dissolved oxygen and damages aquatic life, as well as the nuclear pollution issued from pouring nuclear reactors in the water.

1.4.2. Biological pollution

Pathogenic bacteria, parasites and viruses are examples of biological contaminants. Human and animal secretions are the origins of these pollutants. They enter the water when agricultural drainage water or sewage mixes with it, causing human infection with a variety of illnesses such as cholera (Al-Taai, 2021).

1.4.3. Chemical pollution

The presence of excessive levels of dissolved salts, acids, fluorides, metals, organic compounds, fertilizers and pesticides causes this sort of pollution. The majority of organic compounds are dissolvable in water. They are either organic compounds that can be dissolved by the bacteria in the water or non-soluble materials such as insecticides and detergents. Fertilizers are primarily phosphorous and nitrogen and their presence in water promotes the growth of aquatic plants. This may cause the lakes to prematurely age, eventually transforming them into dry grounds or marshes. Similarly, Metals, especially some poisonous ones like mercury, cadmium and lead which are mainly soluble in water to some extent. Non-toxic metals include copper, magnesium, sodium, calcium and iron. However, their

accumulation can cause various disorders. For example, a super high sodium concentration makes the water unpleasant and increases the risk of heart and renal illnesses, as well as plant poisoning.

1.4.4. Metal pollution

Heavy metal pollution has emerged as a result of anthropogenic activity, primarily from foundries, metal mining, smelting and other metal related industries, as well as the metals washed away from various sources like landfills, waste dumps, excretion, livestock, runoffs and automobiles. Heavy metal can also result from use of fertilizers, pesticides and insecticides used in agriculture. Natural volcanic activity, metal evaporation from soil and water, soil erosion, metal corrosion can elevate heavy metal pollution (Briffa *et al*., 2020).

Metals present in the soil may be absorbed by plants, causing severe plant metabolic dysfunction. High levels of metals can limit the photosynthetic rate, influence the reproduction of plants by reducing pollen and seed viability, disrupt enzymes involved in chlorophyll formation and harm cell membranes. Heavy metals accumulate quickly in plants and access the human and animal food chains leading to metal poisoning. Heavy metal poisoning can go from moderate nose, skin and eye irritations to hematemesis, dizziness, extreme headaches, diarrhea and organ malfunction such as gastrointestinal distress, hypertension, cirrhosis, low blood pressure and necrosis (Adejumoke *et al*., 2018).

1.4.4.1. Heavy metals

Heavy metals term refers to the group of metals and metalloids. They are defined as elements with an atomic density greater than 5 $g.cm^{-3}$ and an atomic number more than 20, which must display metal characteristics. Heavy metals are divided into two types: essential and non-essential heavy metals. Essential metals are those that are necessary for living organisms to carry out essential activities such as growth and metabolism. Plants require various essential heavy metals such as Co, Zn, Fe, Cu, Ni and Mn because they create cofactors that are physically and functionally important for enzymes and other proteins. Heavy metals such as Cd, Pb, Hg, Cr and Al are not essential for any metabolism related processes, even in low levels, thus, not necessary for the growth of plants and animals (Raychaudhuri *et al*., 2021). Heavy metals damage the soil owing to the entrance of industrial wastewater, sewage sludge, fertilizers, the use of treated wastewater in land application and weathering of soil minerals (Vardhan *et al*., 2019).

1.4.4.2. Toxicity of heavy metals

Heavy metals toxicity is determined by pollutant concentration, the organ exposed,

length and amount of exposure and the oxidation state. High levels of heavy metals in soil can cause changes in soil quality by altering pH, porosity and natural components, leading to low growth and loss of many plant species, corrosion and eutrophication (Sankhla *et al*., 2016).

Their buildup in water causes major difficulties for humans and ecosystems. Thus, decreased drinking water quality as well as decreased water resources for all living beings. In plants, they can damage roots or leaves, disrupt mineral absorption and affect photosynthesis. Heavy metal toxicity in animals is shown in the decreased body weight, liver and kidney damages and DNA damage. They can also cause kidney damage, liver and lung damages and numerous forms of cancer in humans. When heavy metals are not digested by the organism, they become poisonous and concentrate in different organs. They enter the human body by ingestion polluted water, inhalation or via skin absorption (Ungureanu and Mustatea, 2022).

Biochemical processes can be affected by these metals, causing a variety of health issues in the bone system (bone mineralization), reproductive system and neurons (Alzheimer's, Parkinson's, depression and dementia). Because of the generation of ROS, it can also cause RNA and DNA damage, cancer of the bladder and lungs (Balali-Mood *et al*., 2021).

1.4.4.3. Lead

Lead (Pb) is a naturally existing metal that forms lead compounds when it attaches to two or more elements. It's a bluish gray metal that's uncommon in the earth's crust. Lead is denser than most common heavy metals with an atomic weight of 207.2 $g.mol^{-1}$ and it is mostly found as lead ore, the most important of which is the lead sulfide (galena). The principal application of lead is in the production of batteries. It is also frequently employed in the manufacture of paint and alloys, in industry of electronic conductors, sheet lead, rubber, waterproof plates, ceramic glazes and toys. Furthermore, it is utilized in the formulation of various ointments like lead acetate. Lead arsenate is used as an insecticide in agriculture (Dökmeci, 2020).

1.4.4.3.1. Lead speciation

The oxidation states under which the lead exists are Pb0, Pb^{2+} and Pb^{4+}, but in the environment it is mainly in the Pb^{2+} state. The Pb^{4+}only occur in oxidizing conditions. The Pb^{2+} degree is stable, in all environmental conditions. There are three lead oxides known: lead monoxide (PbO), lead dioxide (PbO_2) and lead tetroxide (Pb_3O_4), often known as minium (Haynes 2014).

Lead is rarely in its elemental form. It exists in two metallic forms. Inorganic structure; when it is associated with certain compounds to form lead salts. The most frequently

encountered are those of nitrate, sulfates, chromate, phosphates and chlorides. The organic structure most often comes in the form of tetramethyl lead and tetraethyl. Because of their toxic effects, the use of these organic lead compounds, particularly in gasoline, is currently restricted (Abdulla, 2020).

The speciation of lead has an important influence on its bioavailability and therefore on the health effects predictable for a given dose. There are many mineral phases capable of trapping lead: carbonates (cerussite $PbCO_3$) and hydrocerussite ($Pb(CO_3)_2(OH)_2$), sulfides (galena PbS) in a reducing medium, phosphates (pyromorphite $(PO_4)3Cl$), sulfates (anglesite $PbSO_4$), oxides (trimming PbO). In the aqueous phase, lead can be found either in the form of free ions (Pb^{+2}) or in the form of complexes. Its speciation in the aqueous phase is strongly controlled by the two parameters which are the pH and concentration of the complexing agent present in the solution (Glorennec *et al*., 2007).

1.4.4.3.2. Toxicity of lead

Occupational exposures such as dermal contact and inhalation are the indirect routes for lead's intake. However, ingestion of Pb polluted food and water is the direct and the main route for its accumulation. Lead has a half-life of about 30 days in the blood. It binds to hemoglobin in erythrocytes before diffusing into soft tissues like the kidneys, brain and liver. As a result, these organs are particularly vulnerable to lead toxicity. Following that, it is transported as lead phosphate to bones, teeth and hair (Luz *et al*., 2018).

Lead poisoning produces ROS such as hydroperoxyl, hydrogen peroxide and singlet oxygen. Pb generates these free radicals, causing oxidative stress and cellular damage. When there is an imbalance between antioxidants and ROS and in the body, it suffers from oxidative stress. Oxidative stress destroys cells and tissues, increasing the chance of negative health consequences such as cardiovascular disease and cancer.

Blood with a high lead content impairs the functioning of the central nervous system, resulting in encephalopathy and edema mostly affecting the cerebellum. A high level of lead in the body during pregnancy might result in miscarriage. Prolonged lead exposure was observed to reduce male potency (Debnath *et al*., 2019).

The International Agency for Research on Cancer (IARC) has categorized lead as a potential human carcinogen (group 2B) and its inorganic compounds as likely human carcinogens (group 2A). Lead poisoning has been linked to an increased risk of lung, stomach and bladder cancer. Mitogenesis, changes in gene transcription and many indirect genotoxicity processes have been suggested as causes of lead carcinogenicity (Fenga *et al*., 2017).

Children are more sensitive to the effects of lead than adults because they are exposed more often through hand-to-mouth activity and their blood-brain barrier and liver detoxification mechanisms are physiologically immature. They absorb lead from the gastrointestinal system more effectively, which can result in neurodevelopment abnormalities and multiorgan damage, decreased attention span, increased irritability, increased dullness and shorter attention span in the central nervous system, which eventually results in seizures, headache, coma and even death (Al osman *et al*., 2019).

Lead impact on the animals also includes damaged tissues and organs, damaged immune system, damaged reproductive system, high blood pressure and neurological impairment. However, at higher levels, the Pb poisoning can cause damage to the nervous system, paralysis and death. Lead is the most dangerous metal that is designated a priority pollutant as an industrial contaminant. It enters the environment through soil, air and water/wastewater.

Lead contamination enters the soil and ground water through natural sources as well as industrial effluents. Excessive lead concentrations in the atmosphere affect all ecosystem elements. Lead polluted soils cause plants to accumulate it, leading to cellular damage. Lead poisoning of plants has a significant impact on metabolic processes such as photosynthesis, thus, inhibiting their growth (Verma *et al*., 2020).

1.4.4.4. Heavy metals and legislation

- International standards

The World health organization had set heavy metal limitations guidelines in wastewaters as shown in (Table 1) (Who, 2002; 2003).

Table 1. International standards for the discharge of industrial effluents (Who, 2002; 2003).

Metalic element	**Maximal limit** ($mg.L^{-1}$)
Pb	0.01
Cd	0.003
Cr	0.05
Hg	0.001
Ni	0.02
Cu	1.20

❖ Algerian standards

The official journal of the Algerian republic n° 26 has fixed the normative limits regarding the discharge of industrial effluents, according to the decree n° 06-141 corresponding to April 19, 2006. The maximum values are fixed for a temperature of 30°C and a pH which must be between 5.5 and 8.5 (Official Journal of the Algerian Republic, 2006). The limits values of heavy metals and others are shown in (Table 2).

Table 2. Algerian standards for the discharge of industrial effluents (Official Journal of the Algerian Republic, 2006).

Metalic element	**Maximal limit** ($mg.L^{-1}$)
Al	3
Cd	0.2
Cr^{3+}	3
Cr^{6+}	0.1
Fe	3
Hg	0.01
Ni	0.5
Pb	0.5
Cu	0.5
Zn	3

1.5. Conventional technologies of wastewater treatment

Heavy metals are one of the most dangerous types of pollutant worldwide, due to their toxicity, difficult degradation and accumulation in the living organisms. Thus, treatment of polluted wastewater resulted from different metal based industries is very important for the protection of the environment and human health (Simeonidis and Mitrakas, 2021). For that, different technologies of treatment mentioned in this section have been used and developed during the years.

1.5.1. Solid-liquid separation technologies

They consist of transforming soluble metal species into insoluble species (precipitation, electrolysis) or retaining them on a solid matrix (ion exchange, adsorption) (Inglezakis *et al*., 2020).

1.5.1.1. Precipitation

Chemical precipitation is widely used in industry and is regarded as one of the most successful processes, in which metals are dissolved or suspended in solution and solid precipitate is formed. It is frequently followed by sediment removal, which involves the use of coagulants such as polymers to collect the tiny suspended particles into bigger precipitates. The effectiveness of a chemical precipitation is controlled by the type and dose of ionic metals present in solution, the precipitant utilized, the pH of the solution and the presence of additional elements that may block the precipitation reaction (Dahman, 2017).

Conventional chemical precipitation processes include hydroxide precipitation and sulphide precipitation. An alkaline agent is employed in hydroxide precipitation to raise the pH of the solution, resulting in a decrease in metal ion solubility and hence their precipitation from the solvent. Most commonly utilized for this purpose is lime or sodium hydroxide (Qasem *et al*., 2021).

Heavy metal ion removal can also be accomplished by metal sulfide precipitation. Because sulfide precipitates are not amphoteric, they can accomplish a high degree of metal removal in less time over a wider pH range than hydroxide precipitation. Metal sulfide precipitation can be accomplished with a number of precipitants, including sodium sulfide (Na_2S), sodium hydrosulfide (NaHS), calcium sulfide (CaS), barium sulfide (BaS), iron sulfide (FeS), ammonium sulfide ($(NH_4)_2S$) and sodium thiosulfate ($Na_2S_2O_3$) (Pohl, 2020). Carbonate precipitation is an alternate precipitation process that works well at lower pH levels. It is possible to accomplish this using sodium carbonate or calcium carbonate (Moghal *et al*., 2020).

1.5.1.2. Coagulation-flocculation

The coagulation-flocculation process is the major physicochemical treatment method used in industrial wastewater treatment due to its simplicity and effectiveness. This method eliminates turbidity from water as well as other impurities such fine particulate matter, bacteria and colors.

Coagulation is a process in which pollutants, suspended particles, collide with opposing particles and agglomerate to produce an insoluble agglomeration complex (a floc) that may be readily filtered. In general, the coagulation/flocculation process consists of four steps: charge neutralization, sweep coagulation, bridging and patch flocculation. The medium pH, coagulant dose and settling time all have a significant impact on the coagulation-flocculation process (Al-Anzi *et al*., 2022).

Coagulation-flocculation treatments are performed by adding coagulant and auxiliary

coagulant. Polychlorinated aluminium, ferum chloride and aluminium sulphate are often used as coagulant. Polymer coagulant is used as auxiliary coagulant. Chemical coagulants involve synthetic cationic polymers (aminomethyl polyacrylamide, polyalkylene, polyethylenimine, polyamine), hydrolyzing metallic salts (ferric chloride, ferric sulphate, magnesium chloride and alum) and pre-hydrolyzing metallic salts (poly aluminum chloride), poly ferric chloride, poly ferrous sulphate and poly aluminum ferric chloride) and Natural coagulant are either microorganism based material (bacteria, microalgae, fungal), animal based material (chitosan and isinglass) and plant based material (seed and plant extracts and fruit waste) (Sukmana *et al*., 2021).

1.5.1.3. Ion exchange

Ion exchange is a reversible process that involves the exchange of ions between solid and liquid phases that contain unwanted metal ions. Because the solid phase is insoluble in liquid and contains exchangeable ions, it is referred to as an ion exchanger. Furthermore, they are highly stable and do not undergo structural changes during reactions. Ion exchangers are divided into two types: cation exchangers and anion exchangers. Physiochemical stability, ion exchange capacity, hydrophilicity, effective surface area, economic value and particle size are some of the primary parameters that define the quality of ion exchangers.

Depending on the kind of application, a broad selection of ion exchange resins is now available. Synthetic resins are more prevalent than natural resins and are commonly employed in wastewater treatment. There are several varieties of ion exchange resins available, including strong-acid cation resins, strong base anion resins, weak acid cation resins, weak base anion resins and metal selective chelating resins. Strong acid cation resins were mostly composed of sulfonic acid functional groups or other strong acid functional groups. Strong base anion resins may include ethanol functional groups or several methyl groups. They also have distinct properties, such as improved stability in the case of methyl groups but higher efficiency in the case of ethanol groups (Khan and Ahn 2018).

Weak acid cation resins have carboxylic functional groups, whereas weak base anion resins have phenol formaldehyde with amine groups connected to it. Metal selective chelating resins are more effective against heavy metals, because they have a particular affinity for these metals. Ions in solution are transferred to the resin via an exchange with Na^+ or H^+ cations (for cationic resins) or Cl^- or OH^- anions (for an anionic resin) (Al-Asheh and Aidan, 2020).

1.5.1.4. Electrolysis

Electrochemical technologies are considered green processes since they create oxidizing agents using electrons (electric current), eliminating the usage of toxic chemicals. Furthermore, they do not produce any secondary waste. The fundamental limitation restricting their wide-scale adoption is connected to technological and economic factors.

One of the procedures used to extract metals from wastewater streams is electrolytic recovery. A current is passed through an aqueous metal bearing solution including a cathode plate and an insoluble anode in this procedure. The flow of electrons from one element to another can create electricity. The electrochemical technique for treating heavy metal containing wastewater is to precipitate the heavy metals as hydroxides in a mild acidic or neutralized catholyte. Electrochemical wastewater treatment methods include electro-deposition, electro-coagulation, electro-flotation and electro-oxidation (Reza and Singh, 2010).

Electrolysis is an electrochemical wastewater treatment process that is gaining popularity as well as substantial scientific advancement. The process takes place in an electrolyte, which is a watery or salt melting solution that allows ions to be transferred between two electrodes. When an electrical current is provided, positive ions flow to the cathode and negative ions flow to the anode. The metal recovered from the water load can be of high purity, allowing for valuable material extraction.

Many different electrodes may be employed as anode materials in electrochemical water treatment; dimensional stable anode (DSA) and boron doped diamond (BDD) have shown to be the most superior electrodes due to their elevated qualities in wastewater treatment (Tien and luu, 2020).

1.5.1.5. Adsorption

Among the different existing approaches on water treatment, the adsorption technique stands out due to its versatility in operation and design procedures and it appears to have a considerable impact on the toxicity, biological availability and transport of heavy metals in wastewater. The three basic stages of adsorption onto solid sorbent are transport of hazardous substance from aqueous solution onto the accessible surface of the adsorbent by physical or chemical interactions, adsorption onto solid surface and transit within sorbent particle.

Electrostatic attraction causes charged pollutants to adsorb on oppositely charged adsorbents. Heavy metals have a great attraction for hydroxyl or other functional groups on the surface. Adsorbents can be regenerated for multiple cycles because it is often reversible and it can be followed by a desorption process (reverse process of adsorption in which

adsorbate ions are desorbed from adsorbent surface), making it a cost-effective and high-efficiency process to produce high-quality treated effluents (Gupta *et al*., 2021).

1.5.2. Membranes based technologies

Membrane technologies have become more appealing for treating and reusing wastewater in different industrial sections, because of their great efficiency, ease of operation and cheap cost. Membrane separation technologies and applications have advanced dramatically in recent years. The procedure consists in forcing the solution through a porous membrane and extracting permeate or clean water flow of the membrane at air pressure (Noor *et al*., 2019).

1.5.2.1. Ultrafiltration

Ultrafiltration (UF) technology has been broadly used in wastewater treatment and reclamation because of its low energy consumption, high efficiency and the absence of chemical pretreatment. Ultrafiltration is a low pressure process that uses transmembrane pressures ranging from 0.5 to 5 bars, depending on the material to be treated. Organic (polymer) and inorganic materials can be used to make ultrafiltration membranes. Polysulfone, polyethersulfone, polyacrylonitrile, cellulosics, polyimide, polyetherimide and aliphatic polyamides are some of these materials. Inorganic materials such as alumina and zirconia have also been employed (Youcai, 2019).

Ultrafiltration separates heavy metals, macromolecules and suspended particles from inorganic solutions using a permeable (selective) membrane based on the pore size (5-20 nm) and molecular weight of the separating components. Depending on the membrane parameters, UF can achieve more than 90% of removal efficiency with a metal concentration ranging from 10 to 112 $mg.L^{-1}$ at pH ranging from 5 to 9.5 and at a pressure of 2-5 bar (Chaemiso and Nefo, 2019).

1.5.2.2. Microfiltration

Microfiltration (MF) is typically used as a pretreatment for other separation procedures like ultrafiltration and as a post-treatment for granular media filtration. The usual particle size for microfiltration is between 0.1 and 10 µm. These membranes can separate macromolecules with estimated molecular weights of less than 100,000 $g.mol^{-1}$. It is similar to other technologies like as ultrafiltration and reverse osmosis, with the sole variation being the particle size and pressure employed.

MF membranes have pore sizes ranging from 0.1 to 5 µm. Particles larger than 0.1 µm in diameter are often separated by a rather open membrane structure. Because of their low

hydrodynamic resistance, such membranes require modest hydrostatic pressures (0.5-5 bar) to achieve high contaminant rejection and solvent flow (Anis *et al*., 2019).

1.5.2.3. Reverse osmosis

Reverse osmosis (RO) is a membrane-based method used to either clean water or extract soluble solids (known as dewatering) such as ions from a given solution. It is a diffusion-controlled method in which permeant mass transfer occurs via a dense membrane with pore diameters ranging from 0.0001 µm to 0.001 µm, using a controlled solution-diffusion mechanism.

The needed osmotic pressure (20-100 bar) is far higher than that required for MF. Permeants dissolve in membrane material before diffusing through it. Because RO membranes are usually hydrophilic, water will quickly seep into and out of the membrane polymer structure. Because RO membranes are prone to concentration polarization and fouling, pretreatment is one of the primary elements for a successful and cost-effective operation. Pretreatment is intended to improve RO performance by reducing fouling, scaling, membrane deterioration and breaking (Trishitman *et al*., 2020).

RO is effective for the removal of soluble chemicals and heavy metals such as nitrate, sodium, cryptosporidium, fluoride, sulfides, arsenic, mercury, uranium, radium and lead. As the water travels through the thin semi-permeable membranes, it also removes dangerous germs and chloride. RO systems are simple to construct and run, have low maintenance requirements and are modular in nature, making system extension easy. Reverse osmosis membrane technologies may remove both organic and inorganic contaminants at the simultaneously (Ahuchaogu *et al*., 2018).

1.5.2.4. Electrodialysis

Electrodialysis (ED) is a wastewater treatment membrane based method. It is one of the suggested treatment techniques for wastewater containing heavy metal ions such as lead, chromium, cadmium and nickel. In an ED system, ion exchange membranes are positioned between the anode and cathode. Ionic molecules in the feed water begin to migrate across ion exchange membranes with the help of an electrical driving force. By passing an electrical current between the anode and cathode, the cations in the solution migrate toward the cathode and the anions migrate toward the anode.

Cations flow through the cation exchange membrane (CEM), whereas anion exchange membrane (AEM) retains them. Anions, on the other hand, travel through the anion exchange membrane (AEM) but are trapped by the cation exchange membrane. The electrolyte solution is used to maintain system conductivity and eliminate gases created by electrode reactions.

The ED performance depends on different operating factors such as ion exchange membrane structure, feed water ion concentration, current density, pH, flow rate and ED cell structure (Juve *et al*., 2022).

Foulants such as organics, colloids and biomass on the membrane's internal structure or exterior surface reduce the separation efficiency, increase the consumption of energy and lower the membrane selectivity. As a result, certain approaches for reducing fouling in ED systems are offered, such as feed solution pretreatment, zeta potential management and flow rate optimization (Akhter *et al*., 2018).

1.5.3. Biological technologies

These processes exploit certain resistance mechanisms developed by plants or microorganisms (bacteria, algae, fungi and yeasts), which are capable of fixing and to accumulate metals.

1.5.3.1. Biosorption

Biosorption technology is a quick and energy-free process in which biological materials or biopolymers serving as sorbents may remove contaminants such as heavy metals, synthetic organic materials and waste nuclear compounds from wastewater via metabolically mediated or physicochemical absorption mechanisms.

Because of the affinity between biosorbent and adsorbates, mechanisms such as absorption, adsorption, ion exchange, surface complexion and precipitation are involved in the biosorption process. The advantages of biosorption over traditional removal techniques include the utilization of inexpensive and plentiful renewable biomaterials. Because of the quick kinetics, a large amount of wastewater may be treated and specific heavy metals recovery (Kumar and Ngueagni, 2022).

1.5.3.2. Phytoremediation

Phytoremediation is a green technology that employs the combined action of plants, plant-derived microbes or associated microbiota to remove contaminants from soil, groundwater and wastewater by retaining, eliminating, degrading or transforming toxic elements such as pesticides, explosives, radionuclides and heavy metals such as arsenic, lead, mercury, chromium, nickel and cadmium. The advantages of phytoremediation compared to conventional techniques are lower cost, ecofriendly impact, public acceptance, potentiality to remediate various pollutants and further it does not affect people living and working in the surrounding areas (Lakshmi *et al*., 2017).

2. Adsorption

In this section we mainly focus on the liquid-solid interface, since it describes the type of interaction that occurs in adsorption related to water treatment.

2.1. Concept of adsorption

Adsorption is superficial phenomenon that refers to the capacity of solid or liquid materials to attract or draw molecules of gases or liquid solutions to their surface to come into direct contact with them (Figure 1), forming an interface layer. The term adsorbents refers to the solid or liquid materials used to adsorb gases or solutes, whereas adsorbate refers to the removed particles. The desorption process is the inverse of the adsorption process (desorption). The nature of the adsorbent in terms of shape, size, radius, polarity, presence of functional groups, molecular weight and solubility influences the interaction between the adsorbent surface and the adsorbed particles (Soliman and Moustafa, 2020).

In the case of water treatment, the process occurs at the interface between solid adsorbent and the contaminated water. When the solution and adsorbent come into contact, the solute molecules attract to the adsorbent's surface via the functional groups on the surface

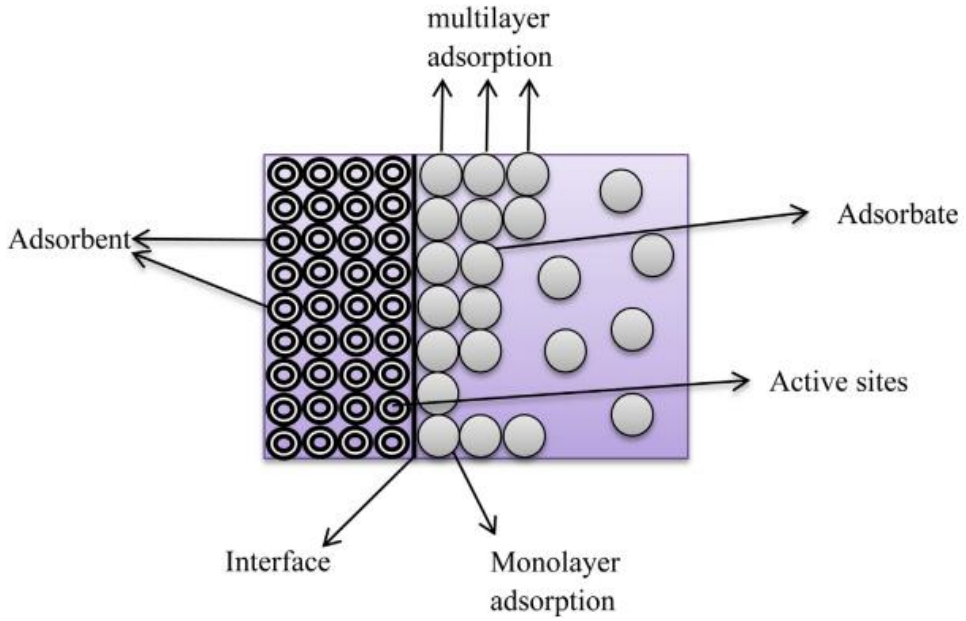

Figure 1. Adsorption process (Soliman and Moustafa, 2020).

2.2. Types of adsorption

Adsorption may be classified into two forms based on the nature of the interactions that connect the adsorbate to the adsorbent's surface; physical adsorption and chemical adsorption.

2.2.1. Physiosorption

Physical adsorption is the simplest type of adsorption, in which the adsorbate are attached to the surface of the adsorbent through weak bonds such as Van Der Waals forces, hydrogen bonding, hydrophobic interactions or electrostatic forces. The main characteristic of physiosorption are rapidity of the process, low binding energy, easy desorption, preserved molecule individuality, process temperature relatively low and possibility of multilayer and monolayer formation (Benjelloun *et al*., 2021).

2.2.2. Chemiosorption

The process of chemisorption of the adsorption technique, also known as chemical adsorption, is defined as the adsorption that occurs under the formation of chemical bond as forces of attraction between the adsorbed molecules and the adsorbent. This makes the chemiosorption irreversible . Chemisorption occurs slowly at high temperature and adsorption energy. Chemiosorption results in a monolayer of the adsorbates attached to the surface of the adsorbent (Adeleke *et al*., 2019).

Table 3. Comparison between chemiosorption and physiosorption (Adeleke *et al*., 2019).

Characteristic	**Physiosorption**	**Chemiosorption**
Activation energy	Low	High
Operating temperature	Relatively low	Very high
Type of bonds	Physical weak bonds	Strong chemical bonds
kinetic	Fast	Slow
Desorption	Reversible	Mostly irreversible
Type of formation	Monolayer and multilayer	Monolayer

Adsorbents are usually classified into conventional and non-conventional adsorbents, which they can have either natural or synthetic origin.

- ❖ Conventional adsorbents: commercial activated carbons (coals, wood, peat, etc.), inorganic materials (zeolites, activated alumina and silica gel), ion-exchange resins (polymeric organic resins and non-porous resins).
- ❖ Non-conventional adsorbents: natural materials (clinoptilolite, siliceous materials and clays), industrial by-products (fly-ash, sludge, red mud, etc.), activated carbons from solid wastes (date pits and bagasse), miscellaneous adsorbents

(hydrogels and cotton waste), biosorbents (fungi, yeast, orange peel and pomegranate peel like the current study) (Hussain *et al*., 2021).

2.3. Adsorption mechanism

The process of adsorption can be summarized in four consecutive steps:

Step 1- The diffusion of the bulk: diffusion of the adsorbate from the outer liquid phase towards the boundary layer or surface film that surrounds the adsorbent particle.

Step 2- Film diffusion or external mass diffusion: external mass transfer from the bulk solution over the boundary layer to the adsorbent's outer surface.

Step 3- Pore diffusion or intraparticle diffusion: diffusion that takes place in the adsorbent particles, by which the adsorbate solution enters the adsorbent pores.

Step 4- Physical and/or chemical bonding: the creation of physical or chemical bonds of the adsorbate at the active sites in the pores of the adsorbent (Wang *et al*., 2020). (Figure 2) shows an illustration of a conventional adsorption process.

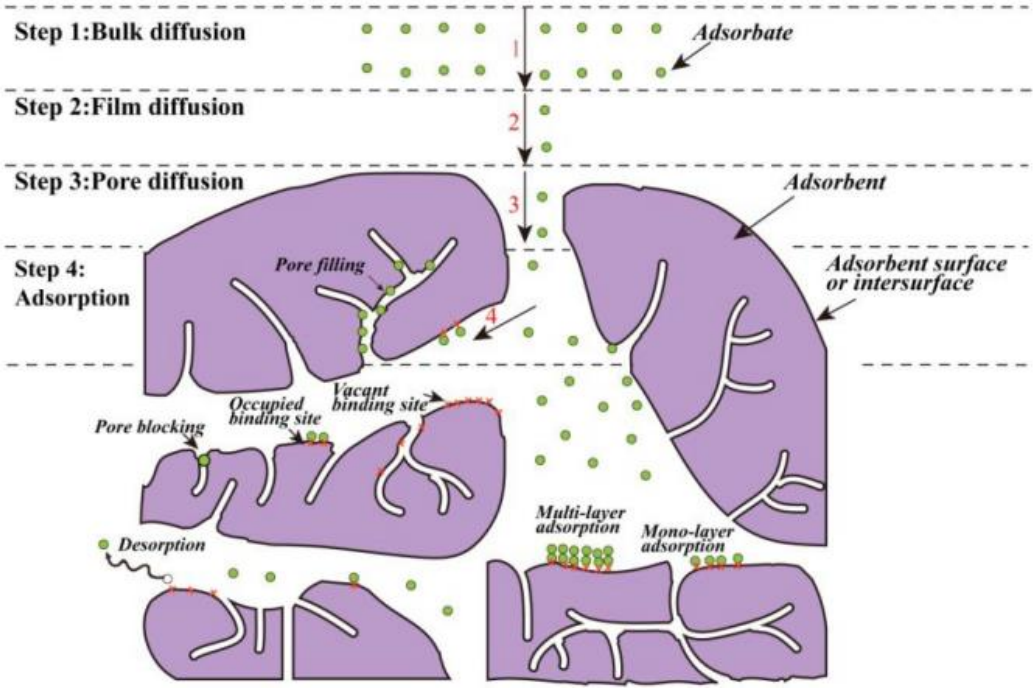

Figure 2. Illustration of a conventional adsorption process (Wang *et al*., 2020).

2.3.1. Estimation of adsorption efficiency

The effectiveness of adsorbents is evaluated through the adsorption, the adsorption percentage (removal rate) and the parameters related to adsorption kinetics. The adsorption capacity and adsorption percentage make it possible to understand the quantity of material required, while the kinetic make it possible to estimate the contact time between the sorbent and the adsorbate.

2.3.2. Adsorption capacity

The capacity of adsorption is the amount of adsorbate that can adhere on the adsorbent per unit mass or volume of the adsorbent (Mokhatab *et al*., 2019), while the adsorption percentage represents the total removal efficiency of the adsorbent (Elkhaleefa *et al*., 2021). These parameters can be calculated using the following equations:

$$Q_e = \frac{(C_e - C_0) \times V}{m} \qquad (1)$$

$$R\% = \frac{(C_0 - C_e) \times 100}{C_0} \qquad (2)$$

Where, Q_e is the amount of adsorbate adsorbed per unit weight of the adsorbent ($mg.g^{-1}$); V is the volume of solution containing the adsorbate (L); C_0 is the initial adsorbate concentration ($mg.L^{-1}$); C_e is the equilibrium concentration of the adsorbate ($mg.L^{-1}$) and m is the mass of the biosorbent (g).

2.4. Adsorption kinetics

2.4.1. Definition

Adsorption kinetics determination is very important to choose the appropriate adsorption conditions. It also demonstrates how the residence time of the adsorbed material at the solution interface affects the adsorption rate. The value of kinetic parameters determined from kinetic models predicts the adsorption rate. Mass transfer resistances constrain mass transfer from the solution to the adsorption sites within the adsorbent particles, which determine the time required to reach equilibrium (Worch, 2021).

As mentioned earlier, the adsorption occurs in four steps, bulk diffusion, external mass diffusion, pore diffusion and physical and/or chemical bonding. The equal distribution of the adsorbent and adsorbate in solution can decrease the effect of mass transfer resistance, making the elimination of the initial bulk diffusion step possible if the solution is evenly stirred. Considering the fact that last step happens fast, the adsorption kinetic is mostly controlled by film diffusion and/or pore diffusion (Wang *et al*., 2020).

2.4.2. Adsorption kinetics models

There are different kinetic models that describe adsorption phenomenon from pseudo-first order (Lagergren) model, the pseudo-second order model, the Elovich or the intra-particle diffusion model and the Weber-Morris model (Obradovic, 2020). In this section we

focus on the most common models used in the kinetic studies, which are in conformity with the experimental data (Table 4).

2.4.2.1. Pseudo-first order model (Lagergren model)

The pseudo-first order model equation is for the adsorption in a liquid-solid system. It considers that one ion is adsorbed on top of one adsorption site (Lagergren, 1898; Abedi *et al.*, 2016). The Lagergren equation is given as follow:

$$\frac{dQ_t}{dt} = K_1 (Q_e - Q_t)$$

The linear form of pseudo-first order model equation is:

$$\text{Log } (Q_e - Q_t) = \text{Log } Q_e - K_1 t$$

Q_e and Q_t represent the concentration of the adsorbate on the adsorbent at equilibrium and at time t, respectively ($mg.g^{-1}$), K_1 is the first-order model constant (min^{-1}). K_1 and Q_e are obtained from the slope and intercept of the plot Log (Q_e - Q_t) versus t.

2.4.2.2. Pseudo-second order model

The pseudo-second order model equation is founded on chemisorption and proposes that one ion is adsorbed on top of two adsorption sites (Ho and McKay, 1999; Abedi *et al.*, 2016). The equation is given as follow:

$$\frac{dQ_t}{dt} = K_2 (Q_e - Q_t)^2$$

The linear form of pseudo-second order model equation is:

$$\frac{t}{Q_t} = \frac{1}{K_2 Q_e^2} + \frac{1}{Q_e} \times t$$

Where Q_e and Q_t are the concentration adsorbate on the biosorbent at equilibrium and at time t, respectively ($mg.g^{-1}$), K_2 is the second-order model constant ($g.mg^{-1}.min^{-1}$). K_2 and Q_e are obtained from the slope and intercept of the plot t/Q_t versus t.

2.4.2.3. Intraparticle diffusion model

Webber-Morris observed that in most adsorption processes the concentration of

adsorbates varies proportionally with the square root of contact time ($t^{1/2}$) (Weber and Morriss, 1963; Ebelegi *et al*., 2020). The equation is given as follow:

$$Qt = k_{IPD}\, t^{1/2} + C$$

Where Qt is the concentration of the adsorbate at time t ($mg.g^{-1}$), K_{IPD} is the intra-particle diffusion constant ($mg.g^{-1}.min^{1/2}$) and C is the thickness of boundary layer (intercept).

Table 4. Kinetic models and their equations. (Lagergren, 1898; Weber and Morriss, 1963; Ho and McKay, 1999).

Kinetic model	Non-linear equation	Linear equation
Pseudo-first order model	$\frac{dQ_t}{dt} = K_1 (Q_e - Q_t)$	$\text{Log}\,(Q_e - Q_t) = \text{Log}\, Q_e - K_1 t$
Pseudo-second order model	$\frac{dQ_t}{dt} = K_2 (Q_e - Q_t)^2$	$\frac{t}{Q_t} = \frac{1}{K_2 Q_e^2} + \frac{1}{Q_e} \times t$
Intraparticle diffusion model	$Qt = k_{IPD}\, t^{1/2} + C$	

2.5. Adsorption equilibrium

2.5.1. Adsorption isotherm models

The adsorption isotherm is a mathematical description of the relationship between the amounts of the solute adsorbed on the adsorbent and the concentration of dissolved adsorbate in the liquid at equilibrium and at a constant temperature. The adsorption equilibrium takes place when the concentration of adsorbate in the solution is in dynamic balance with that of the interface.

The parameter C_{eq} corresponds to the concentration of the metal ion remained in the solution and Q_{eq} refers to the amount of metal ion adsorbed per unit weight of adsorbent (Yousef *et al*., 2020). There are several models; Langmuir, Freundlich, Sips, Dubinin-Radushkevich and Temkin. In this section we focused on the most commonly used isotherms

model at solid-liquid interface and that they are in accordance with the experimental data (Table 5).

2.5.1.1. Langmuir isotherm model

Langmuir models propose that adsorption occurs on adsorbent surfaces with a monomolecular layer structure in which all adsorption sites are identical and there is no contact between the molecules that have been adsorbed (Langmuir, 1918). The Langmuir equation is given as follow:

$$Q_e = \frac{Q_m K_L C_e}{1 + K_L C_e}$$

The linear form of Langmuir isotherm equation is:

$$\frac{C_e}{Q_e} = \frac{C_e}{Q_m} + \frac{1}{Q_m K_L}$$

Where Q_e is the equilibrium concentration of the adsorbate on the adsorbent ($mg.g^{-1}$), Q_m is the theoretical maximum adsorption capacity ($mg.g^{-1}$), C_e is the equilibrium concentration of adsorbate ($mg.L^{-1}$) and K_L is the Langmuir constant ($L.mg^{-1}$). The values of Q_m and K_L constants and coefficients of regression for Langmuir isotherm are obtained from the plot of C_e/Q_e versus C_e.

The important characteristic of the Langmuir isotherm is the dimensionless constant separation factor or the equilibrium parameter, R_L, given as follow:

$$R_L = \frac{1}{1 + bC_0}$$

The value of R_L gives an idea about the form of the isotherm. When it is $R_L > 1$ it indicates an unfavourable isotherm, $R_L = 1$ indicates a linear isotherm, $0 < R_L < 1$ indicates a favourable isotherm, while $R_L = 0$ indicates an irreversible adsorption (Edet and Ifelebuegu, 2020).

2.5.1.2. Freundlich isotherm

Freundlich models propose that the molecules are adsorbed as a monomolecular layer or multilayer structure on heterogeneous adsorbent surfaces and that there is contact between the

molecules that have been adsorbed (Freundlich, 1928). The Freundlich equation is given as follow:

$$Q_e = K_f C_e^{1/nf}$$

The linear form of Freundlich isotherm equation is:

$$\text{Log } Q_e = \text{Log } K_f + \frac{1}{n_f} \text{Log } C_e$$

Where K_f is the Freundlich isotherm constant ($mg.g^{-1}(L.mg^{-1})^{1/n}$), n_f is the adsorption intensity, C_e is the equilibrium concentration of adsorbate ($mg.L^{-1}$) and Q_e is the equilibrium concentration of the adsorbate on the adsorbent ($mg.g^{-1}$). K_f ($L.g^{-1}$) and n_f are Freundlich constants and they represent the adsorption capacity and the adsorption intensity, respectively. The values of K_f and n_f are obtained from the slope and intercept of the plot Log Q_e against Log C_e (Edet and Ifelebuegu, 2020).

2.5.1.3. Sips isotherm model

The Sips isotherm is a hybrid model that joins both Langmuir and Freundlich models (Sips, 1948). Sips model can describe the homogeneous or heterogeneous systems at a wide range of pressures. When C_e approaches a low value, the Sips isotherm effectively reduces to Freundlich, while at high C_e, it predicts the Langmuir monolayer sorption characteristic. (Wang and Guo, 2020).

$$Q_e = \frac{Q_m K_s C_e^{n_s}}{1 + K_s C_e^{n_s}}$$

The linear form of Sips isotherm equation is:

$$\frac{1}{Q_e} = \frac{1}{Q_m K_s}\left(\frac{1}{C_e}\right)^{\frac{1}{n_s}} + \frac{1}{Q_m}$$

Where Q_e is the equilibrium concentration the adsorbate on the adsorbent ($mg.g^{-1}$), C_e is the equilibrium concentration of adsorbate ($mg.L^{-1}$), Q_m is the theoretical maximum adsorption capacity ($mg.g^{-1}$), K_s ($L.mg^{-1}$) and n_s are the Sips constants.

The Sips isotherm equation is characterized by the dimensionless heterogeneity factor,

n_s, which can also be employed to describe the system's heterogeneity when n_s is between 0 and 1. When n_s =1, the Sips equation reduces to the Langmuir equation and it implies a homogeneous adsorption process (Kumara *et al*., 2014).

Table 5. Adsorption isotherm models and their equations (Langmuir, 1918; Freundlich, 1928; Sips, 1948).

Isotherm model	Non-linear equation	Linear equation
Langmuir	$Q_e = \frac{Q_m K_L C_e}{1 + K_L C_e}$	$\frac{C_e}{Q_e} = \frac{C_e}{Q_m} + \frac{1}{Q_m K_L}$
Freundlich	$Q_e = K_f C_e^{1/nf}$	$\text{Log } Q_e = \text{Log } K_f + \frac{1}{n_f} \text{ Log } C_e$
Sips	$Q_e = \frac{Q_m K_s C_e^{n_s}}{1 + K_s C_e^{n_s}}$	$\frac{1}{Q_e} = \frac{1}{Q_m K_s}\left(\frac{1}{C_e}\right)^{\frac{1}{n_s}} + \frac{1}{Q_m}$

3. *Punica Granatum* L.

3.1. Botanical description and taxonomy

The pomegranate plant is a bushy small tree of 3-8 m high, evergreen in the tropics and deciduous in subtropical and temperate climates. The harvest season is from September to November in the northern hemisphere and from March to May in the southern hemisphere. The fruit is classified as nonclimacteric; they do not ripen off the tree and should be harvested. There are dwarf cultivars that do not reach 1.5 m height (Erkan and Dogan, 2018).

The pomegranate, *Punica granatum* L., is classified as a berry, but it belongs to the Punicaceae family, it is native to central Asia and is one of the oldest known edible fruits. The name pomegranate derives from the Latin name of the fruit Malum granatum which means grainy apple. From its origin in what is now Iran and Afghanistan, the pomegranate spread east to India and China and west to mediterranean countries such as Turkey, Egypt, Tunisia, Morocco, Algeria and Spain, among others. Spanish missionaries introduced pomegranate to the Americas in the 1500s (Kumari *et al*., 2012; Shukla *et al*., 2016).The full classification of *Punica granatum* L. is shown in (Table 6) below.

Table 6. Taxonomy of *Punica granatum* L. (Kumari *et al*., 2012; Shukla *et al*., 2016).

Botanical classification	
Botanical name	*Punica granatum*
Kingdom	Plantae
Class	Magnoliopsida
Order	Myrtales
Family	Punicaceae (Lythraceae)
Genus	*Punica* L
Species	*P. granatum*

The fruit is connected to the tree by a short stalk and it consists of many closely packed red arils and irregular segments separated by non-edible white piths and thin membranes. The multi-ovule chambers (locules) are separated by membranous walls (septum) and fleshy mesocarp (Kumar *et al*., 2020).

The chambers are filled with numerous seeds, surrounded by a juicy layer that develops entirely from outer epidermal cells of the seed. The fruit size can vary from 6-12 cm in diameter and weighs 200 to 650 grams. It has a tough, leathery, brown to red, bitter skin (peel or pericarp), which is easily peeled. The skin color of a pomegranate fruit ranges from yellow,

green or pink overlain with pink to deep red or indigo to fully red, pink or deep purple cover, depending on the variety and stage of ripening (Kalaycıoğlu and Erim, 2016). The different parts of pomegranate fruit are shown in (Figure 3) below.

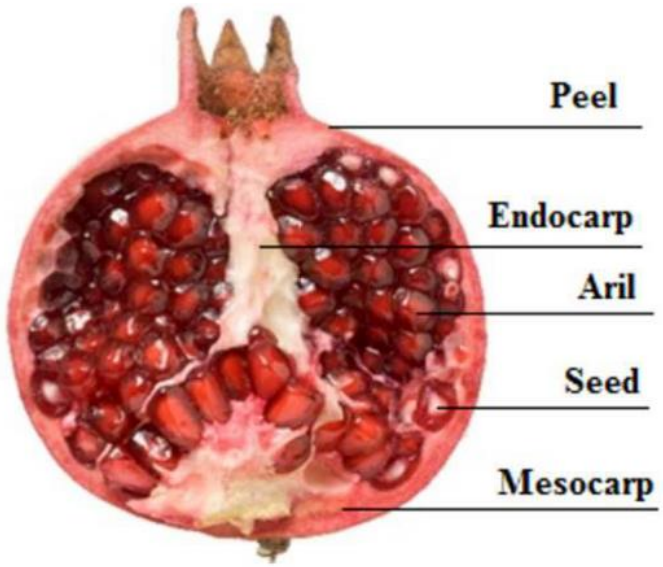

Figure 3. Anatomy of pomegranate fruit (Kalaycıoğlu and Erim, 2016).

3.2. Physiochemical composition

Pomegranate fruits have been largely utilized as a high nutritional value source in ancient plants. 46 % of the whole fruit is juice, the peel represent 43 % and the seeds represent 11 % of the fruit total weight (Ko *et al*., 2021).

3.2.1. Peels

The major minerals found in the peels powder are Ca, P, K, Na and Mg at levels of 342, 120, 150, 68 and 56 mg/100 g of dry peels powder, respectively. Other minerals such as Zn, Mn, Cu, Fe and Se were present at concentrations of 1.08, 0.86, 0.65, 6.11 and 1.07 mg/100 g dry peels, respectively. The peels content in moisture, ash, protein, total fat, carbohydrate and cellulose are 7.27, 4.32, 3.74, 0.85, 66.51 and 15.32 %, sequentially**.**

The most dominant vitamin the peels is vitamin C with a content of 11.54 to 13.26 mg/100 g. Pomegranate peels are also rich in vitamins, in which vitamin C (l-ascorbic acid) is the most dominant with a content of 13.26 mg/100 g of dry matter. However, vitamins B1 (thiamine), B2 (riboflavin), E (α -tocho- ferol) and A (retinol) exist in lower concentrations with 0.141, 0.09, 4.13 and 0.181 mg/100 g of dry peels, respectively (Omer *et al*., 2019).

(Table 7) shows the mineral and chemicals components in the pomegranate peels.

The peels also have various organic acids, such as citric, malic, acetic, oxalic, tartaric, lactic, ascorbic and fumaric acids, which have a potential correlation with biological activities (Magangana *et al*., 2020).

Table 7. Mineral and chemical composition of pomegranate peels (Ranjitha *et al*., 2018).

Minerals (mg/100 g dry peels)		Nutrients (%)	
Macro-elements		Moisture	7.27
Calcium (Ca)	342	Protein	3.74
Phosphorus (P)	120	Ash	4.32
Potassium (K)	150	Crude fibre	17.31
Sodium (Na)	68	Fat	0.85
Magnesium (Mg)	56	Carbohydrate	66.51
Micro-elements		Cellulose	15.32
Zinc (Zn)	1.08		
Manganese (Mn)	0.86		
Copper (Cu)	0.65		
Iron (Fe)	6.11		
Selenium (Se)	1.07		

3.2.2. Seeds

The seeds contain high content of fat with 4.8 ± 0.29 % and protein with 9.2 ± 0.35. In addition, the amount of Moisture, Ash, Crude Fiber, Vitamin C, Cellulose and Carbohydrate is 20.8 ± 0.45, 5.3 ± 0.19, 12.6 ± 0.26, 20.6 ± 0.01, 3.35 ± 0.78 and 64.85 ± 0.07 %, respectively.

Pomegranate seed fat fraction contains 14 fatty acids like stearoleic acid, stearic acid, heptadecanoic acid and others, the most abundant of which is punicic acid. Pomegranate seeds are also rich in mineral elements. Ca, Mn and Na are the major minerals with concentrations of 99.49 ± 13.66, 110.31 ± 16.78 and 73.24 ± 3.71 mg/100g of dry matter. The seeds also contains vitamin C with a concentration of 3.25 ± 0.36 mg/100 g (Peng, 2019). (Table 8) shows detailed chemical and nutritional content of pomegranate seeds.

Table 8. Mineral and chemical composition of pomegranate seeds (Peng, 2019).

Minerals (mg/100 g dry peels)		Nutrients (%)	
Macro-elements		Moisture	20.8 ± 0.45
Calcium (Ca)	99.49 ± 13.66	Protein	9.2 ± 0.35
Sodium (Na)	73.24 ± 3.71	Ash	5.3 ± 0.19
Magnesium (Mg)	110.31 ± 16.78	Crude fibre	12.6 ± 0.26
		Fat	4.8 ± 0.29
Micro-elements		Carbohydrate	64.85± 0.07
Zinc (Zn)	4.47 ± 1.45	Cellulose	3.35 ± 0.78
Manganese (Mn)	1.40 ± 0.74		
Copper (Cu)	0.15 ± 0.06		
Iron (Fe)	9.14 ± 2.51		

3.2.3. Juice

The pomegranate juice moisture percentage is 79.45 ± 0.96 %, with 3.99 ± 0.4 % of protein and 0.2 % fat. Carbohydrates and Ascorbic acid are present with a concentration of 14.1 ± 0.45 g/100 g and 0.26 ± 0.07 mg/100g, respectively (Dżugan *et al*., 2018).

Table 9. Mineral and chemical composition of pomegranate juice (Dżugan *et al*., 2018).

Minerals ($mg.L^{-1}$) of juice)		Nutrients	
Macro-elements		Moisture (%)	79.45 ± 0.96
Calcium (Ca)	29.62 ±17.60	Protein (%)	3.99 ± 0.4
Phosphorus (P)	143.19 ±24.03	Fat (%)	0.2 ± 0.0
Potassium (K)	2 691.80 ±585.30	Carbohydrates	14.1 ± 0.45 g/100 g
Sodium (Na)	13.79 ±6.10	Vitamin C	0.26 ± 0.0731 mg/100g
Magnesium (Mg)	49.15 ±30.73		
Sulfur (S)	132.19 ±29.96		
Micro-elements			
Zinc (Zn)	0.718 ±0.597		
Manganese (Mn)	0.620 ±0.188		
Copper (Cu)	0.453 ±0.115		
Iron (Fe)	2.440 ±2.118		

The chemical and nutritional profile of the juice is shown in (Table 9) above. The pomegranate juice is also rich in malic and citric acid, which play an essential role in preserving beverages quality (Esposto *et al*., 2021).

3.3. Bioactive compounds

The pomegranate fruit and its different parts (peels, seed and arils) have various bioactive compounds, such as phenolic acids, hydrolysable tannins, condensed tannins, anthocyanins and flavonoids, as well as other bioactive constituents that are in relation with the biological activities of *Punica granatum* L.

Pomegranate peel is an excellent source of precious bioelemnts, which have numerous beneficial health effects, including phenolic acids (hydroxycinnamic and hydroxybenzoic acids), flavonoids (anthocyanins and catechins) and hydrolyzable tannins (ellagic acid, gallic acids, pedunculagin, punicalin and punicalagin), all of them were proven. The amount of total phenolic content of pomegranate peels is between 18 and 510 mg/g dry matter varying on the species, extraction solvents and extraction methods (Mo *et al*., 2022).

Pomegranate Seeds are rich in punicic acid (95 %), sterols and ellagic acid (Jauhar *et al*., 2018).The ethanolic seeds extract of *Punica granatum* L. has a total phenolic content of 28.01 ± 11,53 µg GAE/mg of dry weight (Mouas *et al*., 2021). The aqueous and methanolic extracts both have 7.94 ± 1.25 and 11.84 ± 1.92 mg GAE/g of dry weight, successively (Elfalleh *et al*., 2012). The characteristic color of pomegranate juice is due to the presence of polyphenols such as anthocyanins and flavonoids. Other biocompounds with significant presence in the juice are hydroxycinnamic acids (caffeic acid, chlorogenic acid, p-cumaric acid), catechins, proanthocyanidins, quercetin and elagitannins such as punicalin and punicalagina (Coronado-Reyes *et al*., 2022). The total polyphenolic content of the natural pomegranate juice is 7 436.93 ± 76.60 mg GAE/L (Dżugan *et al*., 2017).

3.3. Biological activities

All the pomegranate fruit parts (peels, seeds and juice) are proven to have an antioxidant effect through their radical scavenging activity (DPPH, ABTS and iron chelating activity). It also shown that the regular consumption of pomegranate fruit increases the glutathione (GSH) levels significantly, which is a natural antioxidant present in our bodies (Loizzo *et al*., 2019). Pomegranate juice has been shown to significantly lower systolic blood pressure. It contains potassium, which can help avoid artery stiffness and atherosclerosis. It increases blood flow to the heart and lowers the risk of heart attack.

Pomegranate juice is also high in antioxidants such as anthocyanins and tannins, which may aid to prevent cholesterol accumulation in arteries and so protect the heart (Syed *et al*.,

2018). Pomegranate peels also contain phytochemicals that have the ability to decrease the activity of the angiotensin converting enzyme (ACE), which is involved in the control of blood pressure in the renin-angiotensin system. In fact, a polyphenols-rich extract (mostly gallic acid, p-coumaric acid, cinnamic acid, caffeic acid and chlorogenic acid) is effective as an ACE inhibitor.

One therapeutic approach to decrease postprandial hyperglycemia is to suppress the production and/or absorption of glucose from the gastrointestinal tract through inhibition of α -glycosidase enzyme. In fact, the different parts of pomegranate fruit (peel, seed and juice) and its ethanol extracts showed a high inhibitory activity towards α-glycosidase enzyme which can modulate its activity (Mouas *et al*., 2021).

In breast cancer, pomegranate and its biocompounds are shown to exhibit an anti-aromatase and anti-estrogenic activities, to regulate the transforming growth factor beta (TGF- β)/Smads pathway, to exert anti-inflammatory effects through the reduction of pro-inflammatory cytokines/chemokines, downregulates the expression of the genes involved in the damage of DNA , downregulates the estrogen-responsive genes and disrupts estrogen receptor (ER) and Wnt/β-catenin signaling pathways (Moga *et al*., 2020).

The pomegranate juice also has an antiviral activity. The use of juice a concentration of 70° Brix of on MDCK (Madin-Darby canine kidney) cells for infection with the virus inhibit the proliferation significantly (Coronado-Reyes *et al*., 2020). Biocompounds found in pomegranate peels, such as punicalin, punicalagin, gallic acid and ellagic acid, have an important role in antiviral activity, modifying respiratory infections and influenza. The antiviral activities are mostly due to polyphenolic extracts inhibiting influenza virus RNA replication. Punicalagin at doses up to 40 $mg.mL^{-1}$ effectively inhibited viral RNA replication (Mo *et al*., 2022). Antimicrobial activity has also been confirmed using assays with dried Pomegranate seeds extract in a study with meat pâté, which demonstrated the extract's effectiveness against different strains of *Listeria monocytogenes* and liquid Pomegranate seeds extract against *Salmonella enterica* and plant pathogenic fungi such as *Penicillium italicum*, *Botrytis cinerea* and *Rhizopus stolonifer* (Melgarejo-Sánchez *et al*., 2021).

In developmental biology, cellular differentiation is the process through which a less specialized cell becomes a more specialized cell type. Pomegranate fruit has been demonstrated to induce the differentiation of osteoblastic MC3T3-E1 cells and influence their function. The seed has been demonstrated to boost keratinocyte proliferation in monolayer culture without affecting fibroblast function, facilitating skin healing and promoting dermal and epidermal regeneration. Flavonoid-rich fractions of fermented juice and aqueous pomegranate pericarp extracts are strong promoters of differentiation in human HL-60

promyelocytic leukemia cells, as measured by nitro blue tetrazolium reducing activity, nonspecific esterase activity, specific esterase activity and phagocytic activity (Rahimi *et al*., 2012).

3.4. *Punica granatum* L. and traditional medicine

Pomegranate has been consumed by people from all over the world since ancient times. It grows as a sign of life, permanence, happiness, fertility, knowledge and immortality. Dried pomegranate peel extract, bark and flower infusions were used to cure diarrhea, intestinal worms, nose hemorrhage and ulcers in ancient Indian culture. To soothe sore throats, it was frequently gargled in liquid form. Pomegranate has been used in dentistry to alleviate bleeding gums and plaque in periodontitis patients.

Pomegranate was used to treat jaundice, spleen issues, heart choking and severe coughing in the Islamic tradition. It also helps to smooth the voice and clean the face. "Pomegranate flower cuts the bleeding and strengthens the gums, Pomegranate powder treats the old wounds, Pomegranate bark is useful for treating inflammation, liver, cough and sore" as Abu-Ali Sina remarked (Ge *et al*., 2021).

Several infusions or decoctions of the plant flowers have been used in traditional medicine to treat vaginal discharge and pancreatic inflammation. This extract, together with pomegranate peel, is commonly gurgled to reduce pancreas pain. *Punica granatum* L. fruit juice is indicated to treat gallbladder disorders.

The peel of the fruit and the bark of the pomegranate tree were used in ancient Ayurvedic traditional medicine to treat diarrhea, dysentery and intestinal parasites, nose bleeds and gum bleeding, skin tone and hemorrhoids. Pomegranate juice was used as an eye drop to decrease the progression of cataracts. Pomegranate seeds and rind were also used as a vaginal suppository for contraception and abortifacient purposes (Alshammari *et al*, 2017).

4. Oxidative stress

Many of our bodies' basic biological activities generate dangerous chemicals known as free radicals. Our body's natural antioxidant system normally destroys free radicals. If this system fails to function properly, oxidative stress arises and free radicals cause a damaging chain reaction in the body. Sies defined oxidative stress for the first time in 1985 as an imbalance between oxidants and antioxidants favoring the oxidants, resulting in a disturbance of redox signaling and regulation and/or molecular damage (Sies, 1985). Moreover, oxidative stress is caused by an imbalance between the generation of reactive species such as reactive oxygen species (ROS) and reactive nitrogen species (RNS) and an organism's decreased capacity to eliminate these reactive intermediates or repair the damage they cause, which can

lead to cell and tissue damage as well as disruption of signaling pathways (Hameister *et al*., 2020).

4.1. Forms of reactive species

In physiological normal conditions, the role of ROS in all types of macromolecules, including proteins, lipids and DNA, is mainly directed toward redox signaling rather than oxidative destruction. The reactive species ROS/RNS comprise both free radicals, containing one or more unpaired electrons, such as superoxide (O2$^{\bullet}$), hydroxyl-($^{\bullet}$OH), nitric oxide, alkoxyl (RO$^{\bullet}$) or peroxyl-(ROO$^{\bullet}$) radicals, along with non-radical ROS, which include hydrogen peroxide (H_2O_2), organic hydroperoxides (ROOH), ($ONOO^-$) Peroxynitrite and hypochloride (HOCl) (Table 10) (Di Meo *et al*., 2016).

Table 10. The radical and non-radical ROS/RNS species (Di Meo *et al*., 2016).

Radical species	$O2^{\bullet-}$ Superoxide anion $^{\bullet}$OH Hydroxyl NO$^{\bullet}$ Nitric oxide $NO_2^{\bullet}$Nitrogen dioxide
Non-radical species	H_2O_2 Hydrogen peroxide HOCl Hypochlorous acid $ONOO^-$Peroxynitrite

4.2. Endogenous ROS/RNS sources

The seven isoforms of the growing family of transmembrane NADPH oxidases (NOXs) are among the cytosolic enzyme systems that produce ROS. An electron from NADPH is transferred to a FAD cofactor by the cytosolic domains of NOX. The electron is then transferred to a haem group, which donates it to O_2 on the membrane's extracellular side, creating $O_2^{\bullet-}$. Diverse NADPH oxidases can cause various cellular changes with significantly different biological effects depending on the unique NADPH oxidase expressed in various cells. The specificity in ROS production and its impact on typical physiological signaling and homeostasis are demonstrated by the NADPH oxidase family of enzymes (Krumova and Cosa, 2016).

Mitochondria is known to quickly produce cytotoxic species such $O_2^{\bullet-}$ and H_2O_2. There are a number of elements whose activity results in the formation of ROS, including complex III and mitochondrial complex I (NADH dehydrogenase). Molecular oxygen is converted into $O_2^{\bullet-}$ via the flavoprotein portion of NADH dehydrogenase; however, $O_2^{-\bullet-}$ generation may also

be boosted by the backward electron flow (from complex III to complex I) due to a lack of NAD+ linked substrate, which is controlled by ATP hydrolysis. In order to reduce the cytochrome b complex, which actively reduces molecular oxygen into $O_2^{\bullet-}$, fully reduced ubiquinone (complex III) donates its electron to cytochrome C1. This causes the backward production of semiquinone radicals, which later reduce $O_2^{\bullet-}$ into hydrogen peroxide (H_2O_2) via SOD dismutation.

The enzyme complexes found inside the mitochondrial matrix are likewise susceptible to the production of ROS. ROS are generated either directly or indirectly by aconitase and l-Galactono-gama-lactone dehydrogenase (GAL). MnSOD and APX are the other two most significant enzymes that facilitate the conversion of $O2^{\bullet-}$ into hydrogen peroxides. When reduced Fe and Cu combine with hydrogen peroxide (H_2O_2), highly hazardous hydroxyl bioradicals are produced that easily pass through cell membranes. ROS levels in mitochondria are maintained by the matrix alternate oxidase (AOX) level (Mandal *et al*., 2022).

A number of intracellular enzymes, such as the flavoenzyme in the endoplasmic reticulum, xanthine oxidase, cyclo-oxygenases, cytochrome p450 enzymes, lipoxygenases, oxidases for polyamines and amino acids and nitric oxide synthases that produce oxidants as part of their normal enzymatic function, are other cellular sources of ROS production. In a process known as the Fenton reaction, free copper ions or iron ions that are released from iron-sulfur clusters, haem groups or metal-storage proteins can change $O_2^{\bullet-}$ and/or H_2O_2 to $OH^{\bullet}$ (Di Meo *et al.*, 2016).

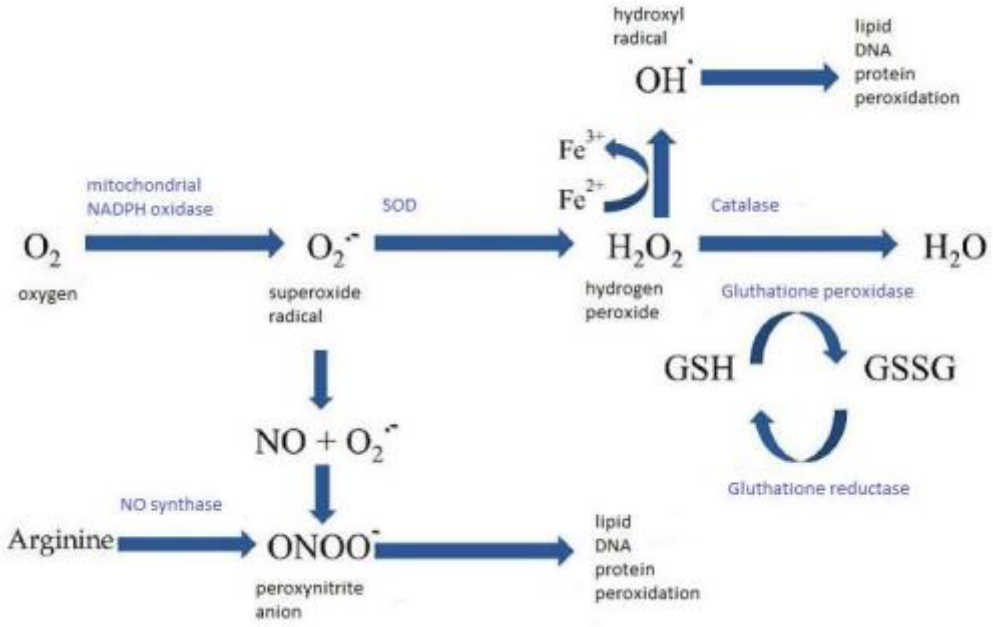

Figure 4. Generation of reactive oxygen and nitrogen species (Rifler, 2018).

Another potential source of cellular singlet oxygen is the oxidation of halide ions by the phagocyte enzyme myeloperoxidase and the action of Phox (NOX of phagocytes, primarily in neutrophils and macrophages), which is activated in inflammatory regions (MPO). Additionally, enzymes and nonenzymatic chemical processes quickly transform superoxide and NO into reactive, nonradical species, such as singlet oxygen, hydrogen peroxide or peroxynitrite ($ONOO_2$) (Kurutas, 2016). (Figure 4) above shows the different reactions involved in ROS production.

Enzymatic routes are the primary means of liberating endogenous NO. Nitric oxide synthase (NOS) catalyzes the enzymatic synthesis of NO. It is created when reduced nicotinamide adenine dinucleotide phosphate (NADPH), oxygen and the amino acid arginine react with NOS. Endothelial NOS (eNOS), neuronal NOS (nNOS) and inducible NOS (iNOS) are the three isoforms of NOS. While the intracellular Ca^{2+}/calmodulin tandem regulates the activity of eNOS and nNOS, which are constitutive enzymes, iNOS is an enzyme that is induced under many conditions and requires the involvement of the gene transcription apparatus. In response to pro-inflammatory mediators, macrophages and other tissues express these Ca^{2+} independent NOS (Alhasawi *et al*., 2019).

4.3. Exogenous ROS/RNS sources

Tobacco, alcohol, medications (cyclosporine, tacrolimus, gentamycin and bleomycin), industrial solvents, cooking (smoked meat, waste oil and fat), radiation X-rays, γ-rays, ultraviolet A, visible light in the presence of a sensitizer, chemical reagents such as heavy or transition metals (Cd, Hg, Pb, As, metal ions such as Fe^{2+} and Cu^{+}), HONOO, ozone, N_2O_2, deoxyosones, ketamine, H_2O_2, HOCl and HOBr, environmental pollutants (aromatic hydrocarbons, pesticides, polychlorinated biphenyls, dioxins and many others), microbial infections, drugs and their metabolites are examples of exogenous sources of reactive species, which the body metabolizes into free radicals (Martemucci *et al*., 2022).

4.4. Reactive species molecular targets

These extremely reactive species have the potential to harm major types of biological components, including nucleic acids, lipids and proteins.

4.4.1. Deoxyribonucleic acid (DNA)

Guanine is the most common base affected by oxidative DNA damage. Because of its low oxidation potential, it is particularly vulnerable to singlet oxygen, resulting in the creation of (8-oxo-7,8-dihydroguanine). Guanine oxidation may also occur in the nucleotide pool. During replication, 8-oxoG can be integrated into DNA. 8-oxoG may affect cellular activity

and cause genomic instability (Poetsch, 2020).

ROS may cause DNA damage in a variety of ways, including oxidized purines and pyrimidines, single-strand breaks (SSBs), double-strand breaks (DSBs) and abasic (AP; apurinic/apyrimidinic) sites. The AP-site appears often in malignant tumors and/or after ionizing radiation exposure and it is an intermediary and/or result of several DNA damage processing pathways. AP sites are potentially mutagenic and fatal lesions that can obstruct important biological processes including DNA replication and transcription. SSBs are formed when AP sites are cleaved by AP-endonucleases or AP-lyases and they can be transformed into DSBs during DNA replication (Stefanou *et al*., 2022).

Deoxyribose and nitrogenous bases react with ROS in DNA, leading to substantial oxidative reactions that cause mutations, carcinogenesis, apoptosis, necrosis and genetic illnesses may result from this. The rupture of nucleosomes, which are essential for the order of DNA within chromosomes, forces DNA to fragment, which interferes with the compaction and folding of DNA within chromatin that is crucial for the control of gene transcription, therefore changes to its functional characteristics may cause mutagenesis.

RNS, particularly peroxynitrite, react with guanine to form nitrative and oxidative DNA lesions such as 8-nitroguanine and 8-oxodeoxyguanosine. The formed 8-nitroguanine is not stable and can be eliminated spontaneously, resulting in an apurinic site; on the other hand, adenine can pair with 8-nitroguanine during DNA synthesis, which results in G-T transversions. Thus, 8-Nitroguanine is a carcinogenic DNA lesion implicated in carcinogenesis (Martemucci *et al*., 2022).

4.4.2. Ribonucleic acid (RNA)

Although 8-hydroxyguanosine is the only oxidized base that has been identified in RNA, both $HO^{\bullet}$ and H_2O_2 can damage RNA. This suggests that RNA is also subject to the same oxidative alterations as DNA. Guanine can react with $HO^{\bullet}$ and then undergo oxidation to generate 8-hydroxyguanosine, or it can react with singlet oxygen and then undergo reduction. This oxidative alteration is the most harmful, because 8-hydroxyguanosine has the capacity to wrongly couple with adenine in RNA with similar or greater efficiency than it does with cytosine and produces mutations at the transcriptional level. It has been shown that RNS affect RNA the same way as ROS (Petřivalský and Luhová, 2020).

4.4.3. Lipids

Free radicals (e.g., hydrogen peroxide (H_2O_2), superoxide ($O_2^{\bullet-}$) and the hydroxyl radical ($^{\bullet}OH$) attack lipids containing carbon-carbon double bonds, particularly polyunsaturated fatty acids (PUFAs) of the plasma membrane in a biochemical process

known as lipid peroxidation (Chen *et al*., 2021). Lipid peroxidation comprises in three major steps: start, chain propagation and termination. An initiation reaction will results in 200-400 propagation cycles, increasing unsaturated aldehydes (4-hydroxy-2-nonenal and acrolein), dialdehydes (malondialdehyde and glyoxal) and ketoaldehydes (4-oxo-2-nonenal and isoketals). Some of them are super reactive and are considered as secondary harmful messengers, which magnify oxidative damage. The most known aldehydes are 4-hydroxynonenal (4-HNE) and malondialdehyde (MDA). Peroxidation of lipids can disrupt membrane construction, resulting in changes in fluidity and permeability, changes in ion transport and inhibition of metabolic activities. Disorders in the mitochondria caused by lipid peroxidation can lead to increased ROS production (Catalá and Díaz, 2017).

4.4.4. Proteins

Protein oxidation is defined as the covalent alteration of a protein brought on by indirect reaction with secondary oxidative stress byproducts or by direct interactions with reactive oxygen species (ROS). Protein fragmentation or protein-protein cross-linkages can emerge from ROS-induced oxidation of amino acid side chains and protein backbones. Although all amino acids can undergo oxidative modification, cysteine and methionine are more vulnerable because of the sulfur group's high reactivity in those amino acids. Proteins' physical and chemical characteristics, such as conformation, structure, solubility, susceptibility to proteolysis and enzyme activity, might alter as a result of oxidative changes (Zhang *et al*., 2013).

Reactive oxygen species (ROS) and reactive nitrogen species (RNS), which are capable of oxidizing or altering proteins, can be produced in greater quantities by stressed cells. Two broad kinds of protein oxidation can be distinguished. While one is reversible, the other one is irreversible. Proteolysis and protein aggregation are frequently caused by irreversible oxidation. Protein carbonyls, nitrotyrosine and sulfonic acids are produced as a result of this type of oxidation (Yan, 2014).

Through oxidation/nitration pathways, peroxynitrite derivatives can alter proteins, enabling changes in protein function with biological relevance by developing new functions, protein aggregation, turnover, signaling and immunological processes. Peroxynitrite is a chemical that plays a role in cell signaling pathways. Some peroxynitrite-modified proteins have also been shown to be immunogenic and have been linked to the etiology of a number of disorders. Tyrosine-nitrated proteins are of particular importance when it comes to the molecular side effects of peroxynitrite. Many processes, particularly those connected to oxidative stress, such inflammatory, neurological and cardiovascular illnesses have been

linked to nitrate tyrosine residues (Pérez de la Lastra *et al*., 2022).

4.5. Oxidative stress related diseases

4.5.1. Cardiovascular diseases (CVDs)

The primary cause of morbidity and mortality in the elderly is cardiovascular disease (CVDs). In fact, as people age, their ability to withstand oxidative stress decreases due to lower levels of the antioxidant enzymes GSH-Px and SOD, which promotes the onset of CV changes. It has been demonstrated over time that oxidatively modified LDL (oxLDL) and increased arterial stiffness are significantly correlated. Because of the prooxidant and proinflammatory conditions that are characteristic of elderly persons, the increase in oxLDL with aging may intensify LDL atherogenicity.

The primary causes of endothelial dysfunction are inflammation and oxidative stress. The inactivation of nitric oxide NO by a number of oxidative enzyme systems, including NADPH oxidase, xanthine oxidase, cyclooxygenases, lipoxygenases, myeloperoxidases, cytochrome P450 monooxygenase, uncoupled NOS and peroxidases, represents a crucial mechanism causing endothelial dysfunction by increasing the level of superoxide anion ($O_2^{\bullet-}$) (Senoner and Dichtl, 2019).

4.5.2. Diabetes

Increasing mitochondrial oxygen consumption, impairing mitochondrial function or activating the evolutionarily conserved ROS-producing enzyme nicotinamide adenine nucleotide phosphate oxidase (NOX) are some of the mechanisms by which chronic hyperglycemia causes ROS overproduction. Oxidative stress, which causes dysfunctions in β-cells and insulin resistance, is a significant contributor to diabetes mellitus. It is caused by either increased ROS production or decreased endogenous antioxidant activity or both. Furthermore, Diabetes complications, which cause both death and long-term disability in patients, are strongly correlated with oxidative stress (Zhang *et al*., 2020).

Beta-cell activity is compromised by oxidative stress in a number of different molecular ways. It significantly lowers the amount of insulin produced, hinders the insertion of proinsulin vesicles into the plasma membrane and lessens their exocytosis in response to blood glucose levels. It can also cause pancreatic cells to undergo apoptosis, which results in cell death and the loss of beta cells (Yaribeygi *et al*., 2020).

4.5.3. Cancer

Reactive oxygen species (ROS) and free radicals are produced in large quantities as a result of oxidative stress, which damages the structure of DNA molecules, proteins and

increases lipid peroxidation. Numerous factors, ranging from genetics to an unbalanced lifestyle, can disrupt oxidative homeostasis. Numerous chemicals are created during these harmful activities, including malondialdehyde, 4-hydroxy-2-nonenal and 8-OH deoxyguanosine, which contribute to increasing the risk of mutagenesis and are strongly connected with carcinogenesis (Fatima Zahra *et al*., 2021).

The release of a lot of ROS and RNS by cells that are chronically inflamed attracts more immune cells that are already activated, which amplifies dysregulated processes and finally results in a preneoplastic situation. Unrepairable oxidative damage to nucleic acids, lipids and proteins may result in genetic and/or epigenetic changes that disrupt the regulation of oncogenes and tumor suppressor genes if the level of cellular ROS/RNS production is high enough to overwhelm the endogenous antioxidant response.

The failure to stop these processes could lead to genetic and epigenetic alterations that trigger the start of carcinogenesis. In addition, ROS change the expression of the p53 suppressor gene, which is essential for apoptosis. As a result, oxidative stress alters gene expression and influences cell growth and apoptosis, which is a key factor in the development of tumors (Jelic *et al*., 2021).

4.5.4. Other Oxidative stress related diseases

Oxidative stress has also been connected to a wide range of unfavorable health issues, including aging, immune function issues, allergies and neurodegenerative and inflammatory diseases (Figure 5) (Fleming and Luo, 2021).

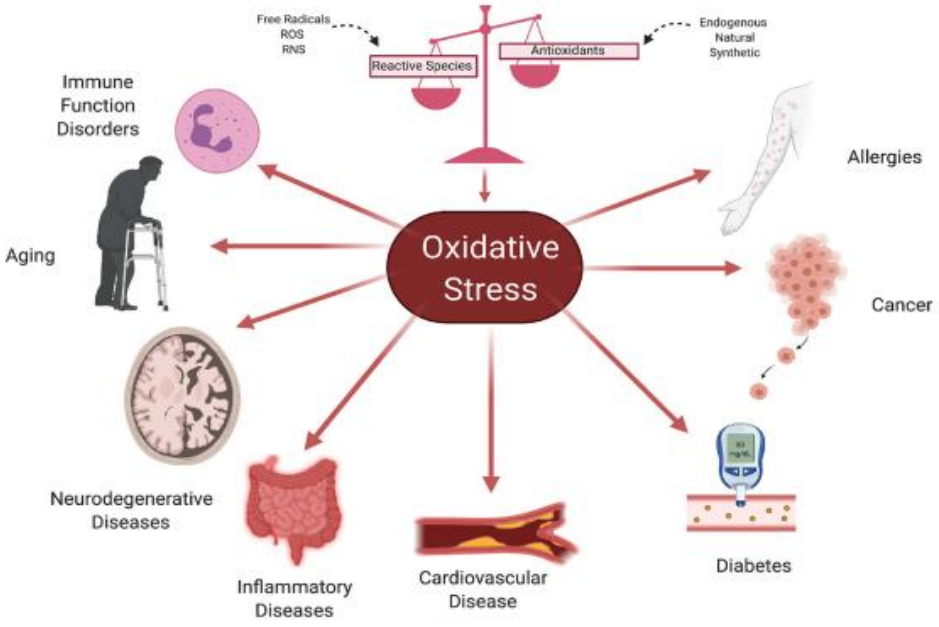

Figure 5. Oxidative stress related diseases (Fleming and Luo, 2021).

4.6. Antioxidants

Antioxidants are enzymatic or non-enzymatic substances that control the level of reactive species in order to neutralize them and minimize oxidative damage.

4.6.1. Enzymatic antioxidants

4.6.1.1. Superoxide dismutases (SOD)

(SOD) is a metalloprotein that serves as one of the first lines of defense against the harmful effects of free radicals. As a result, SODs are able to remove the superoxide anion $O_2^{\bullet-}$ by a disproportionation reaction, creating one molecule of oxygen and one molecule of hydrogen peroxide H_2O_2 from two superoxides. Three isoenzymes are known to exist in humans: extracellular SOD3 (Cu/Zn-SOD), mitochondrial SOD2 (Mn-SOD) and cytosolic SOD1 (Cu/Zn-SOD) (Eddaikra A and Eddaikra N, 2020).

4.6.1.1. Glutathione peroxidase (GPx)

Glutathione peroxidase (GPx) transforms glutathione (GSH), which is a tripeptide composed of cysteine, glutamic acid and glycine into oxidized glutathione, also named glutathione disulfide, (GSSG). Throughout this process it converts lipid peroxides to their corresponding alcohols and hydrogen peroxides (H_2O_2) to water, primarily in the mitochondria and occasionally in the cytoplasm. Most of the time, selenium, a micronutrient cofactor, is required for its function. Humans have at least eight GPx enzymes, numbered GPx1 through GPx8. The most prevalent selenoperoxidase is GPx1, which is found almost practically in every cell (Ighodaro and Akinloye, 2018).

4.6.1.2. Catalase (CAT)

Catalase is found nearly in all aerobic organisms. It is a tetrameric protein localized in the peroxisomes. Two hydrogen peroxide molecules (H_2O_2) are broken down by catalase into one oxygen molecule and two molecules of water. Among bacteria that express CAT are *H. pylori* and enterobacteriaceae family of bacteria, including *Escherichia coli* and *Salmonella*, produce CAT to thwart against host defenses and persist inside of it (Gagnière and Bonnet, 2017).

4.6.2. Non-enzymatic antioxidants

Non-enzymatic antioxidants can either have endogenous or exogenous sources. Major non-enzymatic antioxidants, include metal binding proteins, glutathione, uric acid, melatonin, bilirubin and polyamines. As well as dietary antioxidants such as vitamin E, vitamin C, carotenoids, some minerals (zinc, manganese, copper and selenium) and polyphenols

(flavonoids, phenolic acids, stilbenes and lignans) (Achike and Murugan, 2020). In this section we mention the main non-enzymatic antioxidants.

4.6.2.1. Glutathione

Glutathione (GSH) is found in all living organisms mainly in the nucleus, mitochondria and cytoplasm and it consists of three amino acids: glycine, cysteine and glutamic acid. It has several redox forms, among which the most predominant is the reduced glutathione (GSH) and oxidized glutathione (GSSG). (GSH) engages in a number of defense mechanisms against ROS. In which, the thiol group gives (GSH) the power to protect other thiol groups in proteins against oxidative damage. These thiol functions interact with metal ions, take a part in oxidation reactions by being oxidized themselves to sulfonic acids and make thiol radicals and disulfides (Moussa *et al*., 2019). Through its antioxidant properties, (GSH) lowers ROS in both enzymatic and non-enzymatic processes. It restores other oxidized antioxidants like vitamin C and vitamin E, helps to maintain the reduced state of protein sulfhydryl moieties and repairs lipids harmed by peroxidation processes (Mironczuk-Chodakowska *et al*., 2018).

4.6.2.2. Uric acid

Circulating uric acid (UA) in human plasma functions as an antioxidant through many pathways. It reacts with a variety of oxidants, including hydrogen radicals, superoxide anions and especially peroxynitrite. (UA) is also a powerful scavenger of peroxyl radicals ($ROO^{\cdot}$). (UA) is far more significant as a water-soluble antioxidant in human plasma than ascorbic acid. The iron chelator UA lowers the oxidative stress reaction that is mediated by iron. It has the capacity to remove reactive oxygen species (ROS) and guard against lipid oxidation and further hemolysis to preserve the erythrocyte membrane (Lin *et al*., 2019).

4.6.2.3. Vitamin C

Vitamin C (ascorbic acid) is an essential water-soluble antioxidant that can function both inside and outside of cells. As a result of its capacity to donate a hydrogen atom and create the relatively stable ascorbyl-free radical, vitamin C has been demonstrated to be a potent scavenger against oxygen and nitrogen oxide species, including the superoxide radical ion, hydrogen peroxide, the hydroxyl radical and singlet oxygen. This feature of vitamin C is crucial for protecting cellular components from harm caused by free radicals. In fact, by reducing tocopheroxyl radicals, vitamin C is efficient in rebuilding the antioxidant form of vitamin E. By using this method, the cell's membranes and other compartments are shielded from deleterious effects brought on by free radicals (Kazmierczak-Baranska *et al*., 2020).

4.6.2.4. Vitamin E

Vitamin E or tocopherol is a fat-soluble antioxidant. The main way that α-tocopherol works is as a free radical scavenger. By binding to free radicals, it prevents oxidative damage to biological components. Carbon-centered radicals in the presence of oxygen produce peroxyl radicals during lipid peroxidation, which react with vitamin E 1,000 times more quickly than they do with PUFAs, stopping the lipid peroxidation chain reaction. However, without vitamin E, peroxyl radicals easily oxidize PUFAs to produce a hydroperoxide and a new carbon-centered radical, which spreads lipid peroxidation even more (Traber and Bruno, 2020).

4.6.2.5. Vitamin A

Vitamin A is a lipid-soluble antioxidant and the most prevalent kind of carotenoids. It can be found in the body as retinol, retinal and retinoic acid. The hydrophobic chain of polyene units, which can quench singlet oxygen, neutralize thiyl radicals and interact with and stabilize peroxyl radicals, confers the antioxidant action of vitamin A and carotenoids. In general, the ability to stabilize peroxyl radicals increases with polyene chain length.

Singlet oxygen scavenging activity can occur either, by physical transfer of the excitation energy from singlet oxygen to the carotenoid and then, dissipating it as heat, while preserving the carotenoid molecule. Or chemically, including the reaction between singlet oxygen and carotenoid pigments, which results in the irreparable destruction of the pigment. Additionally, it was shown that radical species directly oxidized vitamin A, producing a 5,6-retinoid epoxide, hence, stabilizing the lipid radical (Stahl and Sies, 2003).

4.6.2.6. Trace minerals

Trace minerals (TMs) are involved in a great range of biological processes either directly or indirectly, making them essential for the human body. (Zn) functions as cofactor for antioxidant enzymes to preserve the body from oxygen free radicals. Thus, Cu and Zn are components of the SOD enzyme. Moreover, the immunological response, inflammation and oxidative stress in the human body are correlated with the plasma levels of these minerals. (Se) is a cofactor of GPx that is included in various selenoproteins that protect us from the free radicals generated in cellular metabolism. In contrast, other TMs like iron (Fe), cadmium (Cd) or lead (Pb) enable the generation of oxygen free radicals. Thus, behaving as cellular pro-oxidants (Barrientos *et al*., 2020).

4.6.2.7. Polyphenols

Polyphenols are secondary plant metabolites that often occur in a plant's bark, root, leaf,

shell and fruit. They are distinguished by having more than one phenolic hydroxyl group. Out of the hundreds of polyphenols that occur in human's diet, including those found in fruits, herb medicines, red wine, tea and vegetables, over 8,000 have been recorded from plants. Catechins, tannins, lignans, stilbenes, phenolic acids, flavonoids and phenolic acids are the main types of polyphenols (Rudrapal *et al*., 2022).

According to their reactivity with radicals and to their effective concentrations at the reaction site, phenolic substances can reduce the formation of ROS. Every polyphenol has at least one -OH group joined to an aromatic ring and it primarily scavenges free radicals by transferring H-atom from its -OH group(s) to the free radical. In addition, polyphenols, which are primarily flavonoids and contain hydroxyl groups at the 3, 5, 3' and 4' positions as well as carbonyl at the 4 position, have three locations where metal complexes can form. Thus they are qualified as chelators of pro-oxidant metals (Costa *et al*., 2021).

Material and Methods

1. Materials

1.1. Chemicals and equipment

The chemicals used in the study as well as their sources are listed in the (table 11) below:

Table 11. The chemicals used in the study and their sources

Name of chemical	Source
Methanol (99.8%) Ethanol (99.8%) Folin-Ciocalteu reagent Gallic acid Na_3CO_3 (Sodium carbonate) $AlCl_3$ (Trichloro aluminum) Rutin Vanillin Catechin KCl (Potassium chloride) $C_2H_3NaO_2$ (Sodium acetate) DPPH (2,2-diphenyl-1-picrylhydrazyl) BHT (Butylated hydroxytoluene) (2,6-Di-*tert*-butyl-4-methylphenol) ABTS (2,2′- azinobis-3- ethylbenzothiazoline-6- sulfonic acid) $K_2S_2O_8$ (Potassium persulfate) $Na_2HPO_47H_2O$ Sodium phosphate dibasic heptahydrate $NaH_2PO_4H_2O$ Sodium Phosphate Monobasic Monohydrate $K_3Fe(CN)_6$ (Potassium ferricyanide) (TCA) Trichloroacetic acid $FeCl_3$ (Ferric chloride) $FeSO_4$ (Ferrous sulfate) Ferrozine (2,4,6-Tris-2-pyridyl-s-triazine) Na_2EDTA (Ethylenediaminetetraacetic Acid, Disodium Salt) β-carotene Tween 40 Linoleic acid Chloroform KBr (Potassium bromide) NaCl (Sodium chloride)	Sigma Aldrich (MO, USA)
NaOH (Sodium hydroxide) 98%,	Cheminova
HCl (Hydrochloric Acid) 37%	Biochem
Lead nitrate $Pb(NO_3)_2$	Prolabo (France)
Deionized water (20 $\mu s.cm^{-1}$)	ENPEC (National Company of Electrochemical Products, Algeria)

The pH measurement was determined by a glass electrode (Hanna HI 9321). Atomic absorption spectrophotometer (AAS) (PerkinElmer PinAAcle 900H model) working with an air acetylene flame was used to estimate the content of lead in the tested solutions. FT-IR spectrophotometer (SHIMADZU FTIR – 8400S), was used to identify the functional groups of the biomasses in native and binding sorbate-sorbent states.

1.2. Plant material

Two pomegranate peels, red and yellow, used in this study were prepared from *Punica granatum L*. fruit purchased from the local market of Setif (East part of Algeria). In the laboratory, the fruits were washed with tap water and then with distilled water to ensure the removal of dirt or unwanted matter. The peels were obtained by extraction of the juice from the arils and discarding their seeds and then dried in the oven at 40°C for 72 hours until a constant weight was obtained. The dried peels were first grounded to a fine powder and then sieved to obtain a particle size of 500 µm. The raw peels powder was kept in sealed bottles away from the dark at room temperature until their use for extraction and in the adsorption experiments.

1.3. Preparation of stock solution

Stock solution (1000 $mg.L^{-1}$) of lead was prepared by dissolving lead nitrate $Pb(NO_3)_2$ in deionized water. The working solutions were prepared by diluting the stock solution to appropriate volumes. The initial pH value of the solutions was adjusted using 0.1 M sodium hydroxide NaOH or 0.1 M hydrochloric acid HCl. A standard curve of lead was assessed from the stock solution (Figure 6).

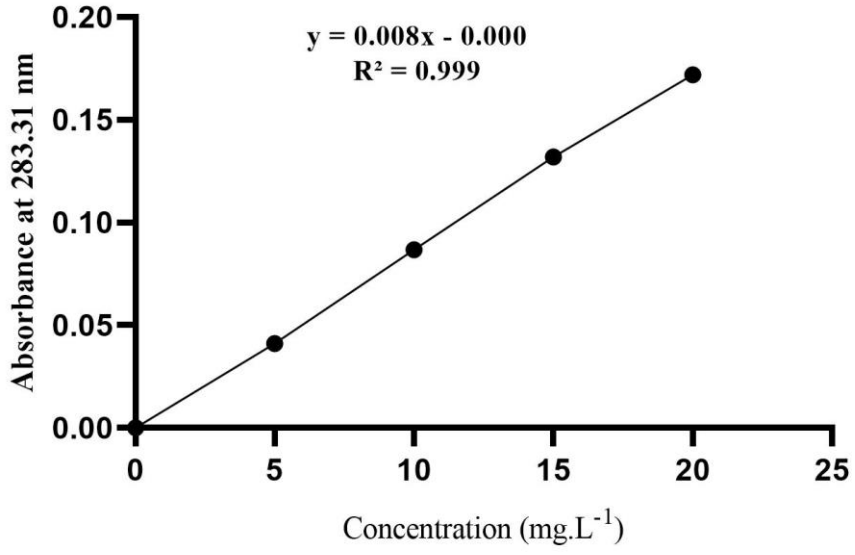

Figure 6. Standard curve of lead with atomic absorption spectrophotometer.

2. Methods

2.1. Adsorption studies

2.1.1. Characterization of the adsorbents

The dried powder of the red (RPP) and yellow (YPP) pomegranate peels (*Punica granatum* L.) with a particle size of 500 µm were used throughout the adsorption experiments.

2.1.1.1. The equilibrium pH of the adsorbent

The contact pH of the adsorbent was established by mixing 0.25 g of the pomegranate peel powder in contact with 25 mL of deionized water. The whole was kept under agitation for 24 h. After 24 h the suspension was filterd and the pH of the filtrate was determined using a pH meter (Tarbaoui *et al*., 2016; Ben-Ali *et al*., 2017).

2.1.1.2. Point of zero charge (pH_{pzc})

The point of zero charge pH_{pzc} is the pH at which the sorbent surface charge becomes zero. At this pH, the cumulative charge of the positive and negative surface sites is equal. The pH_{pzc} controls the behavior and the ionization of functional groups and their interactions with metal species in solution. At a solution with a pH value greater than pH_{pzc} of the adsorbent, the adsorbent surface is negatively charged and may interact with positively charged metal species, whereas at a solution with a pH value lower than the pH_{pzc} of the adsorbent the solid surface is positively charged and may interact with negatively charged metal species (Karna *et al*., 2018).

The point of zero charge was determined using the salt addition method. In a series of 50 mL conical flasks 25 mL of sodium chloride NaCl 0.01 M was added in each flask. The initial pH (pH_i) was adjusted between 2 to 12 using either NaOH 0.1 M or HCl 0.1 M. After adjusting the pH, 25 mg of the peel's powder (500 µm) was added to every flask. The samples were left under agitation for 24 h at room temperature. After 24 hours the final pH of each sample was measured and marked as pH_f. The PZC was obtained from the plot of $\Delta pH = (pH_f - pH_i)$ against pH (Bounaas *et al*., 2019).

2.1.1.3. Surface functional groups

The concentration of acidic and basic sites on the pomegranate peel was determined according to Boehm via the acid-base titration method (Boehm, 1994). Thus, 0.25 g of the adsorbent was treated separately with 25 mL of 0.5 M NaOH and 0.5 M HCl in 50 mL conical flasks for the determination of acid and basic surface functional groups, respectively. The flasks were agitated at room temperature for 24 h. Subsequently, the suspensions were decanted and filtered. 10 mL of each filtrate were taken and the excess acid or base was back-

titrated with 0.5 M NaOH or HCl. The number of functional groups was calculated taking into account that the NaOH neutralizes the phenolic, lactonic and carboxylic groups and HCl neutralizes the basic groups. The total acidity and basicity was expressed in mmol.g^{-1} of adsorbent (Elhleli *et al*., 2020).

2.1.1.4. FT-IR analysis

The FT-IR spectrums of the red peels powder (RPP) and the yellow peels powder (YPP) before and after Pb(II) ions adsorption were taken to establish wavenumber changes in the functional groups of the adsorbents. The adsorbent-adsorbate bonds are usually due to the functional groups characteristic of the adsorbent surface. In order to identify the main chemical functions of the different pomegranate peels powder, we used Fourier transform infrared absorption spectroscopy which is based on radiations-matter interactions (Mohamed *et al*., 2017). The analysis was carried out on a (SHIMADZU FTIR – 8400S) type spectrometer at room temperature, using the technique of the pellet made from potassium bromide (KBr) by adding a mass of finely ground material respecting determined proportions. This action is followed by compression under high pressure. The FT-IR spectra of the KBr pellets were recorded between 400 and 4000 cm^{-1}.

2.1.2. Batch biosorption studies

The biosorption capacity of RPP and YPP towards lead ions (Pb^{2+}) was studied using batch method at room temperature (23-25°C). The working solutions were prepared by diluting the stock solution (1000 mg.L^{-1}) with deionized water to appropriate concentrations and their initial pH was adjusted using 0.1 M sodium hydroxide NaOH or 0.1 M hydrochloric acid HCl.

For this study, a fixed amount of the peels powder (0.0025 – 0.02 g) was placed in a 15 mL flasks containing 10 mL of the metallic lead solution in the range of 5 to 100 mg.L^{-1} at a given pH from 2 to 8 for a contact time varying from 15 to 120 min and then, the flasks were shaken in a rotary orbital shaker at 70 rpm. Finally, the flasks were centrifuged at 3000 rpm for 10 min followed by filtration through 0.45 µm filters. The experiments were carried out in triplicate. The residual concentration of metal ions in the filtrate was determined using atomic absorption spectrophotometer (Bounaas *et al*., 2019). The amount of metal ions sorbed by the biosorbent and the percentage of removal (R%) were calculated using the following equations:

$$Q_e = \frac{(C_e - C_0) \times V}{m} \qquad (1)$$

$$R\% = \frac{(C_0 - C_e) \times 100}{C_0} \qquad (2)$$

Where, Q_e is the amount of heavy metal ions adsorbed per unit weight of the biomass ($mg.g^{-1}$); V is the volume of solution (L); C_0 is the initial lead metal ion concentration ($mg.L^{-1}$); C_e is the equilibrium lead concentration ($mg.L^{-1}$) and m is the mass of the biosorbent (g).

2.1.2.1. Effect of different parameters on the adsorption process

Many factors relating to the biosorbent, the metal and the reaction medium can significantly affect the adsorption process. In this context, the influence of certain experimental parameters has been studied: the pH of the medium, the contact time, the biosorbent dose and the initial metal concentration.

2.1.2.1.1. pH effect

For studying the effect of pH on the adsorption process, we varied the pH values from 2 to 8, while fixing the other parameters. 0.01 g of biosorbent dose and 25 $mg.L^{-1}$ of initial lead concentration were used with a contact time of 60 minutes at ambient temperature.

2.1.2.1.2. Time effect

For studying the time effect on the adsorption process, we varied the contact time from 15 to 120 minutes, while fixing the other parameters. 0.01 g of biosorbent dose and 25 $mg.L^{-1}$ of initial lead concentration were used at pH (5.5) and at ambient temperature.

2.1.2.1.3. Biosorbent dose effect

For studying the biosorbent dose effect on the adsorption process, we varied the doses from 0.0025 g to 0.02 g, while fixing the other parameters. A contact time of 60 minutes and 25 $mg.L^{-1}$ of initial lead concentration were used at pH (5.5) and at ambient temperature.

2.1.2.1.4. Initial metal concentration effect

For studying the effect of metal initial concentration on the adsorption process, we varied the lead initial concentration from 5 to 100 $mg.L^{-1}$, while fixing the other parameters. A contact time of 60 minutes and 0.01 g of biosorbent were used at pH (5.5) and at ambient temperature.

2.1.3. Modeling of adsorption isotherms

Our experimental data were adjusted to the models of Freundlich and Langmuir mentioned earlier (Langmuir, 1918; Freundlich, 1928), which are the most frequently used models in the literature. The adsorption of Pb(II) ions at optimum pH (6) and agitation time (60 min) was accomplished at different Pb(II) ions concentrations ranging from 10 to 4000 $mg.L^{-1}$ and a biosorbent dose of 0.02 g at ambient temperature. The linear form of Langmuir isotherm equation is:

$$\frac{C_e}{Q_e} = \frac{C_e}{Q_m} + \frac{1}{Q_m K_L}$$

Where Q_e is the equilibrium concentration of Pb(II) ions on the biosorbent ($mg.g^{-1}$), Q_m is the theoretical maximum adsorption capacity ($mg.g^{-1}$), C_e is the equilibrium concentration of Pb(II) ions ($mg.L^{-1}$) and K_L is the Langmuir constant ($L.mg^{-1}$). The values of Q_m and K_L constants and coefficients of regression for Langmuir isotherm are obtained from the plot of C_e/Q_e versus C_e. The linear form of Freundlich isotherm equation is:

$$\text{Log } Q_e = \text{Log } K_f + \frac{1}{n_f} \text{ Log } C_e$$

Where K_f is the Freundlich isotherm constant ($mg.g^{-1}(L.mg^{-1})^{1/n}$), nf is the adsorption intensity, C_e is the equilibrium concentration of Pb(II) ions ($mg.L^{-1}$) and Q_e is the equilibrium concentration of Pb(II) ions on the biosorbent ($mg.g^{-1}$). K_f and n_f are Freundlich constants and represent the adsorption capacity and the adsorption intensity, respectively. The values of K_f and n_f are obtained from the slope and intercept of the plot Log Q_e against Log C_e.

2.1.4. Modeling of adsorption kinetics

Two kinetic models such as the Lagergren-first order (Lagergren, 1898) and pseudo-second-order (Ho and Mckay, 1999) were used in this study to describe the adsorption kinetics (effect of contact time). As described earlier the adsorption of Pb(II) ions was assessed at pH (5.5) with a Pb(II) ions concentrations of 25 $mg.L^{-1}$ and a biosorbent dose of 0.01 g at ambient temperature. Adsorption capacity Q_t was determined using the following equation:

$$Q_t = (C_0 - C_t) \times \frac{V}{m}$$

Where Q_t is the amount of heavy metal ion adsorption per unit weight of the biomass at time t ($mg.g^{-1}$) , C_0 and C_t are Pb(II) ions concentrations ($mg.L^{-1}$) at initial time and time t, respectively, V is the volume of the solution (L) and m is the mass of biosorbent (g). The linear form of pseudo-first order model equation is:

$$\text{Log } (Q_e - Q_t) = \text{Log } Q_e - K_1 t$$

Q_e and Q_t represent the concentration of Pb(II) ions on the biosorbent at equilibrium and at time t, respectively ($mg.g^{-1}$), K_1 is the first-order model constant (min^{-1}). K_1 and Q_e are obtained from the slope and intercept of the plot Log (Q_e - Q_t) versus t. The linear form of pseudo-second order model equation is:

$$\frac{t}{Q_t} = \frac{1}{K_2 Q_e^2} + \frac{1}{Q_e} \times t$$

Where Q_e and Q_t are the concentration of Pb(II) ions on the biosorbent at equilibrium and at time t, respectively ($mg.g^{-1}$), K_2 is the second-order model constant ($g.mg^{-1}.min^{-1}$). K_2 and Q_e are obtained from the slope and intercept of the plot t/Q_t versus t.

2.1.5. Batch desorption studies

Desorption studies constitute a very interesting step in the process of depollution of wastewaters that allows to elucidate the nature of the interactions between sorbate and sorbent at interface and by the same way to evaluate the possibility to regenerate the adsorbent for its reuse, which has a positive impact in economic terms.

Desorption experiments were performed by using a simulated solution of Pb(II) at a concentration that mimics its real content in the wastewaters of ENPEC factory (National Company of Electrochemical Products, Setif Algeria) preliminarily determined by atomic spectrophotometry. For that, 10 mL of Pb(II) solution at 50 $mg.L^{-1}$; which represents approximately twice the amount in the effluents of this factory (22 $mg.L^{-1}$), were mixed with 0.02 g of biosorbent for 1 hour under stirring at ambient temperature. This procedure was repeated for 3 cycles in order to determine the actual adsorption capacity of the biomass under optimum conditions.

After each cycle, the collected supernatant was centrifuged at 3000 rpm for 10 min and filtrated on 0.45 µm filters, then the residual Pb(II) content was determined as previously mentioned for quantifying the amount of total lead adsorbed. Before carrying out the

desorption after the third cycle, the lead-loaded biosorbent was first washed with deionized water to remove the free non-adsorbed fraction, then 10 mL of the desorbing or the eluting solution of 1 M hydrochloric acid (HCl) was added and the mixture was stirred during 15, 30, 60 and 120 min. Finally, the amount of desorbed Pb(II) ions in the supernatant was measured as before to allow an evaluation of the desorption rate (Addala *et al*., 2018).

2.2. Plant extraction

At first, we proceeded to extract the polyphenolic compounds from the peels powder, at room temperature, by maceration in three different solvents: water, 50 % ethanol and 50 % methanol with a ratio of 1/10 (W/V) during 24 hours under agitation. The filtrates were collected by filtration under vacuum using fritted glass (G3) and then, the remaining solid phases were subjected to a second extraction under the same conditions for 12 hours to ensure complete recovery of polyphenols. The two filtrates of each extraction were combined and dried at 40°C until a dry residue was obtained that was kept away from the light and moisture.

2.3. Determination of phytochemical content

2.3.1. Determination of total polyphenols content (TPC)

The total polyphenols content (TPC) in the extracts of the peels was estimated by the Folin-Ciocalteu method according to (Li *et al*., 2007), which is based on the reduction in alkaline medium of the phosphotungstic acid ($H_3PW_{12}O_{40}$) and phosphomolybdic acid ($H_3PMo_{12}O_{40}$) of the Folin-Ciocalteu reagent by oxidizable groups of phenolic compounds into blue oxides of tungsten (W_8O_{23}) and molybdenum (Mo_8O_{23}). This reduction leads to the formation of a blue colored product which exhibits an absorption spectrum at 765 nm. The blue color intensity is proportional to the amount of polyphenols present in the sample which is expressed as gallic acid equivalent (GAE).

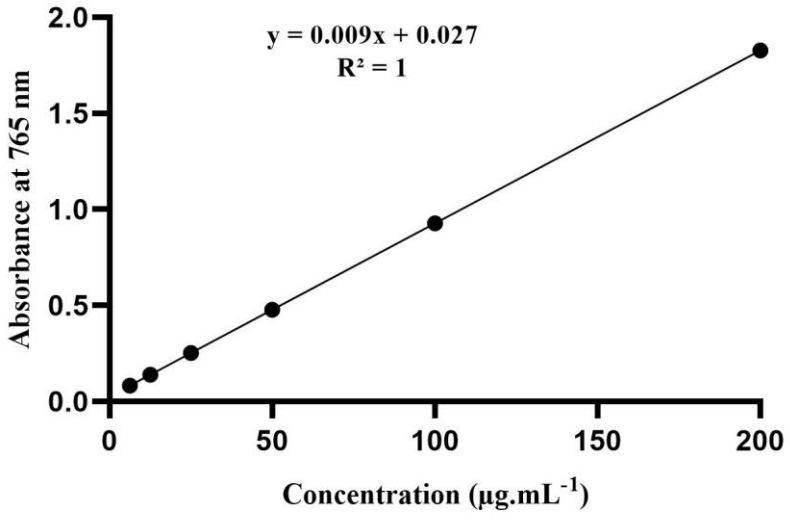

Figure 7. Standard curve of gallic acid used in the determination of (TPC).

The procedure goes as follow; 200 µL of the studied extract was mixed with 1 mL of Folin-Ciolcalteu reagent (10%), after 4 minutes a volume of 800 µl of sodium carbonate solution (75 $g.L^{-1}$) was added. The mixture was than incubated at room temperature away from the light for 120 minutes to react. After incubation, the absorbance was measured at 765 nm using UV-Vis spectrophotometer. A calibration curve using gallic acid as reference was established. The concentration of polyphenols was determined and the results were expressed in mg equivalents of gallic acid per g of extract (mg GAE/g) and mg equivalents of gallic acid per g of dry weight (mg GAE/g DW) (Figure 7).

2.3.2. Determination of total flavonoid content (TFC)

The Total flavonoids content of the extracts was determined using the Trichloro aluminum method described by (Turkoglu *et al*., 2007), which is based on that the aluminum chloride forms acid yellowish stable complexes with the (C-4) keto group and also with the (C-3) or (C-5) hydroxyl group of flavones and flavonols. Additionally, it creates acid labile complexes with the ortho-dihydroxyl groups in the (A-ring) or (B-ring) of flavonoids (Figure 8). The yellow color intensity is proportional to the amount of flavonoids present in the sample which is expressed as rutin equivalent (RE).

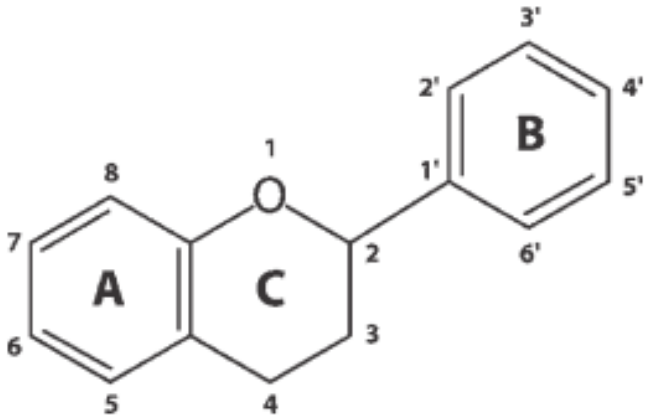

Figure 8. Basic flavonoid structure (Dwivedi *et al*., 2017).

The procedure goes as follow; 1 mL of each extract is mixed with 1 mL of the solution of $AlCl_3$ (2 % in methanol). After 30 min of reaction, the absorbance is determined at 430 nm against a blank. To determine the flavonoids concentration, rutin was used as a standard and the results were expressed as mg equivalent of rutin per g of extract (mg RE/g) (Figure 9).

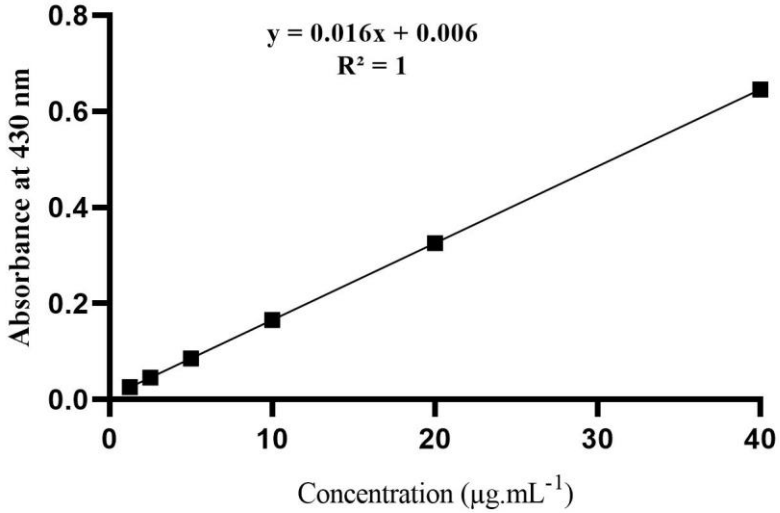

Figure 9. Standard curve of rutin used in the determination of (TFC).

2.3.3 Determination of condensed tannins content (CTC)

The condensed tannins content was determined by the vanillin method with hydrochloric acid (HCl) described by (Julkunen-Titto, 1985). This method depends on the reaction of vanillin with the terminal flavonoid group of condensed tannins in the presence of acid and the formation of red complexes, which is explained by the ability of tannins to transform into red-colored anthocyanidins by reaction with vanillin. The condensed tannins content was expressed as catechin equivalent (CE).

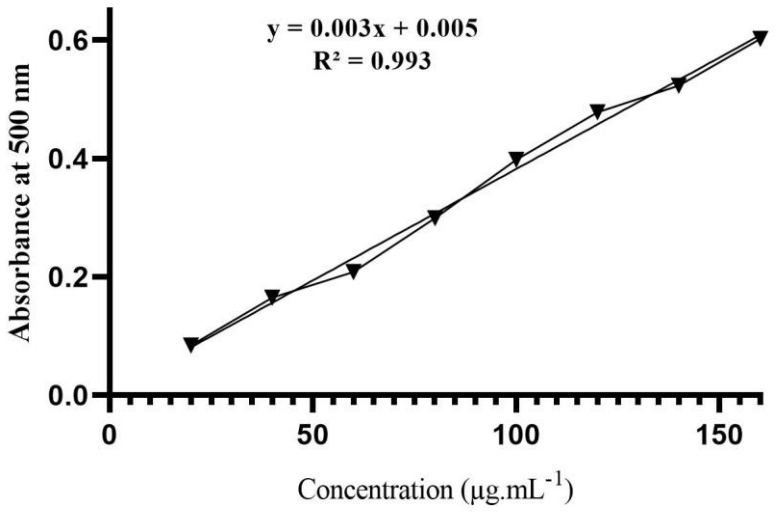

Figure 10. Standard curve of catechin used in the determination of (CTC).

The procedure goes as follow; 500 µL of the tested extract was added to a 750 µL of vanillin (4 % in methanol) and was shaken vigorously, followed by the addition of 375 µl of

HCl (12 M). The mixture was left to react in a water bath at 30°C for 20 minutes. The absorbance was read at 500 nm against a blank. Catechin standard curve was established to calculate the condensed tannins concentrations. The results were expressed as mg equivalents of catechin per g of extract (mg CE/g) (Figure 10).

2.3.4. Determination of anthocyanins content (AC)

The anthocyanins content was determined by pH differentials spectrophotometric method described by (Lako *et al*, 2007) using two buffers: potassium chloride buffer at pH 1.0 (25 mM) and sodium acetate buffer at pH 4.5 (0.4 M). Under the effect of pH, anthocyanins undergo reversible transformation. The structural alteration linked with chromophores modification determines the different colors of anthocyanin solutions depending on pH. At pH 1, the colorful form (oxonium) predominates, whereas the colorless form (hemiacetal) predominates at pH 4.5.

The procedure goes as follow; 200 µL of the tested extract was mixed separately with 1.8 mL of each of the two buffers and the absorbance was measured at 510 nm and 700 nm successively. The final absorbance (Abs) was calculated as follows:

$$Abs = (Abs_{510} - Abs_{700})\ pH_{1.0} - (Abs_{510} - Abs_{700})\ pH_{4.5}$$

The anthocyanins content (AC) of the samples is expressed in mg equivalents of cyanidin-3-glucoside per g of extract (mg C3GE/g) and it is calculated according to the following equation:

$$AC = \frac{Abs.MW.DF.100}{MAC}$$

Where, Abs: is the calculated absorbance; MW; is molecular weight of cyanidin-3-glucoside (449.2); DF is the dilution factor (10) and is MAC; is the molar absorption coefficient of cyanidin-3-glucoside (26900) (Çam *et al*., 2009).

2.4. Antioxidant capacity of *Punica granatum* L. extracts

The antioxidant activity of pomegranate different extracts was evaluated using various methods: the 2-diphenyl-picrylhydrazyl (DPPH) assay, the 2,2'-azino-bis-3-ethylbenzothiazoline-6-sulfonic acid (ABTS) assay, the iron chelating activity, ferric reducing power assay and the β-carotene bleaching test.

2.4.1. Free radical scavenging activity by 2,2-diphenyl-picrylhydrazyl (DPPH) assay

The DPPH free radical is deep purple organic nitrogen radical with a long lifetime. When a DPPH solution is combined with an antioxidant, the color of the matching hydrazine changes from purple to yellow (Figure 11). The effectiveness of antioxidants to reduce DPPH can be assessed by measuring the reduction in absorbance between 515-528 nm. The decrease in absorbance is linearly dependant on antioxidant concentration (Xiao *et al*., 2020).

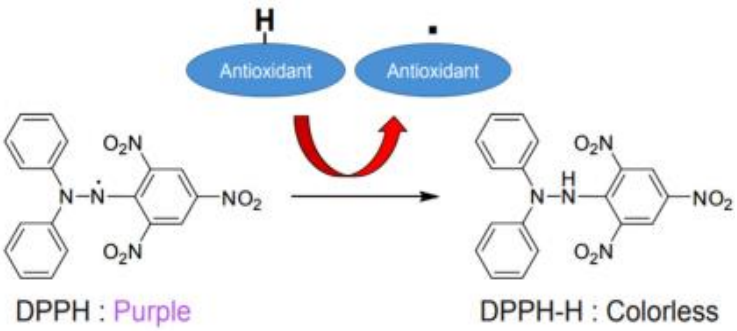

Figure 11. Reaction between DPPH• radical and antioxidant to form DPPH (Xiao *et al*., 2020).

DPPH scavenging activity was assessed based on the method described by (Blois, 1958). In which, 1950 µL of DPPH solution (0.04 mg/mL of methanol) were added to 50 µL of different dilutions of the red and yellow pomegranate peels extracts (aqueous, methanolic and ethanolic) or standard (BHT). The mixture was incubated for 30 min in the dark and the absorbance of each solution was read at 517 nm along with the absorbance of the control using an UV-Vis spectrophotometer. The inhibition percentage was calculated as follow:

$$I\ (\%) = (Abs_C - Abs_E / Abs_C) \times 100$$

Where, Abs_C is the absorbance of the reaction control and Abs_E is the absorbance of the tested extract or standard. The concentration corresponding to 50 % of inhibition (IC_{50}) was calculated from the plot of the inhibition percentage against extract concentration.

2.4.2. 2′-azino-bis-3-ethylbenzothiazoline-6-sulfonic acid (ABTS) radical cation decolorization assay

The addition of potassium persulfate converts ABTS to its radical cation. This radical cation absorbs light at 734 nm and has a blue-green color (Munteanu and Apetrei, 2021). Most antioxidants, including phenolic compounds, thiols and vitamin C, are reactive to the ABTS radical cation. The blue ABTS radical cation is transformed back to its colorless

neutral state during this reaction (Figure 12).

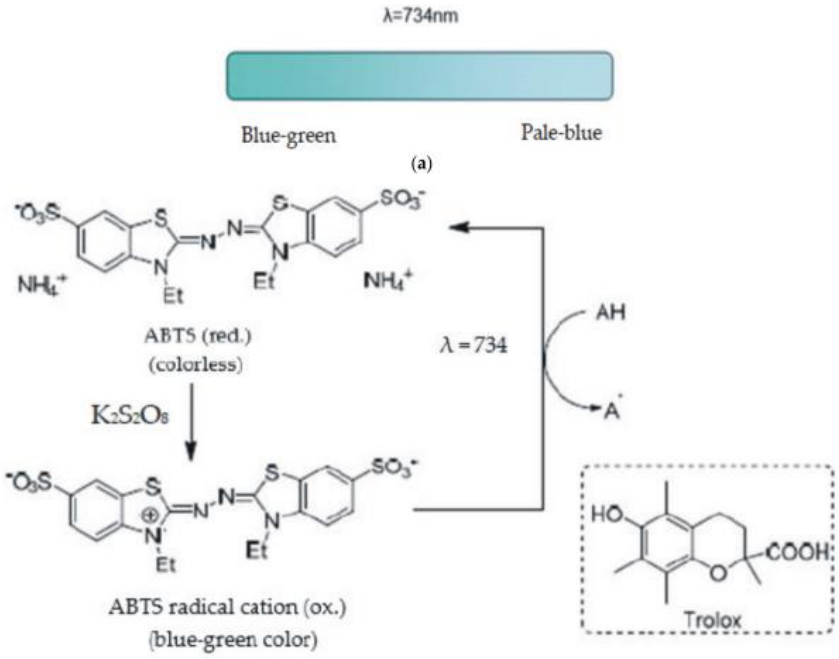

Figure 12. Reaction involved in ABTS• radical cation scavenging activity assay (Munteanu and Apetrei, 2021).

The ABTS assay of the different extracts was established using the method of (Re *et al*., 1999)**.** The $ABTS^{\bullet+}$ solution was prepared by mixing 7 mM ABTS with 2.45 mM potassium persulfate (in water). The solution was left in the dark for activation at room temperature for 16 hours. After activation the ABTS is diluted with water to reach an absorbance of 0.700 ± 0,05 nm. Briefly, 1950 µL of $ABTS^{\bullet+}$ solution was added to 50 µL of different dilutions of extracts or standard (BHT). After 10 min of incubation at room temperature, the absorbance was measured at 734 nm using a UV-Vis spectrophotometer. The percentage of ABTS radical scavenging activity was calculated as follow:

$$I\ (\%) = (Abs_C - Abs_E / Abs_C) \times 100$$

Where, Abs_C is the absorbance of the reaction control and Abs_E is the absorbance of the tested extract or standard. The concentration corresponding to 50 % of inhibition (IC_{50}) was calculated from the plot of the inhibition percentage against extract concentration.

2.4.3. Reducing power assay

The reducing power test technique is based on the idea that compounds with reduction potential react with potassium ferricyanide (Fe^{3+}) to generate potassium ferrocyanide (Fe^{2+}), which then combines with ferric chloride to form ferric-ferrous complex with an absorbance

maximum at 700 nm (Figure 13) (Bhalodia *et al*., 2013).

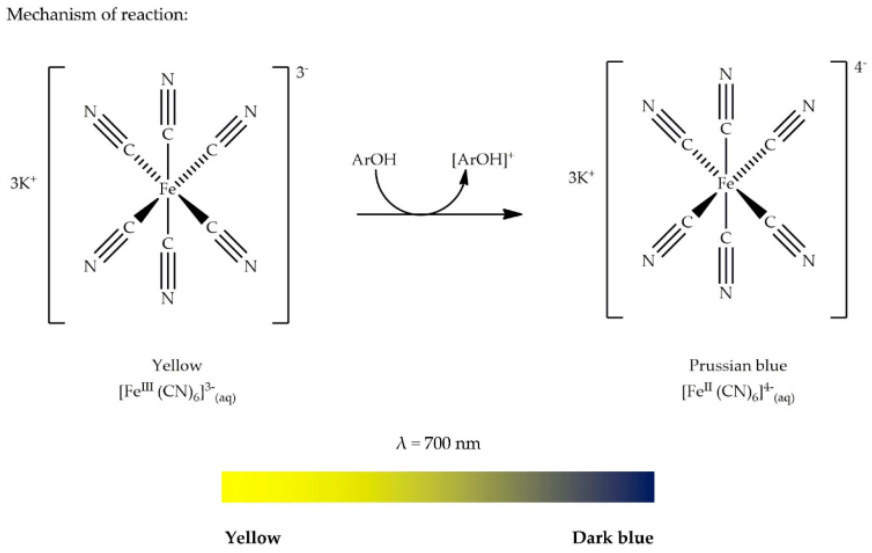

Figure 13. Potassium ferricyanide reaction mechanism (ArOH = Phenol) (Sadeer *et al*., 2020).

The reducing power assay was established according to the method described by (Rohit *et al*., 2012). In which, different concentrations (2.5-200 µg.mL^{-1}) of the extracts and the standard are initially mixed with 2.5 mL of phosphate buffer (200 mM, pH 6.6) and 2.5 mL of Potassium ferricyanide ($K_3Fe(CN)_6$) at 1 % and incubated at 50°C for 20 minutes. After incubation, 2.5 mL of Trichloroacetic acid (TCA) (10 %) are added to the reaction medium, the whole mixture is than centrifuged at 800 rpm for 10 minutes. After that, 2.5 mL of the supernatant are mixed with 2.5 mL of distilled water and 0.5 mL of ferric chloride ($FeCl_3$) (0.1 %) and the absorbance is read at 700 nm against a blank without $FeCl_3$. The absorbance is directly proportional to reducing power. The $A_{0.5}$ values (The absorbance corresponding to 50 % of inhibition) are calculated from the curve of absorbance versus samples concentrations.

2.4.4. Iron chelating activity

Ferrozine can form a complex with free ferrous ions (Fe(II)) to produce a chromophore with a high absorbance at 562 nm. Antioxidants that may chelate Fe(II) reduce the quantity of free Fe(II) in solution, resulting in a decrease in Ferrozine-Fe(II) complex concentration and a reduction in absorbance at 562 nm (Figure 14).

The iron chelating activity was estimated through the ability of the extracts to inhibit the iron(II)–ferrozine complex formation based on the method described by (Le *et al*., 2007) and (Ibrahim *et al*., 2013) with some modifications. Concentrations ranging between (0.0075-1.2 mg.mL^{-1}) of the extracts for both RPP and YPP were tested, in which 0.5 mL of the

extract was mixed with 0.05 mL of ferrous sulfate $FeSO_4$ (2 mM in distilled water). After 5 minutes, 0.05 mL of ferrozine (5 mM in 80% methanol) was added. The mixture was then shaken and incubated for 10 minutes at room temperature and the absorbance of the complex was measured at 562 nm against a reagent blank. The Na_2EDTA (0.001-0.005 $mg.mL^{-1}$) was used as a standard metal chelating agent. The control was prepared with the same manner by replacing the extract with distilled water. The chelating activity percentage was calculated using the following equation:

$$\text{Chelating activity (\%)} = \frac{A_C - A_E}{A_C} \times 100$$

Where, A_C is the absorbance of the control and A_E is the absorbance of the extract or Na_2EDTA. The results were expressed as mg of EDTA equivalent/g of extract.

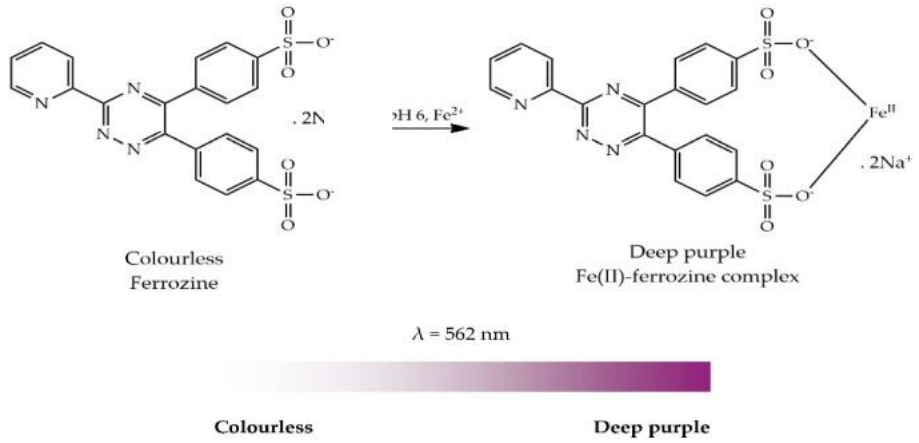

Figure 14. Iron(II)–ferrozine complex formation (Sadeer *et al.*, 2020).

2.4.5. β-carotene bleaching assay

The approach is based on the yellowish coloring of a β-carotene solution caused by the breakdown of π-conjugation by addition reaction of lipid or lipid peroxyl radical (or) to a β-carotene C=C double bond (Figure 15).

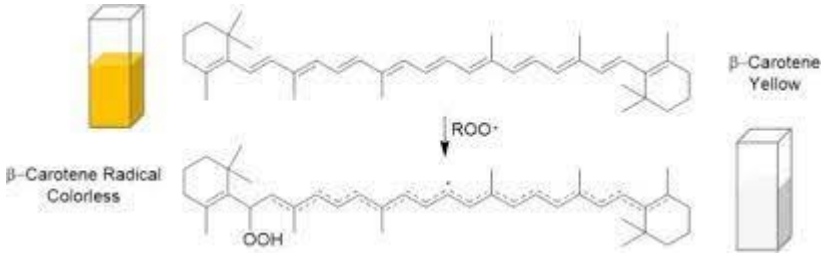

Figure 15. Discoloration of yellowish color of a β-carotene solution (Marchi *et al.*, 2021).

The radical species is formed as a result of heating linoleic acid in an air atmosphere. When the right antioxidant is added to the solution, the discoloration might be delayed due to a competitive interaction between β-carotene and the exposed radicals (Abeyrathne *et al.*, 2021).

The β-carotene bleaching activity of extracts and standard (BHT) was established according to the method of (Marco, 1968). β-carotene emulsion was prepared by initially mixing 0.5 mg of β-carotene with 200 mg of Tween 40 and 25 µL of linoleic acid in 1 mL chloroform. After the vacuum evaporation of chloroform, 100 mL of distilled water saturated with oxygen were then added to the mixture under vigorous stirring. 1250 µL of the emulsion were added to 250 µL of samples (extracts or standard) at a concentration of 2 $mg.mL^{-1}$. The mixtures were well shaken and the absorbance was measured at 470 nm at (t = 0 h), (t = 1 h), (t = 2 h), (t = 4 h), (t = 6 h), (t = 24 h) and (t = 48 h). The methanol and the distilled water saturated with oxygen were used as a negative control. The kinetic of the inhibition percentage was calculated at each time t (t = 0-24 h) using the following equation:

Inhibition percentage % = (Abs of the extract or standard at time (t = 0)/Abs extract or standard at time t = 0-24 h) ×100

2.5. Statistical analysis

The results were given as the mean ± SE for three replicates for each sample. The IC_{50} (DPPH, ABTS and iron chelating assays), $A_{0.5}$ (Reducing power assay) values were calculated by linear regression analysis. The comparison and the significance of the differences among extracts were performed with one way ANOVA and multiple comparisons TUKEY test, the correlation was done using PEARSON test, all these statistical analysis were applied using Graph Pad Prism (version 9.00 for Windows). The adsorption studies results modeling was performed via linear fitting using Origin Pro 64 (version 2021 for Windows).

Results and Discussion

1. Adsorption studies

1.1. Characterization of the adsorbents

The characterization of both RPP and YPP biosorbents was assessed through the equilibrium pH of the adsorbent, point of zero charge (pH_{pzc}), surface functional groups and FT-IR analysis of functional groups.

1.1.1. The equilibrium pH of the adsorbent and surface functional groups

The contact pH of the RPP and YPP were found to be (4.20) and (4.08), respectively. These pH values inform about the adsorbents acidic nature and confirm the Boehm titration results which showed the abundance of the acidic surface functional groups. The total concentration of the acidic functional groups (carboxylic, phenolic and lactonic) on the surface of the RPP and YPP adsorbents was 18.5 $mmol.g^{-1}$ and 16 $mmol.g^{-1}$, which is more important than the concentration of the basic functional groups with 4 $mmol.g^{-1}$ and 2 $mmol.g^{-1}$ for the RPP and YPP, respectively. These results are comparable to the ones found by (Tarbaoui *et al*., 2016) on the pomegrante peels, which found a pH of contact (4.75) with total acidic functional groups of 1.34 $mmol.g^{-1}$.

The characterization of pomegranate peels surface functional groups conducted by (Silveira *et al*., 2014) confirmed the prosperity of acidic groups with 2.82 $mmol.g^{-1}$. Najar-Souissi *et al*., (2019) also reported the acidic nature of pomegranate peels with amount of 4 $mmol.g^{-1}$. The amount of acidic functional groups on the adsorbent has been shown to accelerate the adsorption process, as these groups tend to interact and chelate metals (Paredes-Doig *et al*., 2020). Other studies performed on lemon peels showed acidic functions concentration of 3.9 $mmol.g^{-1}$ (Meseldžija *et al* ., 2020). The orange peels studied by (Ribeiro *et al*., 2017) showed more basic 3.38 $mmol.g^{-1}$ than acidic nature 1.2 $mmol.g^{-1}$.

1.1.2. Point of zero charge (pH_{pzc})

The pH_{pzc} of the RPP and YPP was 5.11 and 4.55 respectively (Figure 16). Therefore, below the pH_{pzc} the surface of the biosorbent is protonated by an excess of protons (H^+) thus, positively charged and may interact with negatively charged metal species. Above pH_{pzc} , the surface of the biosorbent is negatively charged due to its deprotonation by the presence of (OH^-) ions in the solution and may interact with positively charged metal species (Karna *et al*., 2018).

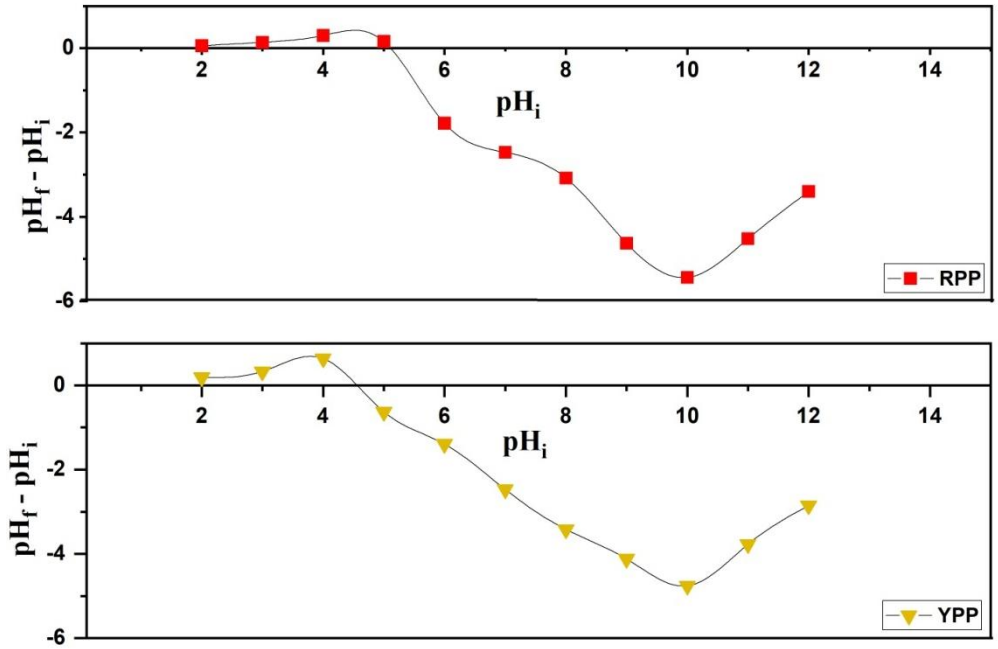

Figure 16. Point of zero charge (pH_{pzc}) of RPP and YPP.

Tunisian pomegranate peel adsorbent had similar pH_{pzc} value of (4.7) (Ben-Ali *et al*., 2017). However, Indian pomegranate peel adsorbent had higher pH_{pzc} value of (7) (Rao and Rehman, 2010) these variations can be explained by the differences in the ratio between acidic and basic functional groups in each variety.

1.1.3. FT-IR analysis

FTIR spectroscopy investigates the interactions between matter and electromagnetic radiation, which appear as a spectrum. Each molecule has a unique spectrum fingerprint that allows it to be recognized from other molecules (Fadlelmoula *et al*., 2022).

The FT-IR analysis of RPP and YPP before and after Pb(II) ions adsorption is shown in (Figure 17) and (Figure 18). For the net powder RPP and YPP, the peaks at 3405 cm^{-1} can be assigned to the stretching vibrations of hydroxyl group (OH) which confirms the presence of carboxylic acids, polysaccharides of cellulose, phenolic compounds and evidently traces of water. The peaks at 1735 cm^{-1} indicate the carbonyl group (C=O) stretching vibration which can be attributed to the CO bonds in cellulose.

The peaks at 1620 and 1623 cm^{-1} can be assigned to the bending of amino group (N–H).The peaks at 1339 and 1352 cm^{-1} can be attributed to the in-plane bending of hydroxylic group (OH). The bands around (1231-1232 cm^{-1}) and (1053-1057 cm^{-1}) can be due to the stretching vibrations of carbonyl group (C–O). These results matches well with the ones found earlier by Boehm titration, thus pomegranate peel powder is rich in acidic functional surface groups that can interact with Pb(II) ions. Earlier studies showed similar spectra of

pomegranate peels powder (Ay *et al*., 2012; Silveira *et al*., 2014).

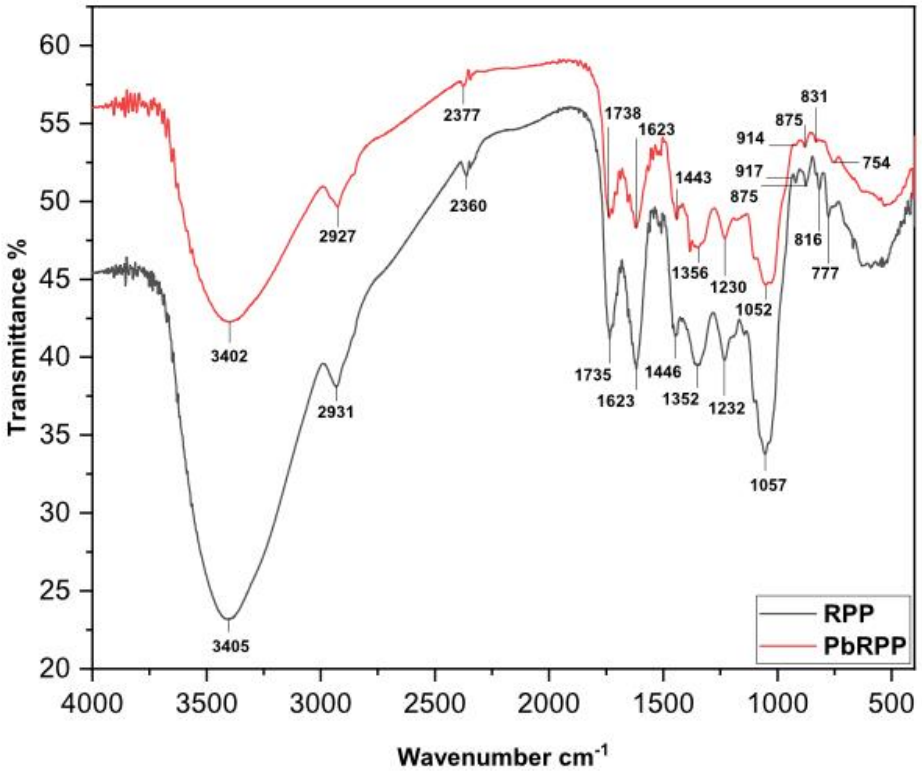

Figure 17. Infrared spectra of RPP.

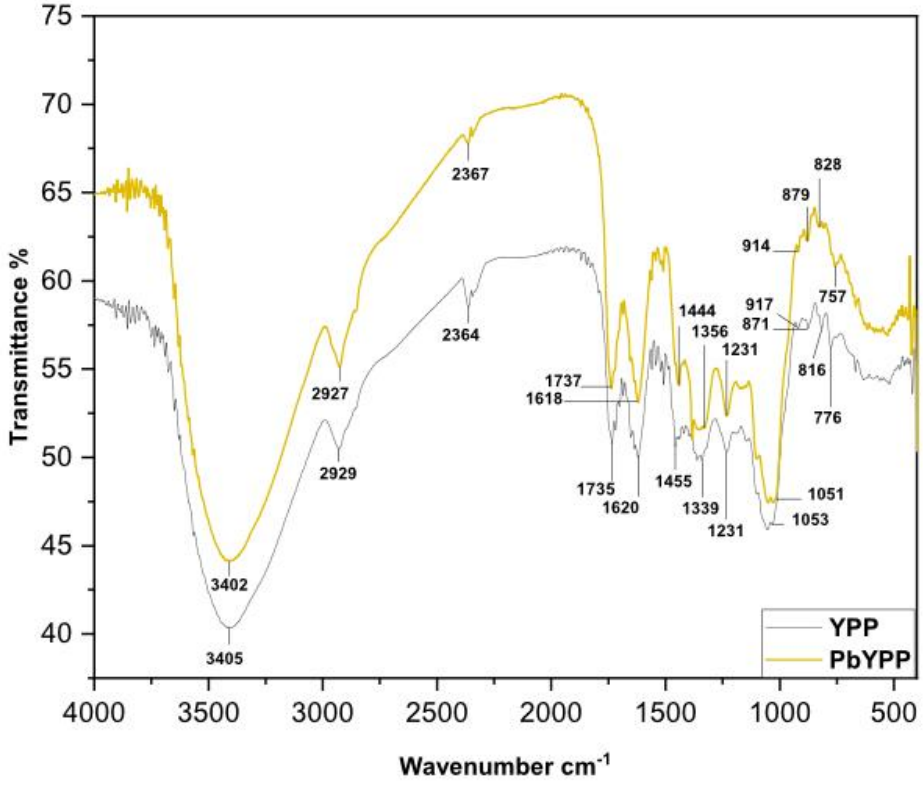

Figure 18. Infrared spectra of YPP.

However, the spectra of the peel powder after adsorption PbRPP and PbYPP showed that the intensities of the peaks were increased as well as the shifting of some bands. This indicates the possible involvement of carbonyl, hydroxyl, carboxyl and amino groups that characterize the biosorbents in the adsorption process.

1.2. Effect of different parameters on the adsorption process

1.2.1. pH effect

The pH is a crucial element that has an impact on the adsorbent metal uptake and the biosorption mechanism because it affects the ionization of the surface functional groups and the speciation of metal ions (Glorennec *et al*., 2007). The effect of pH on the Pb(II) ions adsorption was studied by varying the pH from 2 to 8 (Figure 19). There was an increase in the adsorption capacity of the biosorbent with the increase in pH from 2 to 5 and it attained a maximum adsorption capacity (Q_e) at pH 6 with 18.89 and 17.53 $mg.g^{-1}$ for the RPP and YPP, respectively. Then, it decreased after pH 6 until it reached 15.5 and 15.1 $mg.g^{-1}$ at pH 8 for the RPP and YPP, consecutively.

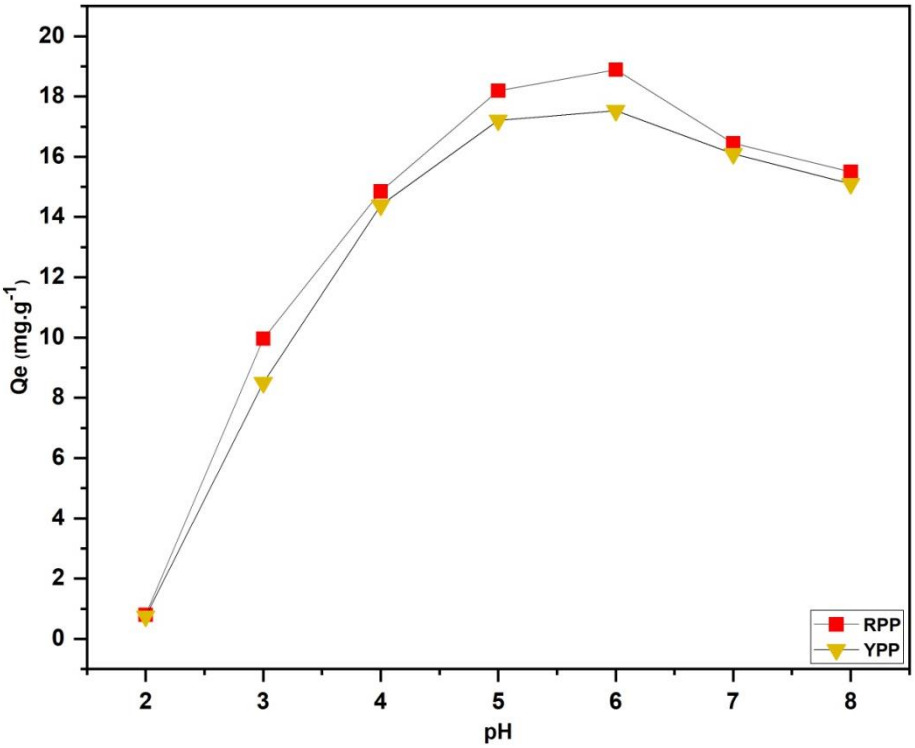

Figure 19. pH effect on the adsorption of Pb(II) ions onto pomegranate peel (Pb(II) dosage = 25 $mg.L^{-1}$, RPP and YPP dosage = 10 mg at pH from 2.0 to 8.0 and for 60 min).

At acidic pH values, more protons are present in the medium; therefore they compete with the Pb(II) cations for the adsorption sites, so the biosorbent surface would be strongly linked with protons H^+. As the pH increases, the concentration of protons

decreases and the surface functional groups of the biosorbent become negatively charged, this makes the biosorbent surface more attractive for metal cations adsorption, thus increasing the adsorption capacity of the biosorbent.

The pH can also affect the metal ion speciation, Pb(II) from pH 2 up to 6 remains with the positive charge, but over pH 6, the Pb^{2+} species concentration decreases remarkably and the concentrations of other lead species increases $Pb(OH)^{+}$, $Pb_3(OH)_4^{2-}$ and $Pb(OH)_2$ and the hydroxide ions (OH^{-}) which causes the precipitation of Pb(II) in the form of $Pb(OH)_2$ (Wang et al., 2017).

In the same manner, the working pH could affect the biosorbent charge. In effect, this pH (6) is above the point of zero charge of the biosorbent (pH_{pzc}) 5.11 and 4.55 for the RPP and YPP, respectively. Thus, the surface of the biosorbent is negatively charged which favorize the adsorption of lead cations. The results obtained in this study are in a good agreement with those reported in previous studies using pomegranate peel powder for heavy metals removal (Fawole *et al*., 2012; Moghadam *et al*., 2013; Ben-Ali *et al*., 2017).

1.2.2. Time effect

Studying effect of time variations on the adsorption helps to better understand the process and establish the adsorption mechanism (Villabona-Ortíz et al., 2022).

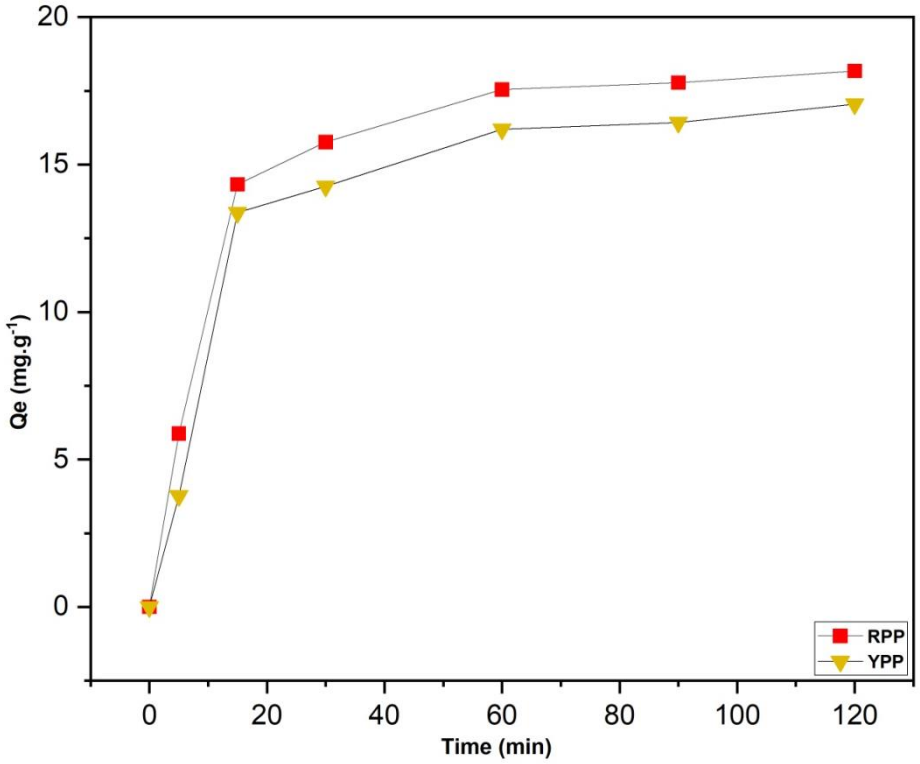

Figure 20. Time effect on the adsorption of Pb(II) ions onto pomegranate peel (Pb(II) dosage= 25 $mg.L^{-1}$, RPP and YPP dosage= 10 mg at pH 5.5 and for 0 to 60 min).

In view of the obtained results, the adsorption of Pb(II) ions increased rapidly between the time of (0-15 min) and then increased slowly to attain equilibrium within 60 min (Figure 20). Any further increase in contact time had no significant effect on the concentration of Pb(II) adsorbed for both RPP and YPP. Thereby, the contact time for subsequent batch experiments was chosen to be 60 min. The detailed study of time effect on lead ions adsorption onto the biosorbents is discussed in the kinetic section below.

1.2.3. Biosorbent dose effect

The biosorption of the Pb(II) was studied in batch mode, varying the mass of the biosorbent from 2.5 to 20 mg. The adsorption experiments were done with 10 mL of Pb(II) ions at a concentration of 25 $mg.L^{-1}$, at a pH of 5.5 and at room temperature. The obtained results shows that the Pb(II) ions removal efficiency increases as the biosorbent dose increases. In fact, the rate of Pb(II) ions removal at a dose of 2.5 mg was 59.2 % and 58.5 % for RPP and YPP, respectively. At high dose of 20 mg, this rate reached 76.4 % and 74.6 % for both biosorbents, successively (Figure 21). This can be explained by the disponibility of more adsorption sites which allows more metallic ions to occupy the biosorbents and subsequently increase the adsorption potency (Güzel *et al.*, 2012).

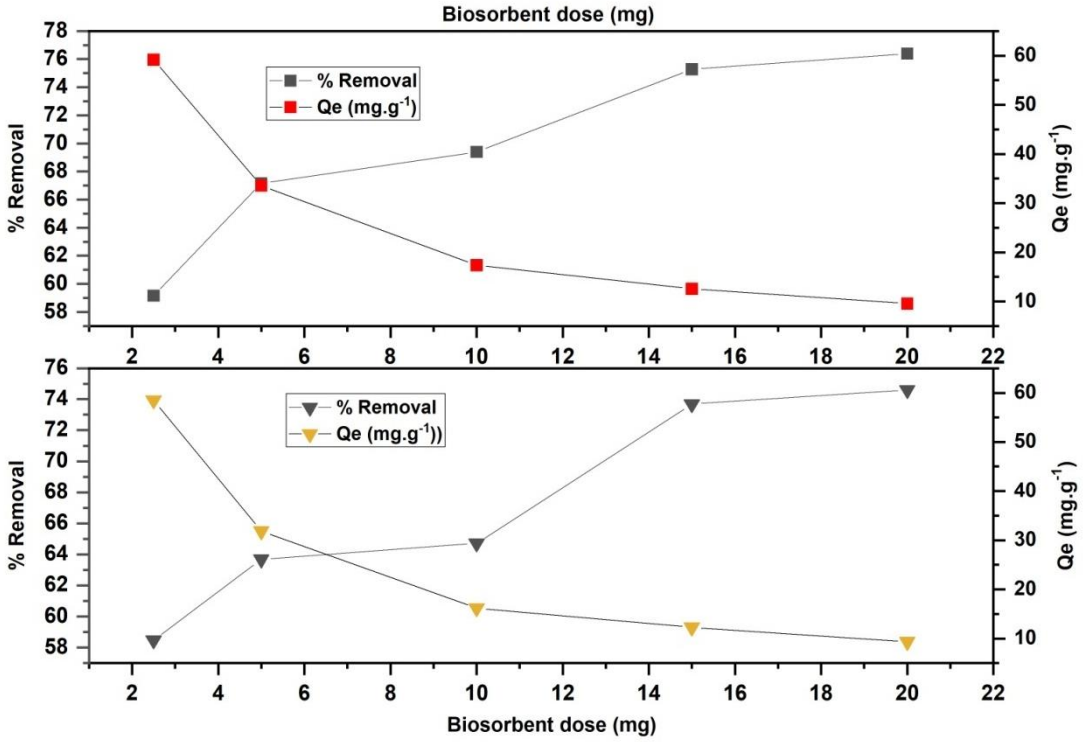

Figure 21. Biosorbent dose effect on lead removal efficiency and on the adsorption of Pb(II) ions onto pomegranate peel (Pb(II) dosage= 25 $mg.L^{-1}$, RPP and YPP dosage = from 2.5 to 20 mg at pH 5.5 and for 60 min).

In contrast, the Pb(II) ions biosorption capacity (Q_e) went from 59.16 and 58.48 $mg.g^{-1}$ at a dose of 2.5 mg to 9.55 and 9.33 $mg.g^{-1}$ at a dose of 20 mg for RPP and YPP, respectively (Figure 21). Thus, the biosorption capacity is inversely proportional to biosorbent dose. Therefore, its increase leads to a direct decrease in adsorption capacity. From a mathematical standpoint, biosorption capacity is inversely related to adsorbent dosage. Thus, its rising produces a direct drop in adsorption capacity, whereas the decrease in biosorption capacity (Q_e) is caused by the superposition and aggregation of biosorption sites, hence the unsaturation of the adsorption sites (Grabi *et al*., 2021).

1.2.4. Initial metal concentration effect

The influence of the initial metal concentration on the adsorption capacity of the YPP and YPP was studied for concentration values of 5, 10, 20, 40, 60, 80 and 100 $mg.L^{-1}$ at pH 5.5 for 60 min at ambient temperature.

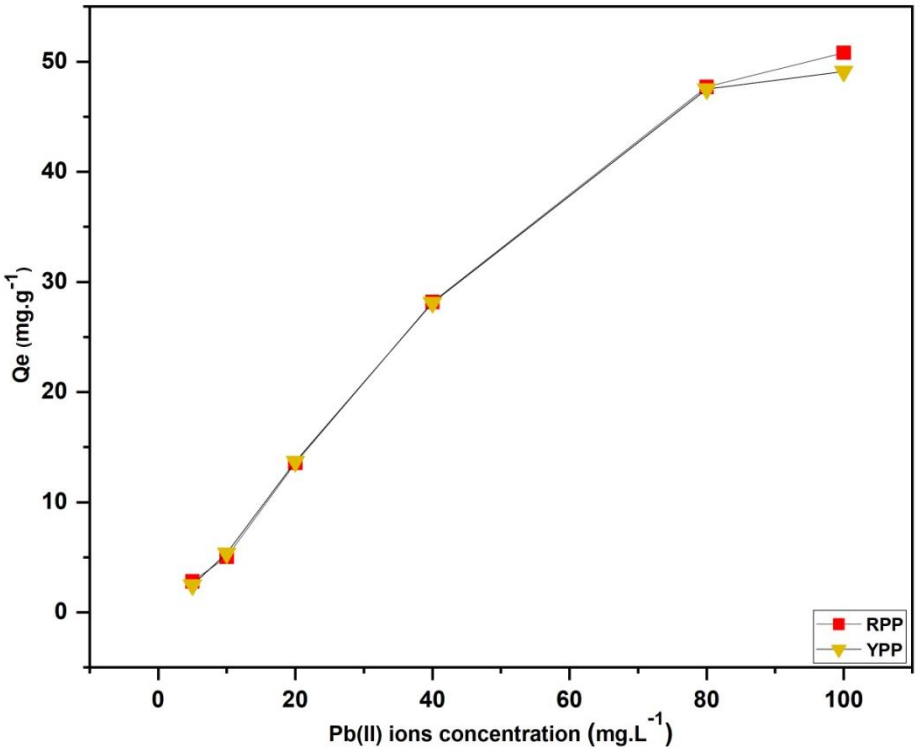

Figure 22. Initial metal concentration effect on the adsorption of Pb(II) ions onto pomegranate peel (Pb(II) dosage = 5 to 100 $mg.L^{-1}$, RPP and YPP dosage = 10 mg at pH 5.5 and for 60 min).

(Figure 22) shows that the adsorption capacity increased with increasing initial Pb(II) ions concentration; the adsorption capacity increases from 2.81 $mg.g^{-1}$ and 2.49 $mg.g^{-1}$ to 50.8 $mg.g^{-1}$ and 49.1 $mg.g^{-1}$ when the initial metal concentration increases from 5 $mg.L^{-1}$ to 100 $mg.L^{-1}$ for the RPP and YPP, respectively. At low concentrations, Pb(II) ions

are adsorbed to a limited number of sites, while with the increase of Pb(II) ions concentration, more sites are occupied and the uptake of adsorbent rises. This shows that the initial metal concentration plays an important role in the adsorption capacity of Pb(II) ions on the biosorbent (Gorzin and Abadi, 2018).

1.3. Modeling of adsorption isotherms

The parameters obtained from isotherm modeling provide important information on the adsorption mechanism, surface properties and adsorbent-adsorbate affinities. The two most commonly used two-parameter models are the Langmuir and Freundlich models. As a reminder, Langmuir model suggests that adsorption occurs on homogenous adsorbent surfaces with a monomolecular layer (Langmuir, 1918). However, Freundlich model proposes that the molecules are adsorbed as a monomolecular layer or multilayer structure on heterogeneous adsorbent surfaces (Freundlich, 1928).

The adsorption parameters (Table 12), estimated from the isotherm plots (Figure 23), show that both Langmuir and Freundlich models fit well with the experimental data. However, the theoretical adsorption capacity of the Pb^{2+} ions (Q_e) 91.32 $mg.g^{-1}$ and 91.07 $mg.g^{-1}$ for RPP and YPP, respectively found in Langmuir model are in conformity with the experimentally determined adsorption capacity (Q_{max}) 90 $mg.g^{-1}$ and 89.25 $mg.g^{-1}$ for RPP and YPP , successively. Effectively, the coefficient of correlation (r^2) in Langmuir model is closer to 1 than the one found in Freundlich model. These results are lower than the ones found by (Ay *et al.*, 2012) on the behavior study of pomegranate peels towards lead ions with Q_{max} = 166.63 $mg.g^{-1}$, but the work conducted by (Ben-ali *et al.*, 2017) on the adsorption of copper ions by pomegranate peels showed higher results with Q_{max} = 20.49 $mg.g^{-1}$.

Table 12. Isotherm parameters of Pb(II) ions onto pomegranate peel RPP and YPP.

Material	Langmuir					Freundlich		
	Q_{max} (experimental) ($mg.g^{-1}$)	Q_e (calculated) ($mg.g^{-1}$)	K_L ($L.mg^{-1}$).	R_L	r^2	K_F ($mg.g^{-1}$ $(L.mg^{-1})^{1/n}$)	1/n	r^2
RPP	90.00	91.3242	0.0146	[0.016-0.872]	0.99933	2.0034	0.4153	0.8516
YPP	89.25	91.0746	0.0130	[0.018-0.884]	0.99931	1.9473	0.4226	0.8210

Moreover, the separation factor R_L is in the range of [0.016-0.872] for the RPP and [0.018-0.884] for YPP which is below one < 1, suggesting a favorable adsorption of the Pb(II)

ions onto the RPP and YPP adsorbents. As shown in (Table 12), in Freundlich model 1/n < 1 for both RPP and YPP which means that the Pb(II) ions adsorption is favorable on both biosorbents. Finally, these parameters suggest that the Langmuir isotherm is the better fit for describing the adsorption mechanism than the Freundlich model.

The study established by (Pavan *et al*., 2008) on the uptake of lead ions by ponkan peels revealed better results than the pomegranate peels with a maximum adsorption capacity of Q_{max} = 112.1 $mg.g^{-1}$. Similar results were detected by (Isaac and Sivakumar, 2013) using custard apple fruit shell as biosorbent for lead ions with a maximum uptake of Q_{max} = 90.93 $mg.g^{-1}$. However, the banana peels analyzed by (Anwar *et al*., 2010) showed a low maximum adsorption capacity towards lead ions Q_{max} = 5.71 $mg.g^{-1}$. Comparative study of the adsorption capacity Q_{max} of different natural biosorbents towards Pb(II) ions is shown in (Table 13) below.

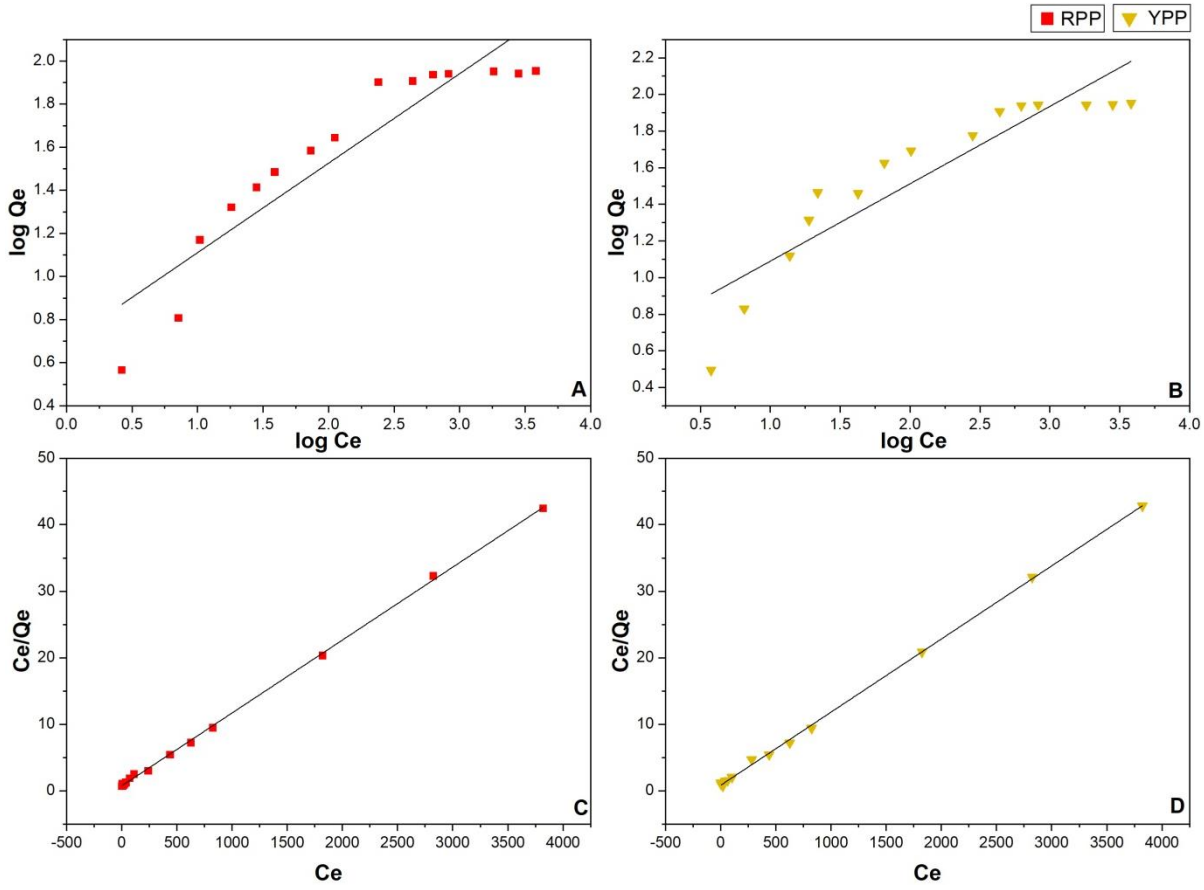

Figure 23. Linear plots of isotherms for Pb(II) ions adsorption onto pomegranate peel: A) RPP Freundlich isotherm B) YPP Freundlich isotherm C) RPP Langmuir isotherm D) YPP Langmuir isotherm (Pb(II) dosage = (10 to 4000 $mg.L^{-1}$), RPP and YPP dosage = 20 mg at pH 6.0 and for 60 min). (Ce = $mg.L^{-1}$).

Table 13. Adsorption capacities of natural biosorbents towards Pb(II) ions.

Adsorbent	Q_{max} ($mg.g^{-1}$)	Reference
Pomegranate peels	89.25-90.00	Current study
Ponkan peels	112.1	Pavan *et al*., 2008
Banana peels	5.71	Anwar *et al*., 2010
Pomegranate peels	166.63	Ay *et al*., 2012
Rapeseed biomass	21.29	Morosanu *et al*., 2017
Leucaena leucocephala	25.51	Cimá-Mukul *et al*., 2019
Sugarcane bagasse	0.143	Vera *et al*., 2019
Pinus kesiya	31.04	Huynh *et al*., 2020
Lavandula pubescens	91.32	Alorabi *et al*., 2020
Banana peels	66.67	Afolabi *et al*., 2021
Unripe papaya peels	6.25	Jaihan *et al*., 2022
C. glaucum shells	40.82	Rezaei *et al*., 2022

1.4. Modeling of adsorption kinetics

The determination of adsorption kinetics parameters is very important to choose the appropriate adsorption conditions. The kinetic study explains the effect of residence time of the adsorbed material at the solution interface on the adsorption rate. The most commonly used models to describe the adsorption kinetics and the mechanism of the reaction are the pseudo-first order model and the pseudo-second order model. As previously mentioned, the pseudo-first order model suggests that one ion is adsorbed on top of one adsorption site (Lagergren, 1898) and the pseudo-second order model proposes that one ion is adsorbed on top of two adsorption sites (Ho and McKay, 1999).

Table 14. Kinetic parameters of Pb(II) ions onto pomegranate peel RPP and YPP.

	Pseudo first-order kinetic model				**Pseudo second-order kinetic model**			
Material	Q_e (experimental) ($mg.g^{-1}$)	Q_e (calculated) ($mg.g^{-1}$)	K_1 (min^{-1})	r^2	Q_e (experimental) ($mg.g^{-1}$)	Q_e (calculated) ($mg.g^{-1}$)	K_2 ($g.mg^1.min^{-1}$)	r^2
RPP	17.35	8.25	0.03239	0.94026	17.35	18.35	0.00700	0.99818
YPP	16.18	5.92	0.01998	0.71271	16.18	16.88	0.00623	0.98662

The calculated parameters of kinetics models are shown in (Table 14). From the obtained results, it is shown that the pseudo-second order fits the experimental data better than the pseudo-first order (Figure 24), in view of the similarity between the experimental (Q_e = 17.35 and 16.18 $mg.g^{-1}$) and the calculated (Q_e = 18.35 and 16.88 $mg.g^{-1}$) Pb(II) ions

adsorption capacity (Q_e) for RPP and YPP, respectively. In addition, the pseudo-second order model has the highest regression coefficient r^2 ; (0.99818) for the RPP and (0.98662) for the YPP. Therefore, the adsorption of Pb(II) ions onto the studied biosorbents follows the pseudo-second order model. Former studies conducted on the adsorption of lead ions onto pomegranate peel waste also confirmed that the kinetics follow the pseudo-second order model (El-Ashtoukhy., *et al.*, 2008; Ay *et al.*, 2012).

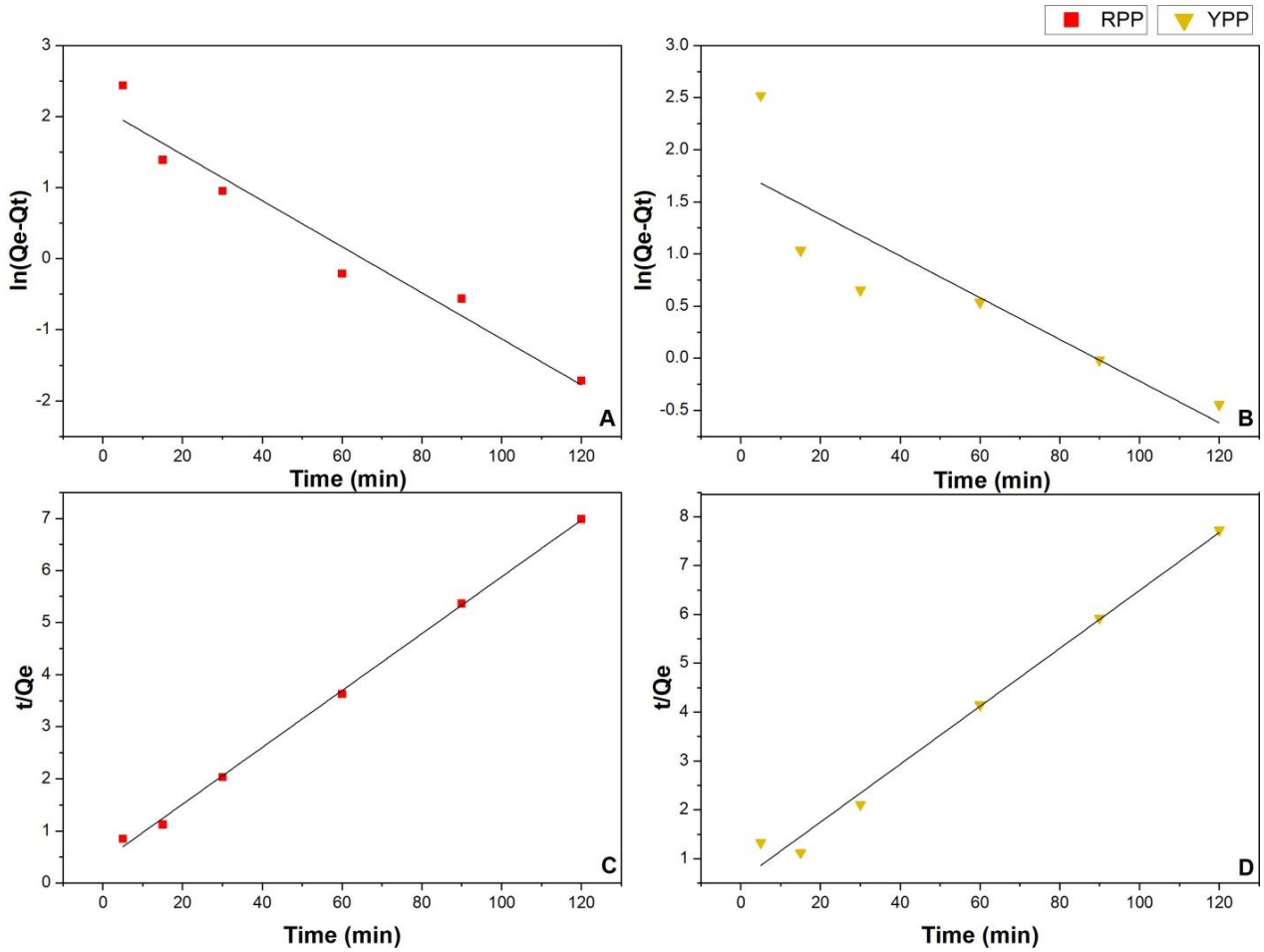

Figure 24. Kinetic linear plots for Pb(II) ions adsorption onto pomegranate peel: A) RPP pseudo-first order model B) YPP pseudo-first order model C) RPP pseudo-second order model D) YPP pseudo-second order model (Pb(II) dosage = 25 $mg.L^{-1}$), RPP and YPP dosage = 10 mg at pH 5.5 and for (0 to 120 min)).

1.5. Desorption studies

Lead removal tests from simulated industrial effluents aim to determine what volume of wastewater can be treated under dynamic conditions in correlation with the actual adsorption capacity of the red and yellow pomegranate peels. For that, 10 mL of Pb(II) solution at 50 $mg.L^{-1}$; which represents approximately twice the amount in the real effluents of this factory (22 $mg.L^{-1}$), were mixed with 0.02 g of biosorbent for 1 hour under stirring at ambient

temperature. This procedure was repeated for 3 cycles in order to determine the actual adsorption capacity of RPP and YPP.

Adsorption capacity of the RPP and YPP was similar for the first and the second cycle; 74.98 %, 74.54 % and 76.4 %, 67.44 %, respectively. After the third cycle, the adsorption capacity lowered by 26.44 % and 30.46 % for the RPP and YPP, successively contrasted to the first cycle (Figure 25).

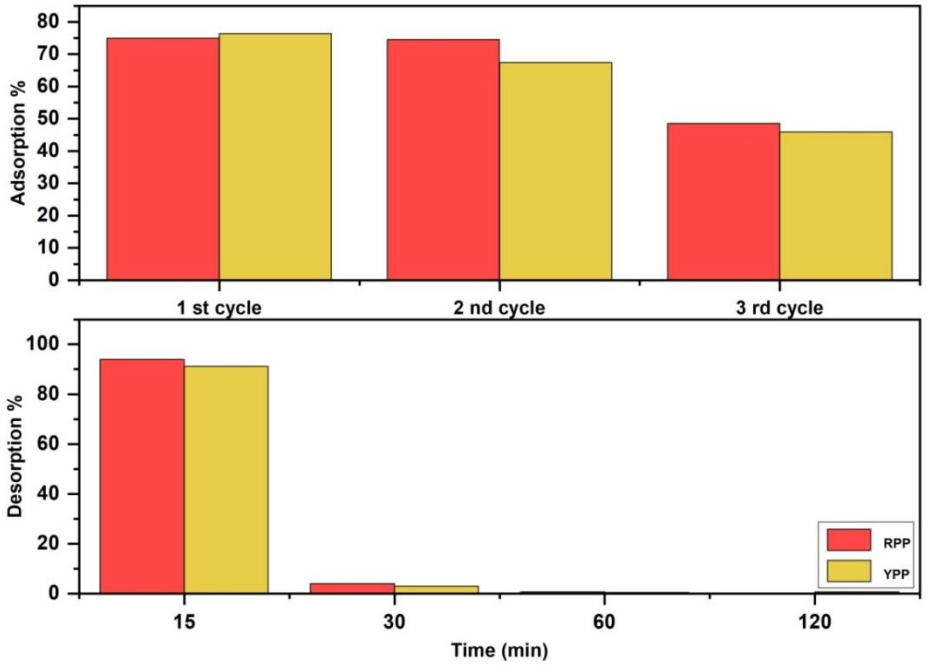

Figure 25. Desorption of Pb(II)-loaded pomegranate peel biosorbents using 1 M HCl for 15 to 120 min (after 3 cycles of adsorption with Pb(II) solution of 50 $mg.L^{-1}$ per cycle, RPP and YPP dosage = 20 mg at pH 6.0 for 60 min).

As to the desorption process, the majority of Pb(II) ions was desorbed after 15 to 30 min with a cumulative percentage of 97.89 % for the RPP and 94.13 % for the YPP as shown in (Figure 25). The rest of the chelated lead was desorbed within the next 1 and 2 hours. These results show that both yellow and red pomegranate peels are effective and efficient adsorbents for Pb(II) ions removal from real industrial effluents with a potential of their regeneration which allows their reusability.

The acidic desorption of Pb(II) ions from the used was reported as successful by (Bayuo *et al.*, 2020), with desorption percentage of 82.1 % from adsorbed lead. The acidic regeneration (nitric acid 0.5 M) of Alginate and Magadiite based composite conducted by (Attar *et al.*, 2019) gave good results with desorption percentage from 88 to 94 % for 10 successive cycles.

2. Extraction yield

The yield of *Punica granatum* L. extracts reported in this study from the initial weight of the used peels powder was affected by extraction time and the extracted solvent. For the RPP, the yield after 24 h was higher in the methanol (R Met and ethanol and R Et) extracts compared to the water extract (R Aq). However, for the YPP the water extract (Y Aq) gave a slightly better yield than the ethanol and methanol extract (Y Met and Y Et) (Table 15).

Table 15. The yield of the six extract of RPP and YPP after 24 and 36 h.

Yield %	24 h		36 h	
Peels	**Red**	**Yellow**	**Red**	**Yellow**
Water	36.9	39.6	50.9	46.7
Methanol	42.2	35.2	53.4	45.6
Ethanol	40.9	37.7	51.7	46.6

Moreover, the yield increased after 36 h in the six extracts as compared to the yield after 24 h; however, there is no significant difference in the extracts yield between 24 and 36 h for each pomegranate variety extracts (Figure 26).

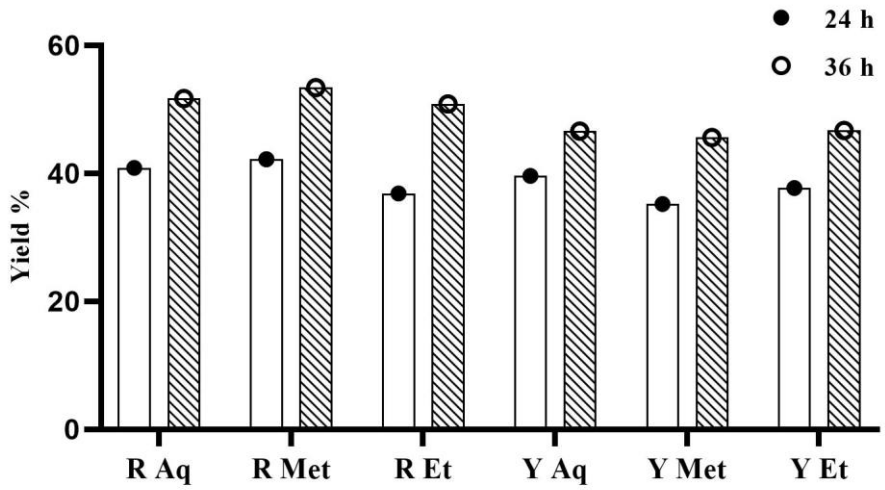

Figure 26. Percentage of yield of the six extract of RPP and YPP after 24 and 36 h.

Extraction is an essential step in the separation, identification and use of phenolic compounds and there is no specific universal extraction technique. The most used conventional extraction method is solvent extraction due to its simplicity, effectiveness and broad application, is the most often used approach for the extraction of phenolic compounds (Alara *et al*., 2021). The efficiency of extraction is known to be a function of process conditions. Several parameters influence extraction yield and desired extract components, including solvent type and concentration, extraction duration, agitation speed, sample-solvent

ratio, temperature and particle size. However, it has been observed that the most significant affecting aspect is the type of solvent used in the procedure (Chormey and Bakırdere, 2018; Maranata *et al.*, 2021).

3. Phytochemical content

3.1. Total phenolic content (TPC)

Phenolic compounds are one of the key contributors to plant antioxidant capacity; it is therefore essential to determine their total content in the selected plant extracts. The total phenolic content of extracts was assessed with the Folin-Ciocalteu method (Li *et al.*, 2007), the results were given as mg gallic acid equivalents per gram extract (mg GAE/g). The Folin-Ciocalteu technique is widely used for measuring phenolics because it is easy, simple, repeatable and cost-effective (Pereira *et al.*, 2018).

All the analyzed extracts were shown to be rich in polyphenolic compounds (Figure 27). In fact, TPC was higher in the methanolic extract (R Met and Y Met) followed by the ethanolic (R Et and Y Et) and aqueous (R Aq and Y Aq) extract for both red and yellow pomegranate peels extracts (Table 16). However, the RPP extracts had the highest TPC for all the extracts (methanol, ethanol and aqueous) in contrast to the YPP extracts.

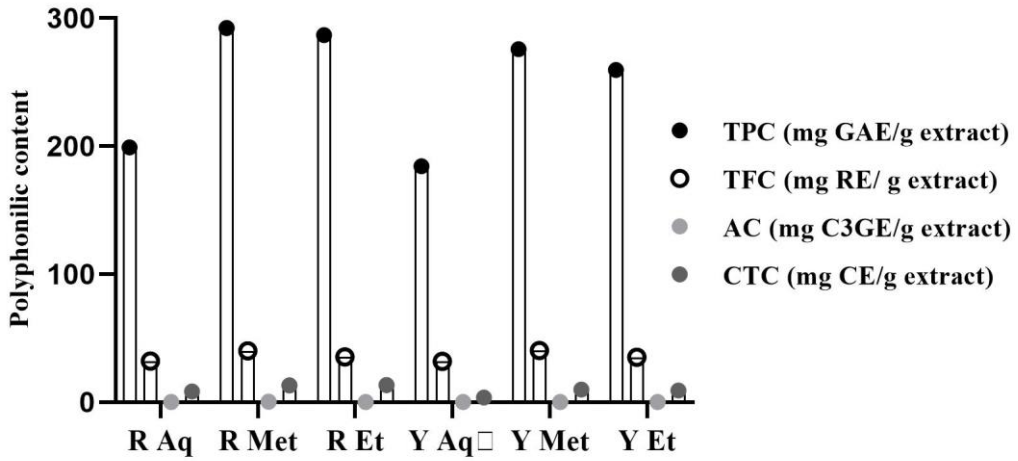

Figure 27. Total phenolic content (TPC), total flavonoids content (TFC), condensed tannins content (CTC) and anthocyanins content (AC) of red and yellow *Punica granatum* L. extracts.

Kennas and Amellal-chibane, (2019) reported that the aqueous extract of *Punica granatum* peels had a TPC of 242.05 ± 7.99 mg GAE/g which is close to our findings. However, the use of pure ethanol, methanol and acetone gave 638.17 ± 10.59, 472.46 ± 2.39 and 580.43 ± 6.49 mg GAE/g of extract, respectively. The TPC of aqueous pomegranate peels extract tested by (Fourati *et al.*, 2020) was close to our results with 178.25 ± 6.22 mg GAE/g.

However, their other extracts gave better results using other extraction solvents; ethyl acetate and acetonitrile with 391.51 ± 10.58 and 281.13 ± 19.25 mg GAE/g, successively.

Our ethanolic extracts for both RPP and YPP gave better results than the study of eight ethanolic extracts of pomegranate peels assessed by (Peršuri *et al*., 2020), which gave TPC ranging from 57.66 to 105.99 mg GAE/g. (Ranjha *et al*., 2020) methanolic and ethanolic (50 %) extracts gave significantly low TPC comparing to our results with 46.28 and 40.29 mg GAE/g extract, sequentially. The variations in TPC reported in different studies can be due to the type and the variety of pomegranate used in each study as well as the operation conditions and the solvents used in the extraction process.

3.2. Total flavonoids content (TFC)

Flavonoids are the major important group of phenolic compounds; these compounds are responsible for the plants antioxidant potency, in which the potency depends on the number and position of free OH groups present in the flavonoids (Aryal *et al*., 2019). Total flavonoids content was determined using the $AlCl_3$ method (Turkoglu *et al*., 2007). The total flavonoids contents were expressed as mg rutin equivalents per gram of extract (mg RE/g).

The TFC of all extracts showed similar results to the TPC. The methanolic extract had the highest TFC in both red and yellow peels extracts (R Met) 40.13 ± 0.4 and (Y Met) 40.38 ± 0.2 mg RE / g extract successively, followed by the ethanolic extracts (Table 16). The aqueous extracts had the lowest TFC compared to the other extracts (R Aq) 32.17 ± 0.4 and (Y Aq) 31.96 ± 0.1 mg RE / g extract for the RPP and YPP, consecutively.

Table 16. Total phenolic content (TPC), total flavonoids content (TFC), condensed tannins content (CTC) and anthocyanins content (AC) of red and yellow *Punica granatum* L. extracts.

Extracts	TPC (mg GAE /g extract)	TFC (mg RE / g extract)	CTC (mg CE / g extract)	AC (mg C3GE/ 100 g extract)
R Aq	199.11 ± 0.8	32.17 ± 0.4	8.44 ± 0.2	13.91 ± 0.001
R Met	292.29 ± 2.0	40.13 ± 0.4	13.22 ± 0.2	35.35 ± 0.001
R Et	286.81 ± 3.5	35.25 ± 0.6	13.33 ± 0.3	22.27 ± 0.002
Y Aq	184.29 ± 1.2	31.96 ± 0.1	3.56 ± 0.2	6.68 ± 0.002
Y Met	275.92 ± 0.3	40.38 ± 0.2	9.78 ± 0.2	9.74 ± 0.001
Y Et	259.70 ± 4.4	35.20 ± 0.2	9.22 ± 0.2	5.57 ± 0.003

Results are (means ± SE) (n = 3). GAE (gallic acid equivalent, RE (rutin equivalent), CE (catechin equivalent), C3GE (cyanidin-3-glucoside equivalent).

The study of three pomegranate varieties by (Campos *et al*., 2022) showed TFC of ethanolic (50 %) peels extract of 8 to 52 mg CATE/g extract, which is close the ones found in the ethanolic extracts in our study of RPP and YPP 35.25 ± 0.6 and 35.20 ± 0.2 mg RE /g extract, respectively.

The TFC of four Moroccan pomegranates peels methanolic extracts were between 46.17 ± 2.18 and 52.12 ± 1.36 mg RE/g of extract in the study conducted by (Sabraoui *et al*., 2020), which is comparable to our TFC results. Other studies reported that the aqueous and ethanolic pomegranate peels extracts had TFC of 45.74 and 50.45 mg Quercitin equivalents/g of dw in succession (Cruz-Valenzuela *et al*., 2022), which is similar to our findings that ranged from 14.88 to 21.44 mg RE / g of peels dry weight.

3.3. Condensed tannins content (CTC)

The condensed tannins are the most abundant secondary plant metabolites, they confer the plants their antioxidants characteristics. The presence of a catecholic B-ring is typical of most condensed tannins and the major aspect determining their antioxidant potential (Gourlay and Constabel, 2019). The condensed tannins content was determined by the vanillin method (Julkunen-Titto, 1985). The results were expressed as mg equivalents of catechin per g of extract (mg CE/g).

The ethanolic (R Et) and the methanolic (R Met) extracts of the red *Punica granatum* L. peels showed a significant content of condensed tannins 13.33 ± 0.3 and 13.22 ± 0.2 mg CE / g extract, successively. However, the other extracts had much lower content (Table 16). The aqueous extract of YPP (Y Aq) showed the lowest CTC among all the tested extracts with 3.56 ± 0.2 mg CE / g extract.

El Moujahed *et al*., (2022), reported that the highest condensed tannins of the aqueous extracts of six morocco pomegranate varieties was 7.7 mg CE/g DW. This result is similar to the one found in the RPP methanolic extract which was 7.1 mg CE/g DW. Saad *et al*., (2012) also reported in a previous study of 4 Tunisian pomegranate cultivars that the highest CTC of the methanolic peels extract was 7.7 mg CE/g DW. Kennas and Amellal-chibane, (2019) reported than the methanol (50 %) extract gave the best CTC with 6.39 ± 0.28 mg CE / g extract and the lowest was present in the acetone extract with 2.32 ± 0.37 CE / g extract. These differences in the tannins contents as well as the differences in TPC and TFC mentioned earlier can be explained to the type of cultivars used and experimental conditions.

3.4. Anthocyanins content (AC)

The anthocyanins are among the most important group of flavonoids in plants, these pigments have a flavylium cation structure (AH^+) which is directly related to its antioxidant

activity due to its reactivity (Tena *et al*., 2020). The anthocyanins content was determined by pH differentials method (Lako *et al.*, 2007). The results are expressed in mg equivalents of cyanidin-3-glucoside per g of extract (mg C3GE/g).

The red *Punica granatum* L. peels extracts exhibited important anthocyanins content (Table 16). The methanolic extract of RPP (R Met) had the highest AC with 35.35 ± 0.001 mg C3GE / g extract followed by the ethanolic and aqueous extracts in succession. However, the YPP extracts had weak AC compared to RPP extracts, the lowest of which 5.57 ± 0.003 mg C3GE / g extract, presented by the ethanolic yellow extract (Y Et). These variations can be explained to differences in variety used in each extraction and the richness of the red *Punica granatum* peels in the red pigments due to its red color.

Zhu *et al.*, (2015) reported that the methanolic peel extracts of three different cultivars had an anthocyanins content ranging from 45.16 ± 1.89 and 344.12 ± 19.56 mg C3GE / 100g extract. These results are higher than ours, which ranged from 5.57 ± 0.003 to 35.35 ± 0.001 mg C3GE / 100g extract for all extracts. The ethanolic peels extract studied by (Azarpazhooh *et al*., 2019) had and AC of 4.02 mg C3G/100 g of dry matter. This result is close to the AC found in the yellow cultivar YPP of all extracts which was between 2.60 and 3.1 mg C3GE / 100g dry matter. However, it was lower than the one found in the red cultivar extracts RPP which ranged from 7.19 to 18.88 mg C3GE / 100 g of dry weight.

These results confirm that the red pomegranate peels extracts have the highest anthocyanins content due to their pigmentations and red color. The variations of AC can be also attributed as mentioned before to the type of variety used, genotype and experimental conditions (El Moujahed *et al*., 2022).

4. Antioxidant capacity of *Punica granatum* L. extracts

4.1. Free radical scavenging activity by 2,2-diphenyl-picrylhydrazyl (DPPH) assay

The antioxidant activities obtained by the DPPH method for the *Punica granatum* L. extracts are presented as IC_{50} in (Figure 28). The one way ANOVA analysis revealed significant differences between various extracts ($p \leq 0.0001$). This activity was compared with that of BHT as a synthetic antioxidant. The results revealed that methanolic red extract (R Met) with an IC_{50} value of 5.943 ± 0.01 $\mu g.mL^{-1}$ is a more effective scavenger than other RPP ethanolic and aqueous extracts with IC_{50} of 6.79 ± 0.02 and 7.94 ± 0.01 $\mu g.mL^{-1}$ and YPP aqueous, methanolic and ethanolic extracts 8.76 ± 0.01, 6.25 ± 0.00 and 7.16 ± 0.02 $\mu g.mL^{-1}$, respectively. (Table 18) shows that is a strong negative correlation between TPC (R = -0.952) and TFC (R = -0.926) with the antiradical activity.

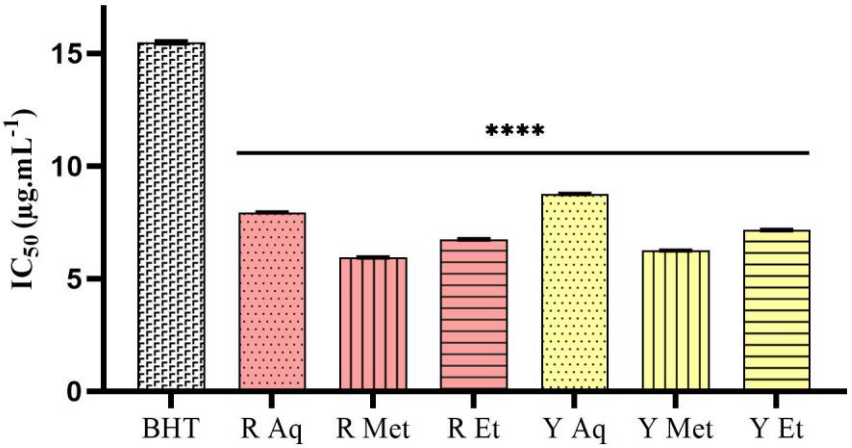

Figure 28. The IC_{50} values in the DPPH radical scavenging activity assay of the extracts.

BHT was used as reference antioxidant .Each value is expressed as a mean ± S.D (n=3).

The DPPH radical is a stable organic free radical with a 517 nm absorption band. When it accepts an electron or a free radical species, it loses its absorption, resulting in a visible discoloration from purple to yellow. It can handle a large number of samples in a short amount of time and is sensitive enough to detect active substances at low concentrations (Platzer *et al*., 2022).

The IC_{50} of an extract is inversely connected to its antioxidant capacity since it expresses the quantity of antioxidant necessary to reduce the DPPH concentration by 50%, which is determined by interpolation from a linear regression study (Becker *et al*., 2019). Our findings revealed that all *Punica granatum* L. extracts scavenge DPPH radicals in a concentration-dependent manner.

The DPPH scavenging activity of extracts is generally associated with the phenolic content including flavonoids content (Table 18) (Baliyan *et al*., 2022). In general, extracts with greater total phenolic content exhibited better scavenging efficacy (Teka and Kassahun, 2020).

Our results revealed a strong antiradical scavenging activity comparing to the results reported by (Benslimane *et al*., 2020) IC_{50} of methanolic (70 %) and ethanolic (70 %) pomegranate peels extracts with 700 ± 37 and 220 ± 14 $\mu g.mL^{-1}$. However, the study conducted by (El-Hamamsy and El-khamissi, 2020) showed more close results to ours with IC_{50} values of 14.6 ± 1.2, 23.9 ± 1.3 and 27.6 ± 2.9 $\mu g.mL^{-1}$ for the ethanol, isopropanol and cold water *Punica granatum* peels extracts.

The lyophilized pomegranate peel nanoparticles methanolic extract studied by (Morsy *et al*., 2018) reported an IC_{50} of 17.77 $\mu g.mL^{-1}$. The black pomegranate and the red pomegranate peels ethanolic extracts studies by (Chasanah, 2020) showed a significant antioxidant activity

of DPPH radical with IC_{50} of 1.78 ± 0.21and 3.82 ± 0.05 µg.mL^{-1}, successively.

4.2. 2′-azino-bis-(3-ethylbenzothiazoline-6-sulfonic acid (ABTS) radical cation decolorization assay

The antioxidant activities obtained by the ABTS method for the *Punica granatum* L. extracts are presented as IC_{50} in (Figure 29). The one way ANOVA analysis revealed significant differences between various extract ($p \leq 0.0001$). This activity was compared with that of BHT as a synthetic antioxidant. The results revealed that aqueous red extract (R Aq) gave the best scavenging ability of towards ABTS radical with an IC_{50} of 2.26 ± 0.08 µg.mL^{-1} which comparable to that of BHT (no significance difference $p > 0.05$) with IC_{50} of 2.20 ± 0.00 µg.mL^{-1}. The red ethanolic (R Et) and methanolic (R Met) extracts also exhibited a strong scavenging activity according to BHT ($p \leq 0.05$) with IC_{50} 2.93 ± 0.00 and 3.24 ± 0.11 µg.mL^{-1}, respectively. However, the ethanolic ($p \leq 0.001$), methanolic and aqueous ($p \leq 0.0001$) YPP extracts showed less stronger activity with IC_{50} values of 4.86 ± 0.03, 7.87 ± 0.03 and 8.04 ± 0.14 µg.mL^{-1}, successively.

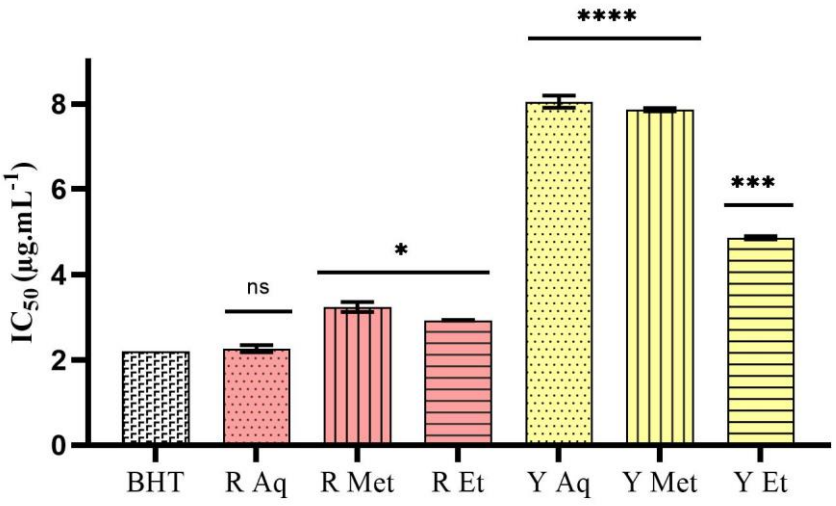

Figure 29. The IC_{50} values in the ABTS radical scavenging activity assay of the extracts.

BHT was used as reference antioxidant .Each value is expressed as a mean ± S.D (n=3).

The $ABTS^{\bullet+}$ radical is one of several radicals used to assess plant antioxidant activity. $ABTS^{\bullet+}$ is a stable organic radical that may get hydrogen from antioxidants that donate hydrogen. Radical scavenging capacity assessments in ABTS assays are a simple, quick and sensitive approach that is commonly used to examine the antioxidant potential of diverse natural compounds (Dorsey and Jones, 2017). Although the underlying principles are the same as DPPH assay, the ABTS scavenging test is preferred since it can assess the radical scavenging potential of both lipophilic and hydrophilic antioxidants (Ilyasov *et al*., 2020).

DPPH, on the other hand, is more selective since it does not react with flavonoids that lack hydroxyl groups in cycle B (Yokozawa *et al*., 1998).

Gigliobianco *et al*., (2022) reported that the ethanolic 30 % extracts of three *Punica granatum* extracts gave a powerful scavenging activity with IC_{50} ranging from 1.00 to 16.0 $\mu g.mL^{-1}$. The use of different ethanol-water ratio for the *Punica granatum* peels extraction conducted by (Laosirisathian *et al*., 2020) , showed that the ethanol 60 gave the best antiradical activity with IC_{50} of 6.48 ± 0.97 $\mu g.mL^{-1}$. Abdealsiede *et al*., (2020) also used different extraction solvents; the acetone peels extract gave the best antioxidant activity with 61 $\mu g.mL^{-1}$. The ethanol peels extract gave IC_{50} of 141 $\mu g.mL^{-1}$. Petroleum ether, chloroform and ethyl acetate gave IC_{50} values ranging from 128 to 159 $\mu g.mL^{-1}$.

These results confirm the potency of our current studied RPP and YPP extracts. The operational conditions and solvent of extraction use can affect the TPC and the antioxidant activity of the extracted biocompounds (Nguyen *et al*., 2021). The correlation results (Table 18) showed that there is a weak negative correlation between TPC and antiradical activity (R = -0.235).

4.3. Reducing power assay

The reducing power assay for the *Punica granatum* L. extracts are presented as $A_{0.5}$ in (Figure 30). The one way ANOVA analysis revealed significant differences between various extract ($p \leq 0.0001$). This activity was compared with that of BHT as a synthetic antioxidant. Activity (absorbance) increased linearly with the increasing amount of extracts. The results revealed that red aqueous extract (R Aq) had the highest reducing power activity with $A_{0.5}$ of 16.05 ± 0.16 $\mu g.mL^{-1}$ compared to BHT ($p \leq 0.05$) with $A_{0.5}$ of 18.71 ± 0.20 $\mu g.mL^{-1}$.

The red methanolic and ethanolic extracts (R Met and R Et) and the yellow ethanolic extract (Y Et) also manifested a good antioxidant activity comparable to the standard ($p > 0.05$) with $A_{0.5}$ values of 18.16 ± 0.3, 17.72 ± 0.2 and 18.64 ± 0.2 $\mu g.mL^{-1}$, respectively. The aqueous and methanolic YPP extracts had the lowest reducing power ($p \leq 0.05$) with $A_{0.5}$ values of (Y Aq) 20.94 ± 0.3 and (Y Met) 20.29 ± 0.1 $\mu g.mL^{-1}$, successively. The Pearson analysis showed a weak negative correlation between TPC and reducing power (Table 18).

The reducing antioxidant power assay measures the reduction of ferric ion (Fe^{3+})-ligand complex to the intensely blue-colored ferrous (Fe^{2+}) complex by antioxidants in an acidic medium (Zhong and Shahidi, 2015). This method is a simple, rapid and reproducible method that provides an estimate of total antioxidant activity (Anwar et al., 2020).

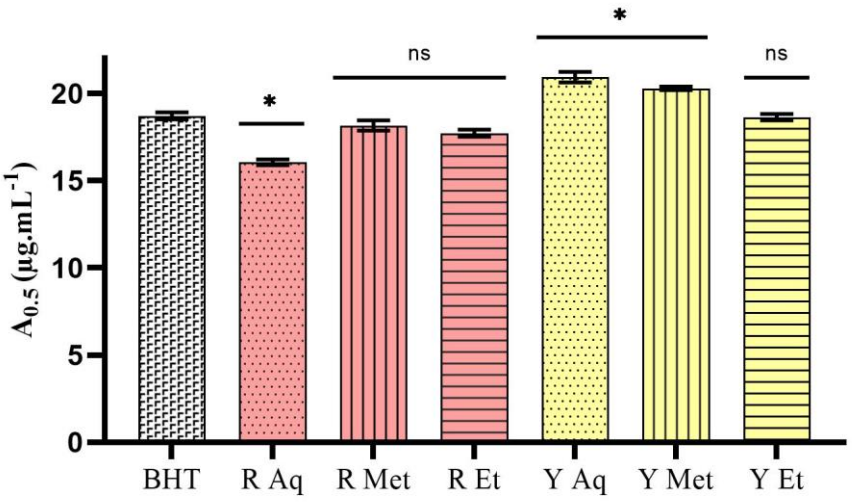

Figure 30. The $A_{0.5}$ values in the reducing power antioxidant capacity of the extracts.

BHT was used as reference antioxidant .Each value is expressed as a mean ± S.D (n=3).

Barathikannan *et al*., (2016) reported that the methanolic extract of the *Punica granatum* peels reached almost 80 % of inhibition activity at a concentration of 500 µg.mL^{-1}. The pomegranate peels extract studied by (Sihag *et al*., 2022) exhibited a powerful reducing potency with $A_{0.5}$ of 0.37 µg.mL^{-1}. Previous study conducted by (Shiban *et al*., 2012), showed that the methanolic (80 %) and water extracts of the *Punica granatum* peels reached $A_{0.5}$ at a concentration around 70 µg.mL^{-1}.

The aqueous and methanolic pomegranate peels extracts reported by (Elfalleh *et al*., 2012) showed a good reducing activity but lower than our current findings with $A_{0.5}$ of 163.50 ± 10.42 and 155.16 ± 13.24 µg.mL^{-1}, successively. Tekin and Küçükbay, (2020) reported that the methanolic extract of the pomegranate peels exhibited the strongest reducing power ($A_{0.5}$ around 6 µg.mL^{-1}) and the activity increased with the increase of the concentrations of extracts.

4.4. Iron chelating activity

Metal chelating is often regarded as the most promising and widely used antioxidant technique. Because of their functional groups that perform metal binding, antioxidants have been shown to have an efficient Fe-binding capacity (Gulcin and Alwasel, 2022).The iron-chelating activity is determined by measuring the absorbance of the iron (II)-ferrozine complex. This combination generated a red chromophore with a maximum absorbance of 562 nm. The chelator agents can grab ferrous ion before ferrozine (Sellal *et al*., 2019).

The iron chelating activity for the *Punica granatum* L. extracts are presented as IC_{50} in (Figure 31). The one way ANOVA analysis revealed significant differences between various extract ($p \leq 0.0001$). This activity was compared with that of EDTA as a synthetic antioxidant

and metal chelator which exhibited IC_{50} of 7.10 ± 0.03 µg.mL^{-1}. The results revealed that the red aqueous extract (R Aq) with an IC_{50} value of 227.2 ± 1.8 µg.mL^{-1} is the most effective iron chelator among the other RPP extracts and YPP extracts.

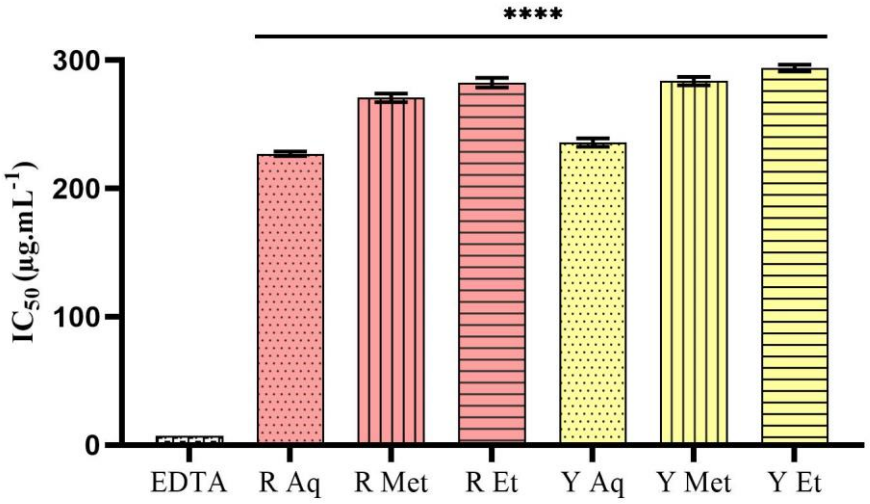

Figure 31. The IC_{50} values in iron chelating activity assay of the extracts.

EDTA was used as reference antioxidant .Each value is expressed as a mean ± S.D (n=3).

The methanolic (R Met) and ethanolic (R Et) red extracts showed IC_{50} values of 270.8 ± 3.4 and 282.7 ± 3.8 µg.mL^{-1}, respectively. The yellow aqueous extract (Y Aq) had the strongest iron chelating activity 235.9 ± 3.2 µg.mL^{-1} compared to the methanolic (Y Met) and ethanolic (Y Et) yellow extracts, which had 283.9 ± 3.6 and 294.0 ± 2.68 µg.mL^{-1}, in succession. The values of IC_{50} and the iron chelating activity in terms of mg EDTA equivalent per gram of extracts are shown in (Table 17). The Pearson analysis showed a good positive correlation between TPC (R = 0.857) and TFC (R = 0.654) and the iron chelating activity of extracts (Table 18).

Table 17. The values of IC_{50} and the iron chelating activity in terms of EDTA equivalent.

Extract	IC_{50} (µg.mL^{-1})	Chelating activity (mg EDTA equiv/g extract)
R Aq	227.2 ± 1.7	31.25
R Met	274.1 ± 3.3	25.9
R Et	282.7 ± 3.7	25.11
Y Aq	235.9 ± 3.2	30.10
Y Met	283.8 ± 3.3	25.01
Y Et	294.0 ± 2.5	24.14
EDTA	7.10 ± 0.03	-

Results are (means ± SE) (n = 3).

Farag *et al*., (2020) reported that the pomegranate peels extract had a powerful iron chelating activity with IC_{50} of 142.651 ± 0.817 µg.mL^{-1}. These results are higher than the ones found in our extracts. The ethyl acetate extract of *Punica granatum*, obtained by Soxhlet extraction gave a strong iron chelating activity with IC_{50} of 18.2 µg.mL^{-1} as reported by (Di Sotto *et al*., 2019).The methanolic extract of the pomegranate peels reported by (Sivaraj *et al*., 2018) manifested a strong iron chelating activity with IC_{50} of 51.69 µg.mL^{-1}.

The methanolic peels extracts of three Moroccan pomegranate cultivars studied by (Sabraoui *et al*., 2020), manifested a strong iron chelating potency ranging from 1.401 ± 0.00 to 2.293 ± 0.00 (µmol EDTA equiv/g dw), when our results (Table 17) ranged from 8.98 to 10.69 (µmol EDTA equiv/g extract). Elkamali and Hamed, (2015) reported that pomegranate peels methanolic and aqueous extracts gave an iron chelation inhibition percentage of 35 ± 0.03 % and 18 ± 0.03 %, respectively at a dose of 5 mg.mL^{-1}. However, our extracts showed an inhibition percentage ranging from 75.07 ± 0.1 to 77.42 ± 0.5 %, at a concentration of 1.2 mg.mL^{-1}.

4.5. β-carotene bleaching assay

The β-carotene bleaching activity for the *Punica granatum* L. extracts is presented as the inhibition percentage during different time (t = 0-24 h). The bleaching activity of the extracts was compared to BHT used as a standard antioxidant and methanol and ethanol used as control (Figure 32). The methanolic (C Met) and aqueous (C Aq) control showed a decrease in the antioxidant activity as the time went on until they reached their lowest after 24 h with inhibition percent of 13.56 and 15.10 %, respectively ($p \leq 0.0001$).

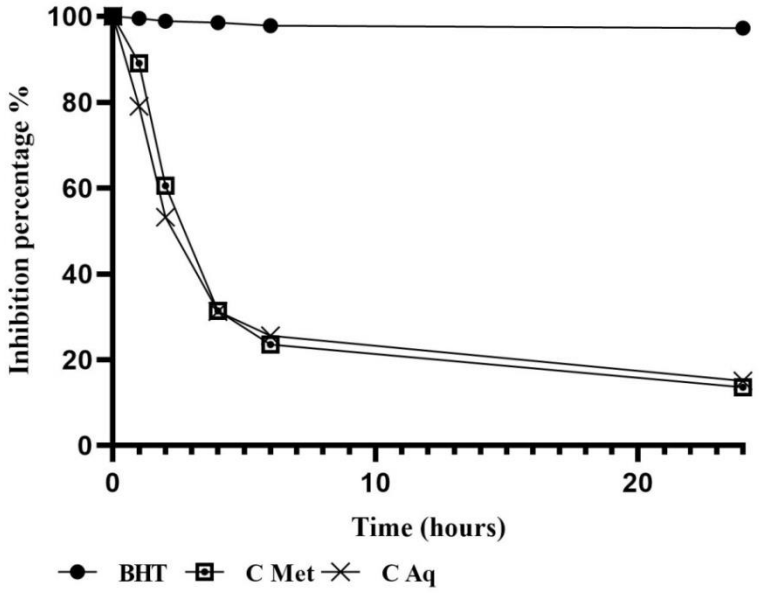

Figure 32. Kinetics and inhibition percentage of β-carotene bleaching assay of the controls.

BHT was used as reference antioxidant .Each value is expressed as a mean ± S.D (n=3).

The methanolic red extract (R Met) gave the best antioxidant activity followed by the ethanolic extract (R Et) as there was no significant difference compared to BHT ($p > 0.05$), However, the aqueous red extract (R Aq) gave the lowest antioxidant activity ($p \leq 0.05$) as shown in (Figure 33). As for the YPP extracts, the methanolic extract (Y Met) also presented the most strong antioxidant activity compared to BHT ($p > 0.05$).

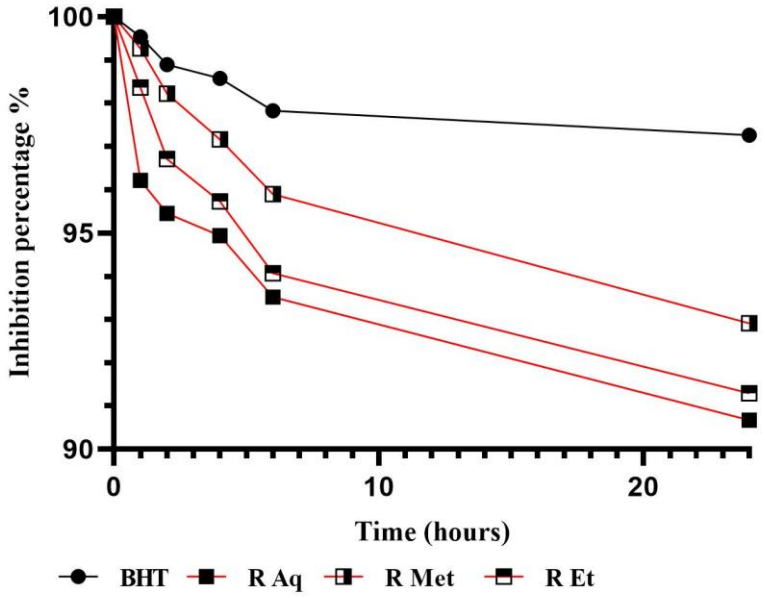

Figure 33. Kinetics and inhibition percentage of β-carotene bleaching assay of the RPP extracts. BHT was used as reference antioxidant .Each value is expressed as a mean ± S.D (n=3).

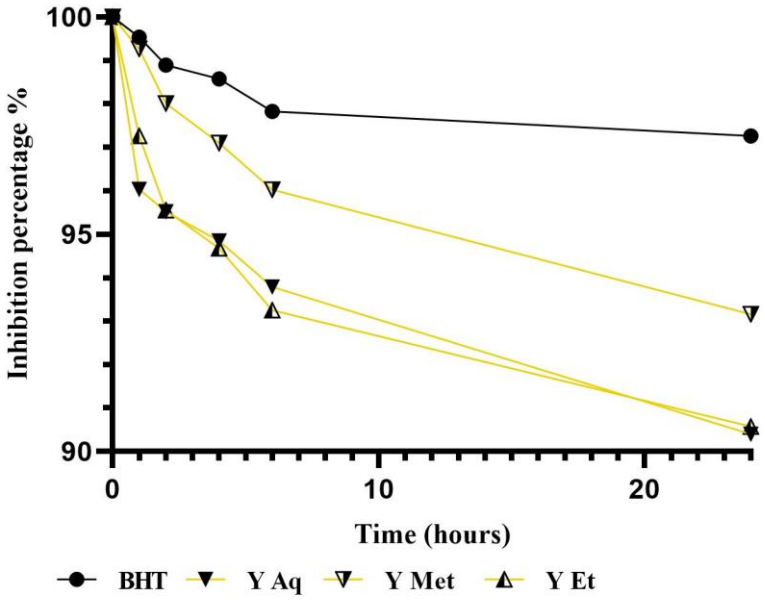

Figure 34. Kinetics and inhibition percentage of β-carotene bleaching assay of the YPP extracts. BHT was used as reference antioxidant .Each value is expressed as a mean ± S.D (n=3).

In contrast, the aqueous (Y Aq) and ethanolic (Y Et) yellow extracts showed lesser

potency (Figure 34) and a significance difference compared to BHT ($p \leq 0.05$). These results show that all the extracts have prevented the discoloration of the β-carotene emulsion throughout the 24 h of the study at a concentration of 2 $mg.mL^{-1}$. The Pearson analysis showed that there is significant positive correlation between TPC (R = 0.702) and TFC (R = 0.951) and β-carotene antioxidant activity (Table 18).

Table 18. Pearson's correlation coefficients (R) of the TPC, TFC, CTC and AC with the antioxidant activities of *Punica granatum* L. extracts.

	TPC	TFC	CTC	AC	DPPH	ABTS	Reducing power	Iron chelation	β-carotene
TPC	1.000								
TFC	0.830	1.000							
CTC	0.891	0.631	1.000						
AC	0.566	0.480	0.753	1.000					
DPPH	-0.952	-0.926	-0.870	-0.610	1.000				
ABTS	-0.235	0.106	-0.628	-0.597	0.230	1.000			
Reducing power	-0.074	0.200	-0.492	-0.408	0.118	0.955	1.000		
Iron chelation	0.857	0.654	0.600	0.098	-0.733	0.053	0.176	1.000	
β-carotene	0.702	0.951	0.569	0.531	-0.850	0.111	0.169	0.426	1.000

TPC total phenolic content, TFC total flavonoids content, CTC condensed tannins content, AC anthocyanins content, DPPH diphenyl-picrylhydrazyl assay, ABTS azino-bis-3-ethylbenzothiazoline-6-sulfonic acid assay. ($p > 0.05$).

The presence of various antioxidants can reduce the degree of β-carotene bleaching by neutralizing the linoleate free radical and other free radicals produced in the system. As a result, absorbance drops fast in samples without an antioxidant, but in the presence of an antioxidant, they keep their color and hence absorbance, for a longer amount of time (Fawwaz *et al*., 2021). The oxidation of β-carotene was prevented by the various extracts and standard. This action is caused by either the prevention of linoleic acid peroxidation or the radical scavenging of hydroperoxides generated during linoleic acid peroxidation.

The methanolic (70 %) extract of *Punica granatum* peels reported by (Benchagra *et al*., 2021) exhibited significantly high antioxidant activity (86.83 ± 1.22 %) at 2 $mg.mL^{-1}$. Our results showed better antioxidant activity as the inhibition percentage didn't go below 90 during 24 h at the same concentration.

Derakhshan *et al*., (2018) reported that the methanolic extracts (80 %) of three studied cultivars peels gave an antioxidant activity ranging from 45 ± 9.94 to 58 ± 10.52 % at 2 $mg.mL^{-1}$. Thus, our extracts showed better and stronger antioxidant activity. However, the water and methanolic extracts analyzed by (Zaki *et al*., 2015) gave antioxidant potency of

45.5 and 80.21%, respectively. These percentages are considered significant regarding that they only used a 100 µg.mL^{-1} of each extract.

Conclusion

Polyphenols, which exist naturally in plants, have been recognized for a long time to have a wide range of health-promoting qualities due to their various biological activities, including antioxidant activity. Their extraction from plants in moderate and effective conditions to better understand their methods of biologic action are scientific challenges that form the foundation of our research.

In the present study, two varieties of *Punica granatum* L. were chosen in order to find new ways of application in the medical and pharmaceutical fields as well as in the environmental fields. The objective of this work was to valorize the pomegranate peels waste as a source of antioxidant proprieties and as a low cost adsorbent for metallic pollutants present in different industrial effluents.

In the first section, the study aimed to investigate the adsorption potential of the red and yellow *Punica granatum* L. peels towards Pb(II) ions in aqueous medium. The characterization of both RPP and YPP showed the acidic nature of both biomasses and their richness in acidic functional surface groups, which may be responsible for these biosorbents affinity to lead ions. The study of different factors on the adsorption process showed that the adsorption capacity increases with pH until pH 6, contact time and initial metal concentration and it decreases with increasing the biosorbent dose. The optimum adsorption conditions were found to be 60 min of contact time at pH (6) with 0.02 g of biosorbent.

The modeling of adsorption isotherms showed that the Langmuir model is more suitable than the Freundlich model for both biosorbents. The adsorption capacity of RPP and YPP was 89.25 $mg.g^{-1}$ and 90 $mg.g^{-1}$, respectively. The kinetics studies showed that the experimental data follow the pseudo-second order better compared to the pseudo-first one with a coefficient of correlation $r^2 = 0.99818$ and r^2 0.98662 for RPP and YPP, successively.

The adsorption-desorption of lead at interface of these biomasses as sorbents was successful with acidic desorption. These results manifested the power of these biomasses as biosorbents for lead ions.

In the second section, the study focused on the extraction of polyphenols and the investigation of the antioxidant potentials of the six extracts. The extraction yields vary depending on the duration, type and physicochemical properties of the solvents employed, particularly their polarity. The hydro-alcoholic extraction using methanol and ethanol (50 %) gave the best yields. The methanolic and ethanolic extracts for both RPP and YPP gave the best TPC and TFC.

All the extracts exhibited a strong radical scavenging activity; however the RPP extracts gave slightly better results than the YPP. The ferric (Fe^{3+}) reducing power and iron (Fe^{2+})

chelating activity were powerful regarding the six extracts. The oxidation of β-carotene was also prevented significantly by all the red and yellow pomegranate peels extracts, they maintained a strong antioxidant activity during 24 hours.

The results of the present study support the traditional use of *Punica granatum* L. peels as a rich source of polyphenolic compounds and as prevention from oxidative stress related diseases induced by lead toxicity. .

At the light of the present study, it would be interesting to conduct a more in-depth study to isolate, purify and identify the molecules responsible for the previous activities.

In view of these given results, pomegranate peels constitute versatile tools for the treatment of lead poisoning in humans through their polyphenols content and their iron chelating antioxidant activity that inhibit reactive oxygen species generated during the oxidative stress induced by lead. In addition and in terms of adsorption, pomegranate peels as an agro-waste, can be used efficiently and advantageously in removing lead pollutant from effluents, which contributes in the protection of the environment from its toxic effects with the possibility of their reuse.

→ Future study should involve more research aiming at identifying, isolating and characterizing the active elements responsible for the high reported antioxidant activity in order to discover the specific mechanism of the antioxidant activity.

→ The adsorption capacity should be further exploited and more factors should be tested.

→ The adsorption capacity of both biomasses should be tested towards different metals.

→ The biomasses should be exploited as natural biosorbents in real industrial effluents.

→ Other types of in vivo antioxidant testing are required.

→ More research on pharmacological and biological activity is needed.

References

Abdealsiede, M. M., Alrasheid, A. A., Ali Omar, M. M., & Elbashir, A. A. (2020). Antimicrobial and antioxidant activity of pomegranate peel extracts obtained by Sequential Extraction Method. *Asian Journal of Pharmaceutical Research and Development*, *8*(2), 14–20.

Abdulla, M. (2020). Lead. In A. S. Prasad & G. J. Brewer (Eds.), *Essential and Toxic Trace Elements and Vitamins in Human Health* (pp. 181–191). essay, Academic Press.

Abedi, M., Salmani, M. H., & Mozaffari, S. A. (2016). Adsorption of CD ions from aqueous solutions by iron modified pomegranate peel carbons: Kinetic and thermodynamic studies. *International Journal of Environmental Science and Technology*, *13*(8), 2045–2056.

Abedi, M., Salmani, M. H., & Mozaffari, S. A. (2016). Adsorption of CD ions from aqueous solutions by iron modified pomegranate peel carbons: Kinetic and thermodynamic studies. *International Journal of Environmental Science and Technology*, *13*(8), 2045–2056.

Abeyrathne, E. D., Nam, K., & Ahn, D. U. (2021). Analytical methods for lipid oxidation and antioxidant capacity in food systems. *Antioxidants*, *10*(10), 1587.

Achike, F., & Murugan, D. D. (2020). Quercetin and antioxidant potential in diabetes. In V. R. Preedy (Ed.), *Diabetes* (Second Edition, pp. 293–302). essay, Academic Press.

Addala, A., Belattar, N., & Elektorowicz, M. (2018). Nigella sativa L. seeds biomass as a potential sorbent of lead from aqueous solutions and Wastewaters. *Oriental Journal of Chemistry*, *34*(2), 638–647.

Adejumoke , I. A., Abimbola , O. P., Tabitha, A.-A. A., Adewumi , D. O., & A, O. T. (2018). Water Pollution: Effects, Prevention, and Climatic Impact. In A. O. Babatunde & M. Glavan (Eds.), *Water Challenges of an Urbanizing World* (pp. 34–53). essay, IntechOpen.

Adeleke, O. A., Latiff, A. A. A., Saphira, M. R., Daud, Z., Ismail, N., Ahsan, A., Aziz, N. A. A., Al-Gheethi, A., Kumar, V., Fadilat, A., & Apandi, N. (2019). Principles and Mechanism of Adsorption for the Effective Treatment of Palm Oil Mill Effluent for Water Reuse. In A. Ahsan & A. F. Ismail (Eds.), *Nanotechnology in Water and Wastewater Treatment: Theory and Applications A volume in Micro and Nano Technologies* (pp. 1–33). essay, Elsevier.

Afolabi, F. O., Musonge, P., & Bakare, B. F. (2021). Bio-sorption of copper and lead ions in single and binary systems onto Banana Peels. *Cogent Engineering*, *8*(1).

Afolabi, F., Musonge, P., & Bakare, B. (2021). Evaluation of lead (II) removal from wastewaterusing Banana Peels: Optimization Study. *Polish Journal of Environmental Studies*, *30*(2), 1487–1496.

Ahmed, J., Thakur, A., & Goyal, A. (2021). Industrial wastewater and its toxic effects. *Chemistry in the Environment*, 1–14.

Ahuchaogu, A. A., Chukwu, O. J., Obike, A. I., Igara, C. E., Nnorom, I. C., & Echeme, J. B. O. (2018). Reverse osmosis technology, its applications and nano-enabled membrane. *International Journal of Advanced Research in Chemical Science*, *5*(2), 20–26.

Ajibade, F. O., Adelodun, B., Lasisi, K. H., Fadare, O. O., Ajibade, T. F., Nwogwu, N. A., Sulaymon, I. D., Ugya, A. Y., Wang, H. C., & Wang, A. (2021). Environmental pollution and their socioeconomic impacts. *Microbe Mediated Remediation of Environmental Contaminants*, 321–354.

Akhter, M., Habib, G., & Qamar, S. U. (2018). Application of electrodialysis in waste water treatment and impact of fouling on process performance. *Journal of Membrane Science & Technology*, *08*(02).

Akhter, M., Habib, G., & Qamar, S. U. (2018). Application of electrodialysis in waste water treatment and impact of fouling on process performance. *Journal of Membrane Science & Technology*, *08*(02).

Al osman, M., Yang, F., & Massey, I. Y. (2019). Exposure routes and health effects of heavy metals on children. *BioMetals*, *32*(4), 563–573.

Al-Anzi, B. S., Naik, M.-ud-din, & Ahmad, M. (2022). The imperative need of metal salt for the treatment of industrial wastewater via the SYNERGIC coagulation-flocculation method. *Polymers*, *14*(9), 1651.

Alara, O. R., Abdurahman, N. H., & Ukaegbu, C. I. (2021). Extraction of phenolic compounds: A Review. *Current Research in Food Science*, *4*, 200–214.

Al-Asheh, S., & Aidan, A. (2020). A Comprehensive Method of Ion Exchange Resins Regeneration and Its Optimization for Water Treatment. In I. A. Moujdin, & J. K. Summers (Eds.), Promising Techniques for Wastewater Treatment and Water Quality Assessment. essay. IntechOpen.

Alhasawi, A., Legendre, F., Jagadeesan, S., Appanna, V., & Appanna, V. (2019). Biochemical Strategies to Counter Nitrosative Stress: Nanofactories for Value-Added Products. In S. Das & H. R. Dash (Eds.), *Microbial Diversity in the Genomic Era* (pp. 153–169). essay, Academic Press.

Alorabi, A. Q., Alharthi, F. A., Azizi, M., Al-Zaqri, N., El-Marghany, A., & Abdelshafeek, K. A. (2020). Removal of lead(II) from synthetic wastewater by *Lavandula pubescens* Decne Biosorbent: Insight into composition–adsorption relationship. *Applied Sciences*, *10*(21), 7450.

Alshammari, N. D., Fatima, N., & Nayeem, N. (2017). *Punica granatum* Rind, a Traditional Herbal Medicine: Effect on wound healing. *International Journal of Pharmaceutical Research & Allied Sciences*, *6*(1), 53–58.

Anis, S. F., Hashaikeh, R., & Hilal, N. (2019). Microfiltration Membrane Processes: A review of Research Trends over the past decade. *Journal of Water Process Engineering*, *32*, 100941.

Anwar, J., Shafique, U., Waheed-uz-Zaman, Salman, M., Dar, A., & Anwar, S. (2010). Removal of Pb(II) and Cd(II) from water by adsorption on peels of banana. *Bioresource Technology*, *101*(6), 1752–1755.

Arana Juve, J. M., Christensen, F. M., Wang, Y., & Wei, Z. (2022). Electrodialysis for metal removal and recovery: A Review. *Chemical Engineering Journal*, *435*, 134857.

Aryal, S., Baniya, M. K., Danekhu, K., Kunwar, P., Gurung, R., & Koirala, N. (2019). Total phenolic content, flavonoid content and antioxidant potential of wild vegetables from western Nepal. *Plants*, *8*(4), 96.

Ashfaq, A., Nadeem, R., Bibi, S., Rashid, U., Hanif, M. A., Jahan, N., Ashfaq, Z., Ahmed, Z., Adil, M., & Naz, M. (2021). Efficient adsorption of lead ions from synthetic wastewater using agrowaste-based mixed biomass (Potato Peels and banana peels). *Water*, *13*(23), 3344.

Attar, K., Demey, H., Bouazza, D., & Sastre, A. (2019). Sorption and desorption studies of Pb(II) and Ni(II) from aqueous solutions by a new composite based on alginate and Magadiite Materials. *Polymers*, *11*(2), 340.

Ay, C. O., Ozcan, A. S., Erdoğan, Y., & Ozcan, A. (2012). Characterization of *Punica granatum* L. peels and quantitatively determination of its biosorption behavior towards lead(II) ions and Acid Blue 40. *Colloids and Surfaces B: Biointerfaces*, *100*, 197–204.

Azarpazhooh, E., Sharayei, P., Zomorodi, S., & Ramaswamy, H. S. (2018). Physicochemical and phytochemical characterization and storage stability of freeze-dried encapsulated pomegranate peel anthocyanin and in vitro evaluation of its antioxidant activity. *Food and Bioprocess Technology*, *12*(2), 199–210.

Balali-Mood, M., Naseri, K., Tahergorabi, Z., Khazdair, M. R., & Sadeghi, M. (2021). Toxic mechanisms of five heavy metals: Mercury, lead, chromium, Cadmium, and arsenic. *Frontiers in Pharmacology*, *12*.

Baliyan, S., Mukherjee, R., Priyadarshini, A., Vibhuti, A., Gupta, A., Pandey, R. P., & Chang, C.-M. (2022). Determination of antioxidants by DPPH radical scavenging activity and quantitative phytochemical analysis of *Ficus religiosa*. *Molecules*, *27*(4), 1326.

Barrientos, G., Alves, J., Pradas, F., Robles, M. C., Muñoz, D., & Maynar, M. (2020). Association between parameters related to oxidative stress and trace minerals in athletes. *Sustainability*, *12*(12), 4966.

Bayuo, J., Abukari, M. A., & Pelig-Ba, K. B. (2020). Desorption of chromium (VI) and lead (II) ions and regeneration of the exhausted adsorbent. *Applied Water Science*, *10*(7).

Becker, M., Nunes, G., Ribeiro, D., Silva, F., Catanante, G., & Marty, J. L. (2019). Determination of the antioxidant capacity of red fruits by miniaturized spectrophotometry assays. *Journal of the Brazilian Chemical Society*.

Ben-Ali, S., Jaouali, I., Souissi-Najar, S., & Ouederni, A. (2017). Characterization and adsorption capacity of raw pomegranate peel biosorbent for copper removal. *Journal of Cleaner Production*, *142*, 3809–3821.

Benchagra, L., Berrougui, H., Islam, M. O., Ramchoun, M., Boulbaroud, S., Hajjaji, A., Fulop, T., Ferretti, G., & Khalil, A. (2021). Antioxidant effect of Moroccan pomegranate (*Punica granatum* L. Sefri variety) extracts rich in punicalagin against the oxidative stress process. *Foods*, *10*(9), 2219.

Benchagra, L., Berrougui, H., Islam, M. O., Ramchoun, M., Boulbaroud, S., Hajjaji, A., Fulop, T., Ferretti, G., & Khalil, A. (2021). Antioxidant effect of Moroccan pomegranate (*Punica granatum* L. Sefri variety) extracts rich in punicalagin against the oxidative stress process. *Foods*, *10*(9), 2219.

Benjelloun, M., Miyah, Y., Akdemir Evrendilek, G., Zerrouq, F., & Lairini, S. (2021). Recent advances in adsorption kinetic models: Their application to dye types. *Arabian Journal of Chemistry*, *14*(4), 103031.

Benslimane, S., Rebai, O., Djibaoui, R., & Arabi, A. (2020). Pomegranate Peel Extract Activities as Antioxidant and Antibiofilm against Bacteria Isolated from Caries and Supragingival Plaque . *Jordan Journal of Biological Sciences* , *13*(3), 403–412 .

Bhalodia, N. R., Nariya, P. B., Shukla, V. J., & Acharya, R. N. (2013). In vitro antioxidant activity of hydro alcoholic extract from the fruit pulp of Cassia fistula Linn. *AYU (An International Quarterly Journal of Research in Ayurveda)*, *34*(2), 209.

Blois, M. A. R. S. D. E. N. S. (1958). Antioxidant determinations by the use of a stable free radical. *Nature*, *181*(4617), 1199–1200.

Boehm, H. P. (1994). Some aspects of the surface chemistry of carbon blacks and other carbons. *Carbon*, *32*(5), 759–769.

Bounaas, M., Bouguettoucha, A., Chebli, D., Reffas, A., Harizi, I., Rouabah, F., & Amrane, A. (2018). High efficiency of methylene blue removal using a novel low-cost acid treated forest wastes, *cupressus semperirens* cones: Experimental results and modeling. *Particulate Science and Technology*, *37*(4), 504–513.

Briffa, J., Sinagra, E., & Blundell, R. (2020). Heavy metal pollution in the environment and their toxicological effects on humans. *Heliyon*, *6*(9).

Çam, M., Hışıl, Y., & Durmaz, G. (2009). Classification of eight pomegranate juices based on antioxidant capacity measured by four methods. *Food Chemistry*, *112*(3), 721–726.

Çam, M., Hışıl, Y., & Durmaz, G. (2009). Classification of eight pomegranate juices based on antioxidant capacity measured by four methods. *Food Chemistry*, *112*(3), 721–726.

Campos, L., Seixas, L., Henriques, M. H., Peres, A. M., & Veloso, A. C. (2022). Pomegranate peels and seeds as a source of phenolic compounds: Effect of cultivar, by-product, and extraction solvent. *International Journal of Food Science*, *2022*, 1–11.

Catalá, A., & Díaz, M. (2016). Editorial: Impact of lipid peroxidation on the physiology and pathophysiology of cell membranes. *Frontiers in Physiology*, *7*.

Chaemiso, T. D., & Nefo, T. Removal Methods of Heavy Metals from Laboratory Wastewater . *Journal of Natural Sciences Research*, *9*(2), 36–42.

Chasanah, U. (2021). Studies on antioxidant activity of red, white, and black pomegranate (*Punica granatum* L.) peel extract using DPPH radical scavenging method. *Farmasains : Jurnal Farmasi Dan Ilmu Kesehatan*, *5*(2), 51–55.

Chaudhry, F. N., & Malik, M. F. (2017). Factors affecting water pollution: A Review. *Journal of Ecosystem & Ecography*, *07*(01).

Chen, X., Kang, R., & Tang, D. (2021). Ferroptosis by lipid peroxidation: The tip of the iceberg? *Frontiers in Cell and Developmental Biology*, *9*.

Chormey, D. S., & Bakırdere, S. (2018). Principles and Recent Advancements in Microextraction Technique. In D. S. Chormey, S. Bakırdere, S. Bakırdere, N. B. Turan, & G. Ö. Engin (Eds.), *Comprehensive Analytical Chemistry* (Vol. 81, pp. 257–294). essay, Elsevier B.V.

Cimá-Mukul, C. A., Abdellaoui, Y., Abatal, M., Vargas, J., Santiago, A. A., & Barrón-Zambrano, J. A. (2019). Eco-efficient Biosorbent based on *leucaena leucocephala* residues for the simultaneous removal of Pb(II) and Cd(II) ions from water system: Sorption and mechanism. *Bioinorganic Chemistry and Applications*, *2019*, 1–13.

Coronado-Reyes, J. A., Cortés-Penagos, C. de, & González-Hernández, J. C. (2022). Chemical composition and great applications to the fruit of the pomegranate (*Punica granatum*): A Review. *Food Science and Technology*, *42*.

Costa, M., Sezgin-Bayindir, Z., Losada-Barreiro, S., Paiva-Martins, F., Saso, L., & Bravo-Díaz, C. (2021). Polyphenols as antioxidants for extending food shelf-life and in the Prevention of Health Diseases: Encapsulation and interfacial phenomena. *Biomedicines*, *9*(12), 1909.

Cruz-Valenzuela, M. R., Ayala-Soto, R. E., Ayala-Zavala, J. F., Espinoza-Silva, B. A., González-Aguilar, G. A., Martín-Belloso, O., Soliva-Fortuny, R., Nazzaro, F., Fratianni, F., Tapia-Rodríguez, M. R., & Bernal-Mercado, A. T. (2022). Pomegranate (*Punica granatum* L.) peel extracts as antimicrobial and antioxidant additives used in alfalfa sprouts. *Foods*, *11*(17), 2588.

Dahman, Y. (2017). Nanopolymers. In *Nanotechnology and Functional Materials for Engineers* (Micro and Nano Technologies, pp. 121–144). essay, Elsevier.

Derakhshan, Z., Ferrante, M., Tadi, M., Ansari, F., Heydari, A., Hosseini, M. S., Conti, G. O., & Sadrabad, E. K. (2018). Antioxidant activity and total phenolic content of ethanolic extract of pomegranate peels, juice and seeds. *Food and Chemical Toxicology*, *114*, 108–111.

Di Meo, S., Reed, T. T., Venditti, P., & Victor, V. M. (2016). Role of Ros and RNS sources in physiological and pathological conditions. *Oxidative Medicine and Cellular Longevity*, *2016*, 1–44.

Di Sotto, A., Locatelli, M., Macone, A., Toniolo, C., Cesa, S., Carradori, S., Eufemi, M., Mazzanti, G., & Di Giacomo, S. (2019). Hypoglycemic, antiglycation, and cytoprotective properties of a phenol-rich extract from waste peel of *Punica granatum* L. var. dente di Cavallo DC2. *Molecules*, *24*(17), 3103.

Dökmeci, A. H. (2020). Environmental Impacts of Heavy Metals and Their Bioremediation. In M. K. Nazal, & H. Zhao (Eds.), Heavy Metals - Their Environmental Impacts and Mitigation. essay, IntechOpen.

Dorsey, B. M., & Jones, M. A. (2017). Healthy components of coffee processing by-products. In C. M. Galanakis (Ed.), *Handbook of Coffee Processing By-Products: Sustainable Applications* (pp. 27–62). essay, Academic Press.

Dwivedi, S., Malik, C., Chhokar, V. (2017). Molecular Structure, Biological Functions, and Metabolic Regulation of Flavonoids. In: Gahlawat, S., Salar, R., Siwach, P., Duhan, J., Kumar, S., Kaur, P. (Eds.) Plant Biotechnology: Recent Advancements and Developments. essay, Springer, Singapore.

Dżugan, M., Wesołowska, M., Zaguła, G., & Puchalski, C. (2018). The comparison of the physicochemical parameters and antioxidant activity of homemade and commercial pomegranate juices. *Acta Scientiarum Polonorum Technologia Alimentaria*, *17*(1), 59–68.

Ebelegi, A. N., Ayawei, N., & Wankasi, D. (2020). Interpretation of adsorption thermodynamics and kinetics. *Open Journal of Physical Chemistry*, *10*(03), 166–182.

Eddaikra, A., & Eddaikra, N. (2021). Endogenous Enzymatic Antioxidant Defense and Pathologies. In (Ed.), Antioxidants - Benefits, Sources, Mechanisms of Action. essay, IntechOpen.

Egendorf, S. P., Groffman, P., Moore, G., & Cheng, Z. (2020). The limits of lead (PB) phytoextraction and possibilities of phytostabilization in contaminated soil: A critical review. *International Journal of Phytoremediation*, *22*(9), 916–930.

El Moujahed, S., Dinica, R.-M., Cudalbeanu, M., Avramescu, S. M., Msegued Ayam, I., Ouazzani Chahdi, F., Kandri Rodi, Y., & Errachidi, F. (2022). Characterizations of six pomegranate (*Punica granatum* L.) varieties of global commercial interest in Morocco: Pomological, organoleptic, chemical and Biochemical Studies. *Molecules*, *27*(12),

El-Ashtoukhy, E.-S. Z., Amin, N. K., & Abdelwahab, O. (2008). Removal of lead (II) and copper (II) from aqueous solution using Pomegranate Peel as a new adsorbent. *Desalination*, *223*(1-3), 162–173.

Elfalleh, W. (2012). Total phenolic contents and antioxidant activities of pomegranate peel, seed, leaf and flower. *Journal of Medicinal Plants Research*, *6*(32).

El-Hamamsy, S., & El-khamissi, H. (2020). Phytochemicals, antioxidant activity and identification of phenolic compounds by HPLC of Pomegranate (*Punica granatum* L.) peel extracts. *Journal of Agricultural Chemistry and Biotechnology*, *11*(4), 79–84.

Elhleli, H., Mannai, F., ben Mosbah, M., Khiari, R., & Moussaoui, Y. (2020). Biocarbon derived from Opuntia Ficus indica for p-nitrophenol retention. *Processes*, *8*(10), 1242.

EL-Kamali, H., & E. M. Hamed, S. (2015). Antioxidant potential of some Sudanese medicinal plants used in traditional medicine. *International Journal of Scientific World*, *3*(2), 192.

Elkhaleefa, A., Ali, I. H., Brima, E. I., Shigidi, I., Elhag, A. B., & Karama, B. (2021). Evaluation of the adsorption efficiency on the removal of lead(ii) ions from aqueous solutions using Azadirachta indica leaves as an adsorbent. *Processes*, *9*(3), 559.

Erkan, M., & Dogan, A. (2018). Pomegranate/Roma—*Punica granatum*. In S. Rodrigues, E. de O. Silva, & S. de Brito (Eds.), *Exotic Fruits: Reference Guide* (pp. 355–361). essay, Academic Press.

Esposto, S., Veneziani, G., Taticchi, A., Urbani, S., Selvaggini, R., Sordini, B., Daidone, L., Gironi, G., & Servili, M. (2021). Chemical composition, antioxidant activity, and sensory characterization of commercial pomegranate juices. *Antioxidants*, *10*(9).

Estrada-Rivera, A., Díaz Fonseca, A., Treviño Mora, S., García Suastegui, W. A., Chávez Bravo, E., Castelán Vega, R., Morán Perales, J. L., & Handal-Silva, A. (2022). The impact of urbanization on water quality: Case study on the Alto Atoyac Basin in Puebla, Mexico. *Sustainability*, *14*(2), 667.

Fadlelmoula, A., Pinho, D., Carvalho, V. H., Catarino, S. O., & Minas, G. (2022). Fourier transform infrared (FTIR) spectroscopy to analyse human blood over the last 20 years: A review towards lab-on-a-chip devices. *Micromachines*, *13*(2), 187.

Farag, R. S., Abdel-Latif, M. S., Abd El Baky, H. H., & Tawfeek, L. S. (2020). Phytochemical screening and antioxidant activity of some medicinal plants' crude juices. *Biotechnology Reports*, *28*.

Fatima Zahra, K., Lefter, R., Ali, A., Abdellah, E.-C., Trus, C., Ciobica, A., & Timofte, D. (2021). The involvement of the oxidative stress status in cancer pathology: A double view on the role of the antioxidants. *Oxidative Medicine and Cellular Longevity*, *2021*, 1–25.

Fawole, O. A., Makunga, N. P., & Opara, U. L. (2012). Antibacterial, antioxidant and tyrosinase-inhibition activities of pomegranate fruit peel methanolic extract. *BMC Complementary and Alternative Medicine*, *12*(1).

Fawwaz, M., Pratama , M., Hasrawati, A., Sukmawati, Widiastuti , H., Rahmawati , & Abidin, Z. (2020). Total carotenoids, antioxidant and anticancer effect of *Penaeus Monodon* shells extract. *Biointerface Research in Applied Chemistry*, *11*(4), 11293–11302.

Fazal-ur-Rehman, M. (2019). Polluted Water Borne Diseases: Symptoms, Causes, Treatment and Prevention. *Journal of Medicinal and Chemical Sciences*, *6*(4), 21–26.

Fenga, C., Gangemi, S., Di Salvatore, V., Falzone, L., & Libra, M. (2017). Immunological effects of occupational exposure to lead. *Molecular Medicine Reports*, *15*(5), 3355–3360.

Fleming, E., & Luo, Y. (2021). Co-delivery of synergistic antioxidants from food sources for the prevention of oxidative stress. *Journal of Agriculture and Food Research*, *3*, 100107.

Fourati, M., Smaoui, S., Ben Hlima, H., Elhadef, K., Chakchouk Mtibaa, A., & Mellouli, L. (2020). Variability in phytochemical contents and biological potential of pomegranate

(*Punica granatum*) peel extracts: Toward a new opportunity for minced beef meat preservation. *Journal of Food Quality*, *2020*, 1–14.

Freundlich,, H. (1928). Über die Struktur der Kolloidteilchen und über den Aufbau von Solen und Gelen. *Berichte Der Deutschen Chemischen Gesellschaft*, *61*(10), 2219–2233.

Gagniere , J., & Bonnet, M. (2017). Molecular Mechanism Underlying the Actions of Antioxidant Molecules in Digestive Disorders. In J. Gracia-Sancho & J. Salvadó (Eds.), *Gastrointestinal Tissue. Oxidative Stress and Dietary Antioxidants* (pp. 197–216). essay, Academic Press.

Ge, S., Duo, L., Wang, J., GegenZhula, Yang, J., Li, Z., & Tu, Y. (2021). A unique understanding of traditional medicine of pomegranate, *Punica granatum* L. and its current research status. *Journal of Ethnopharmacology*, *271*, 113877.

Gigliobianco, M. R., Cortese, M., Nannini, S., Di Nicolantonio, L., Peregrina, D. V., Lupidi, G., Vitali, L. A., Bocchietto, E., Di Martino, P., & Censi, R. (2022). Chemical, antioxidant, and antimicrobial properties of the peel and male flower by-products of four varieties of *Punica granatum* L. cultivated in the Marche region for their use in cosmetic products. *Antioxidants*, *11*(4), 768.

Glorennec, P., Laperche, V., & Guyonnet, D. (2007). Plomb et santé: importance de la spéciation. *Géosciences*, 40–45.

Gorzin, F., & Abadi, B. R. M. M. (2017). Adsorption of cr(vi) from aqueous solution by adsorbent prepared from paper mill sludge: Kinetics and Thermodynamics Studies. *Adsorption Science & Technology*, *36*(1-2), 149–169.

Gourlay, G., & Constabel, C. P. (2019). Condensed tannins are inducible antioxidants and protect hybrid poplar against oxidative stress. *Tree Physiology*, *39*(3), 345–355.

Grabi, H., Derridj, F., Lemlikchi, W., & Guénin, E. (2021). Studies of the potential of a native natural biosorbent for the elimination of an anionic textile dye cibacron blue in aqueous solution. *Scientific Reports*, *11*(1).

Gulcin, İ., & Alwasel, S. H. (2022). Metal ions, metal chelators and metal chelating assay as antioxidant method. *Processes*, *10*(1), 132.

Gupta, A., Sharma, V., Sharma, K., Kumar, V., Choudhary, S., Mankotia, P., Kumar, B., Mishra, H., Moulick, A., Ekielski, A., & Mishra, P. K. (2021). A review of adsorbents for heavy metal decontamination: Growing approach to wastewater treatment. *Materials*, *14*(16), 4702.

Güzel, F., Aksoy, Ö., & Akkaya, G. (2012). Application of Pomegranate (*Punica granatum*) Pulp as a New Biosorbent for the Removal of a Model Basic Dye (Methylene Blue). *World Applied Sciences Journal*, *20*(7), 965–975.

Hameister, R., Kaur, C., Dheen, S. T., Lohmann, C. H., & Singh, G. (2020). Reactive oxygen/nitrogen species (ROS/RNS) and oxidative stress in arthroplasty. *Journal of Biomedical Materials Research Part B: Applied Biomaterials*, *108*(5), 2073–2087.

Hassan Al-Taai, S. H. (2021). Water pollution its causes and effects. *IOP Conference Series: Earth and Environmental Science*, *790*(1), 012026.

Haynes, W. M. (Ed.). (2014). *Crc Handbook of Chemistry and Physics* (95th ed., Vol. 2704). CRC Press.

Hider, R. C., Liu, Z. D., & Khodr, H. H. (2001). Metal chelation of Polyphenols. *Methods in Enzymology*, 190–203.

Ho, Y. S., & McKay, G. (1999). Pseudo-second order model for sorption processes. *Process Biochemistry*, *34*(5), 451–465.

Hubeny, J., Harnisz, M., Korzeniewska, E., Buta, M., Zieliński, W., Rolbiecki, D., Giebułtowicz, J., Nałęcz-Jawecki, G., & Płaza, G. (2021). Industrialization as a source of heavy metals and antibiotics which can enhance the antibiotic resistance in wastewater, sewage sludge and River Water. *PLOS ONE*, *16*(6).

Hussain, A., Madan, S., & Madan, R. (2021). Removal of Heavy Metals from Wastewater by Adsorption. In M. K. Nazal, & H. Zhao (Eds.), Heavy Metals - Their Environmental Impacts and Mitigation. essay, IntechOpen.

Huynh, P.-T., Nguyen, N.-T., Van, H. N., Nguyen, P.-T., Nguyen, T. D., & Dinh, V.-P. (2020). Modeling and optimization of biosorption of lead (II) ions from aqueous solution onto pine leaves (*Pinus kesiya*) using response surface methodology. *Desalination And Water Treatment*, *173*, 383–393.

Ibrahim, G. I., Jalal, A. F., & Ibrahim , B. M. (2013). Evaluation of antioxidant activity, phenolic, flavonoid and ascorbic acid contents of three edible plants from Erbil/Kurdistan. *Tikrit Journal of Pure Science*, *18*(3), 46–51.

Ighodaro, O. M., & Akinloye, O. A. (2018). First Line defence antioxidants-superoxide dismutase (SOD), catalase (CAT) and glutathione peroxidase (GPX): Their fundamental role in the entire antioxidant defence grid. *Alexandria Journal of Medicine*, *54*(4), 287–293.

Ilyasov, I. R., Beloborodov, V. L., Selivanova, I. A., & Terekhov, R. P. (2020). ABTS/pp decolorization assay of antioxidant capacity reaction pathways. *International Journal of Molecular Sciences*, *21*(3), 1131.

Inglezakis, V. J., Balsamo, M., & Montagnaro, F. (2020). Liquid–solid mass transfer in adsorption systems—an overlooked resistance? *Industrial & Engineering Chemistry Research*, *59*(50), 22007–22016.

Isaac, C. P., & Sivakumar, A. (2013). Removal of lead and cadmium ions from water using *annona squamosa* shell: Kinetic and Equilibrium Studies. *Desalination and Water Treatment*, *51*(40-42), 7700–7709.

Jaihan, W., Mohdee, V., Sanongraj, S., Pancharoen, U., & Nootong, K. (2022). Biosorption of lead (II) from aqueous solution using cellulose-based bio-adsorbents prepared from Unripe papaya (*Carica papaya*) peel waste: Removal efficiency, thermodynamics, kinetics and isotherm analysis. *Arabian Journal of Chemistry*, *15*(7), 103883.

Jauhar, S., Ismail-Fitry, M. R., Chong, G. H., Nor-Khaizura, M. A. R., & Ibadullah, W. Z. W. (2018). Polyphenol Compounds from Pomegranate (*Punica granatum*) Extracted via Various Methods and its Application on Meat and Meat Products: A Review . *Journal of Advanced Research in Applied Sciences and Engineering Technology*, *12*(1), 1–12.

Jelic, M. D., Mandic, A. D., Maricic, S. M., & Srdjenovic, B. U. (2021). Oxidative stress and its role in cancer. *Journal of Cancer Research and Therapeutics*, *17*(1), 22.

Julkunen-Tiitto, R. (1985). Phenolic constituents in the leaves of northern willows: Methods for the analysis of certain phenolics. *Journal of Agricultural and Food Chemistry*, *33*(2), 213–217.

Kalaycıoğlu, Z., & Erim, F. B. (2017). Total phenolic contents, antioxidant activities, and bioactive ingredients of juices from pomegranate cultivars worldwide. *Food Chemistry*, *221*, 496–507.

Kandylis, P., & Kokkinomagoulos, E. (2020). Food applications and potential health benefits of pomegranate and its derivatives. *Foods*, *9*(2), 122.

Karna, R., Noerpel, M., Luxton, T., & Scheckel, K. (2018). Point of zero charge: Role in Pyromorphite Formation and bioaccessibility of lead and arsenic in phosphate-amended soils. *Soil Systems*, *2*(2), 22.

Karna, R., Noerpel, M., Luxton, T., & Scheckel, K. (2018). Point of zero charge: Role in Pyromorphite Formation and bioaccessibility of lead and arsenic in phosphate-amended soils. *Soil Systems*, *2*(2), 22.

Kaźmierczak-Barańska, J., Boguszewska, K., Adamus-Grabicka, A., & Karwowski, B. T. (2020). Two Faces of Vitamin C—antioxidative and pro-oxidative agent. *Nutrients*, *12*(5), 1501.

Kennas , A., & Amellal-Chibane, H. (2019). Comparison of five solvents in the extraction of phenolic antioxidants from pomegranate (*Punica granatum* L.) peel . *The North African Journal of Food and Nutrition Research*, *3*(5), 140–147.

Khan, M. D., & Ahn, J. W. (2018). Ion Exchange Processes: A Potential Approach for the Removal of Natural Organic Matter from Water. *Journal of Energy Engineering*, *27*(2), 70–80.

Khatri, N., & Tyagi, S. (2015). Influences of natural and anthropogenic factors on surface and groundwater quality in rural and urban areas. *Frontiers in Life Science*, *8*(1), 23–39.

KILIÇ, Z. (2021). Su Kirliliği Nedenleri, Olumsuz etkileri ve önleme Yöntemleri. *İstanbul Sabahattin Zaim Üniversitesi Fen Bilimleri Enstitüsü Dergisi*, *2*(3).

Killian, B., Yuan, T.-H., Tsai, C.-H., Chiu, T. H., Chen, Y.-H., & Chan, C.-C. (2020). Emission-related heavy metal associated with oxidative stress in children: Effect of antioxidant intake. *International Journal of Environmental Research and Public Health*, *17*(11), 3920.

Ko, K., Dadmohammadi, Y., & Abbaspourrad, A. (2021). Nutritional and bioactive components of pomegranate waste used in food and cosmetic applications: A Review. *Foods*, *10*(3), 657.

Kruk, J., Aboul-Enein, B. H., Duchnik, E., & Marchlewicz, M. (2022). Antioxidative properties of phenolic compounds and their effect on oxidative stress induced by severe physical exercise. *The Journal of Physiological Sciences*, *72*(1).

Krumova , K., Cosa, G., Nonell, S., & Flors, C. (2016). Overview of Reactive Oxygen Species. In *Singlet Oxygen: Applications in Biosciences and Nanosciences* (Vol. 1, pp. 1–21). Essay, The Royal Society of Chemistry.

Kumar, N. V., Godara, A., & Mirza, A. (2020). Characteristics of flowering and fruiting description of pomegranate (*Punica granatum* L.). *International Journal of Current Microbiology and Applied Sciences*, *9*(11), 401–412.

Kumara , P. S., & Ngueagni, T. (2022). Removal of volatile organic carbon and heavy metols through microbial approach. In M. Shah, S. Rodriguez-Couto, & J. Biswas (Eds.), *An Innovative Role of Biofiltration in Wastewater Treatment Plants (WWTPs)* (pp. 285–308). essay, Elsevier.

Kumara, N. T., Hamdan, N., Petra, M. I., Tennakoon, K. U., & Ekanayake, P. (2014). Equilibrium isotherm studies of adsorption of pigments extracted from Kuduk-Kuduk (*melastoma malabathricum* L.) pulp onto TiO_2 nanoparticles. *Journal of Chemistry*, *2014*, 1–6.

Kumari, A., Dora, J., Kumar, A., & Kumar , A. (2012). Pomegranate (*Punica granatum*)-Overview . *International Journal of Pharmaceutical and Chemical Sciences*, *1*(4), 1218–1222.

Kurutas, E. B. (2016). The importance of antioxidants which play the role in cellular response against oxidative/nitrosative stress: Current State. *Nutrition Journal*, *15*(1).

Kwikima, M. M., Mateso, S., & Chebude, Y. (2021). Potentials of agricultural wastes as the ultimate alternative adsorbent for cadmium removal from wastewater. A Review. *Scientific African*, *13*.

Lagergren, S. (1898). Zur Theorie der Sogenannten Adsorption Gelöster Stoffe, Kungliga Svenska Vetenskapsakademiens, *24*(4), 1–39.

Lakey-Beitia, J., Burillo, A. M., La Penna, G., Hegde, M. L., & Rao, K. S. (2021). Polyphenols as potential metal chelation compounds against alzheimer's disease. *Journal of Alzheimer's Disease*, *82*(s1).

Lako, J., Trenerry, V., Wahlqvist, M., Wattanapenpaiboon, N., Sotheeswaran, S., & Premier, R. (2007). Phytochemical flavonols, carotenoids and the antioxidant properties of a wide selection of Fijian fruit, vegetables and other readily available foods. *Food Chemistry*, *101*(4), 1727–1741.

Lakshmi, K. S., Sailaja, V. H., & Reddy, M. A. (2017). Phytoremediation - a promising technique in waste water treatment. *International Journal of Scientific Research and Management*, *5*(6), 5480–5489.

Langmuir, I. (1918). The Adsorption of Gases on Plane Surfaces of Glass, Mica and Platinum. *Journal of the American Chemical Society*, *40*(9), 1361–1403.

Laosirisathian, N., Saenjum, C., Sirithunyalug, J., Eitssayeam, S., Sirithunyalug, B., & Chaiyana, W. (2020). The chemical composition, antioxidant and anti-tyrosinase activities, and irritation properties of Sripanya *Punica granatum* peel extract. *Cosmetics*, *7*(1), 7.

Le, K., Chiu, F., & Ng, K. (2007). Identification and quantification of antioxidants in *Fructus lycii*. *Food Chemistry*, *105*(1), 353–363.

Li, H., Cheng, K., Wong, C., Fan, K., Chen, F., & Jiang, Y. (2007). Evaluation of antioxidant capacity and total phenolic content of different fractions of selected microalgae. *Food Chemistry*, *102*(3), 771–776.

Lin, K. M., Lu, C. L., Hung, K. C., Wu, P. C., Pan, C. F., Wu, C. J., Syu, R. S., Chen, J.-S., Hsiao, P. J., & Lu, K. C. (2019). The paradoxical role of uric acid in osteoporosis. *Nutrients*, *11*(9), 2111.

Lin, L., Yang, H., & Xu, X. (2022). Effects of water pollution on human health and disease heterogeneity: A Review. *Frontiers in Environmental Science*, *10*.

Loizzo, M. R., Aiello, F., Tenuta, M. C., Leporini, M., Falco, T., & Tundis, R. (2019). Pomegranate (*Punica granatum* L.). In S. M. Nabavi & A. S. Silva (Eds.), *Nonvitamin and Nonmineral Nutritional Supplements* (pp. 467–472). essay, Academic Press.

Luz, A. L., Wu, X., & Tokar, E. J. (2018). In J. C. Fishbein & acqueline M. Heilman (Eds.), *Advances in Molecular Toxicology* (Vol. 12, pp. 1–46). essay, Elsevier B.V.

Magangana, T. P., Makunga, N. P., Fawole, O. A., & Opara, U. L. (2020). Processing factors affecting the phytochemical and nutritional properties of pomegranate (*Punica granatum* L.) peel waste: A Review. *Molecules*, *25*(20).

Majumder, A. K., Al Nayeem, A., Islam, M., Akter, M. M., & Carter, W. S. (2021). Critical Review of lead pollution in Bangladesh. *Journal of Health and Pollution*, *11*(31).

Mandal, M., Sarkar, M., Khan, A., Biswas, M., Masi, A., Rakwal, R., Agrawal, G. K., Srivastava, A., & Sarkar, A. (2022). Reactive oxygen species (ROS) and reactive nitrogen species (RNS) in plants– maintenance of structural individuality and functional blend. *Advances in Redox Research*, *5*, 100039.

Manna, K., Debnath, B., & Singh, W. S. (2019). Sources and toxicological effects of lead on human health. *Indian Journal of Medical Specialities*, *10*(2), 66–71.

Maranata, G. J., Surya, N. O., & Hasanah, A. N. (2021). Optimising factors affecting solid phase extraction performances of molecular imprinted polymer as recent sample preparation technique. *Heliyon*, *7*(1).

Marchi, R. C., Campos, I. A. S., Santana, V. T., & Carlos, R. M. (2022). Chemical Implications and considerations on techniques used to assess the in vitro antioxidant activity of coordination compounds. *Coordination Chemistry Reviews*, *451*, 214275.

Marco, G. J. (1968). A rapid method for evaluation of Antioxidants. *Journal of the American Oil Chemists' Society*, *45*(9), 594–598.

Markowitz, M. (2021). Lead poisoning: An update. *Pediatrics In Review*, *42*(6), 302–315.

Martemucci, G., Costagliola, C., Mariano, M., D'andrea, L., Napolitano, P., & D'Alessandro, A. G. (2022). Free radical properties, source and targets, antioxidant consumption and health. *Oxygen*, *2*(2), 48–78.

Martínez Francisco Cavas. (2022). *Advances in design engineering Ii: Proceedings of the Xxx international congress ingegraf, 24-25 June, 2021, Valencia, Spain*. Springer.

Melgarejo-Sánchez, P., Núñez-Gómez, D., Martínez-Nicolás, J. J., Hernández, F., Legua, P., & Melgarejo, P. (2021). Pomegranate variety and pomegranate plant part, relevance from bioactive point of view: a review. *Bioresour. Bioprocess*, *8*(2), 1–29.

Meseldzija, S., Petrovic, J., Onjia, A., Volkov-Husovic, T., Nesic, A., & Vukelic, N. (2020). Removal of $Fe^{2+,}$ Zn^{2+} and Mn^{2+} ions from the mining wastewater by Lemon Peel Waste. *Journal of the Serbian Chemical Society*, *85*(10), 1371–1382.

Mirończuk-Chodakowska, I., Witkowska, A. M., & Zujko, M. E. (2018). Endogenous non-enzymatic antioxidants in the human body. *Advances in Medical Sciences*, *63*(1), 68–78.

Mo, Y., Ma, J., Gao, W., Zhang, L., Li, J., Li, J., & Zang, J. (2022). Pomegranate Peel as a source of bioactive compounds: A mini review on their physiological functions. *Frontiers in Nutrition*, *9*.

Moga, M. A., Dimienescu, O. G., Bălan, A., Dima, L., Toma, S. I., Bîgiu, N. F., & Blidaru, A. (2021). Pharmacological and therapeutic properties of *Punica granatum* phytochemicals: Possible roles in breast cancer. *Molecules*, *26*(4), 1054.

Moghadam, M. R., Nasirizadeh, N., Dashti, Z., & Babanezhad, E. (2013). Removal of fe(ii) from aqueous solution using pomegranate peel carbon: Equilibrium and kinetic studies. *International Journal of Industrial Chemistry*, *4*(1), 19.

Moghal, A. A., Lateef, M. A., Mohammed, S. A., Lemboye, K., C. S. Chittoori, B., & Almajed, A. (2020). Efficacy of enzymatically induced calcium carbonate precipitation in the retention of heavy metal ions. *Sustainability*, *12*(17), 7019.

Mohamed, M. A., Jaafar, J., Ismail, A. F., Othman, M. H. D., & Rahman, M. A. (2017). Fourier Transform Infrared (FTIR) Spectroscopy. In N. Hilal, A. F. Ismail, T. Matsuura, & D. Oatley-Radcliffe (Eds.), *Membrane Characterization* (pp. 3–29). essay, Elsevier.

Mohammed Al-Dulaimi, W. A., & Hassan Al-Taai, S. H. (2021). Pollution and its impact on sustainable development. *IOP Conference Series: Earth and Environmental Science*, *790*(1), 012025.

Mokhatab, S., Poe, W., & Mak, J. Y. (2019). Natural Gas Dehydration and Mercaptans Removal. In *Handbook of Natural Gas Transmission and Processing (Fourth Edition): Principles and Practices* (pp. 307–348). essay, Gulf Professional Publishing.

Morosanu, I., Teodosiu, C., Paduraru, C., Ibanescu, D., & Tofan, L. (2017). Biosorption of lead ions from aqueous effluents by rapeseed biomass. *New Biotechnology*, *39*, 110–124.

Morsy, M. K., Mekawi, E., & Elsabagh, R. (2018). Impact of pomegranate peel nanoparticles on Quality Attributes of Meatballs during refrigerated storage. *LWT - Food Science and Technology*, *89*, 489–495.

Mouas, T. N., Kabouche, Z., Benssuici , C., & Chaoui, L. (2021). *Punica granatum* L. Fruit Parts from Algerian Cultivar Bioactive Compounds and In Vitro Biological Activities: A Comparative Study . *Proceedings* , *65*.

Moussa, Z., Judeh, Z. M. , & Ahmed, S. A. (2019). Nonenzymatic Exogenous and Endogenous Antioxidants. In K. Das, S. Das, M. S. Biradar, V. Bobbarala, & S. S. Tata (Eds.), Free Radical Medicine and Biology. essay, IntechOpen.

Munteanu, I. G., & Apetrei, C. (2021). Analytical methods used in determining antioxidant activity: A Review. *International Journal of Molecular Sciences*, *22*(7), 3380.

Najar-Souissi, S., Saadi, W., Zarroug, M., & Ouederni, A. (2019). Pomegranate peels activated carbon by phosphoric acid activation: Preparation, characterization and evaluation of adsorptive properties. *Journal of Engineering and Applied Sciences*, *14*(18), 6731–6741.

Negi, S., Batoye, S., Singh, K., & Waraich, J. S. (2021). Environmental Pollution, Its Causes and Impact on Ecosystem. In R. Kumar, R. Kumar, & G. Kaur (Eds.), *New Frontiers of Nanomaterials in Environmental Science* (1st ed., Vol. 297). Essay, Springer Singapore.

Nguyen, N.-V. T., Kim, K.-H., Le, P. H., Nguyen, K. T., Pham, T.-L. T., Bui, N. T., Nguyen, K.-N. H., & Duong, N. T. (2021). Effect of extraction solvent on total phenol, flavonoid content, and antioxidant activity of avicennia officinalis. *Biointerface Research in Applied Chemistry*, *12*(2), 2678–2690.

Noor, S. F. M., Ahmad, N., Khattak, M. A., Mukhtar, A., Badshah, S., & Khan, R. U. (2019). Removal of Heavy Metal from Wastewater: A Review of Current Treatment Processes . *Journal of Advanced Research in Materials Science* , *58*(1), 1–9.

Obradovic, B. (2020). Guidelines for general adsorption kinetics modeling. *Chemical Industry*, *74*(1), 65–70.

Official Journal of the Algerian Republic N° 24, April 16. (2006).

Omer, H. A., Abdel-Magid, S. S., & Awadalla, I. M. (2019). Nutritional and chemical evaluation of dried pomegranate (*Punica granatum* L.) peels and studying the impact of level of inclusion in ration formulation on productive performance of growing ossimi lambs. *Bulletin of the National Research Centre*, *43*(1).

Owa, F. D. (2014). Water pollution: Sources, effects, control and management. *Mediterranean Journal of Social Sciences*, *4*(8).

Paredes-Doig, A. L., Pinedo-Flores, A., Aylas-Orejón, J., Obregón-Valencia, D., & Sun Kou, M. R. (2020). The interaction of metallic ions onto activated carbon surface using

computational chemistry software. *Adsorption Science & Technology*, *38*(5-6), 191–204.

Pavan, F. A., Mazzocato, A. C., Jacques, R. A., & Dias, S. L. P. (2008). Ponkan Peel: A potential biosorbent for removal of Pb(II) ions from aqueous solution. *Biochemical Engineering Journal*, *40*(2), 357–362.

Peng, Y. (2019). Comparative analysis of the biological components of pomegranate seed from different cultivars. *International Journal of Food Properties*, *22*(1), 784–794.

Pereira, G. A., Arruda, H. S., & Pastore, G. M. (2018). Modification and validation of Folin-CIOCALTEU assay for faster and safer analysis of total phenolic content in food samples. *Brazilian Journal of Food Research*, *9*(1), 125.

Pérez de la Lastra, J. M., Juan, C. A., Plou, F. J., & Pérez-Lebeña, E. (2022). The nitration of proteins, lipids and DNA by peroxynitrite derivatives-chemistry involved and biological relevance. *Stresses*, *2*(1), 53–64.

Peršurić, Ž., Saftić Martinović, L., Malenica, M., Gobin, I., Pedisić, S., Dragović-Uzelac, V., & Kraljević Pavelić, S. (2020). Assessment of the biological activity and phenolic composition of ethanol extracts of pomegranate (*Punica granatum* L.) peels. *Molecules*, *25*(24), 5916.

Petřivalský, M., & Luhová, L. (2020). Nitrated nucleotides: New players in signaling pathways of reactive nitrogen and oxygen species in plants. *Frontiers in Plant Science*, *11*.

Platzer, M., Kiese, S., Tybussek, T., Herfellner, T., Schneider, F., Schweiggert-Weisz, U., & Eisner, P. (2022). Radical scavenging mechanisms of phenolic compounds: A quantitative structure-property relationship (QSPR) study. *Frontiers in Nutrition*, *9*.

Poetsch, A. R. (2020). The genomics of oxidative DNA damage, repair, and resulting mutagenesis. *Computational and Structural Biotechnology Journal*, *18*, 207–219.

Pohl, A. (2020). Removal of heavy metal ions from water and wastewaters by sulfur-containing precipitation agents. *Water, Air, & Soil Pollution*, *231*(10).

Pratiksha, K., Tomar, S., & Sharma, P. (2020). Effects of Environmental Pollution on Human Health. *Agriculture & Food : e-Newsletter*, *2*(8), 982–983.

Qasem, N. A., Mohammed, R. H., & Lawal, D. U. (2021). Removal of heavy metal ions from wastewater: A comprehensive and critical review. *Npj Clean Water*, *4*(1).

Rahimi, H. R., Arastoo, M., & Ostad, S. N. (2012). A Comprehensive Review of *Punica granatum* (Pomegranate) Properties in Toxicological, Pharmacological, Cellular and Molecular Biology Researches. *Iranian Journal of Pharmaceutical Research*, *11*(2), 385–400.

Ranjha, M. M., Amjad, S., Ashraf, S., Khawar, L., Safdar, M. N., Jabbar, S., Nadeem, M., Mahmood, S., & Murtaza, M. A. (2020). Extraction of polyphenols from Apple and pomegranate peels employing different extraction techniques for the development of functional date bars. *International Journal of Fruit Science*, *20*(sup3).

Rao, R. A. K., & Rehman, F. (2010). Adsorption of Heavy Metal Ions on Pomegranate (*Punica granatum*) Peel: Removal and Recovery of Cr(VI) Ions from a Multi-metal Ion System. *Adsorption Science & Technology*, *28*(3), 195–211.

Ravikumar, Y., Yun, J., Zhang, G., Zabed, H. M., & Qi, X. (2022). A review on constructed wetlands-based removal of pharmaceutical contaminants derived from non-point source pollution. *Environmental Technology & Innovation*, *26*, 102504.

Raychaudhuri, S. S., Pramanick, P., Talukder, P., & Basak, A. (2021). Polyamines, metallothioneins, and phytochelatins—Natural defense of plants to mitigate heavy metals. In Atta-ur-Rahman (Ed.), *Studies in Natural Products Chemistry* (Vol. 69, pp. 227–261). essay, Elsevier.

Re, R., Pellegrini, N., Proteggente, A., Pannala, A., Yang, M., & Rice-Evans, C. (1999). Antioxidant activity applying an improved ABTS radical cation decolorization assay. *Free Radical Biology and Medicine*, *26*(9-10), 1231–1237.

Reza, R., & Singh , G. (2010). Heavy metal contamination and its indexing approach for river water. *Int. J. Environ. Sci. Tech*, *7*(4), 785–792.

Rezaei, M., Pourang, N., & Moradi, A. M. (2022). Removal of lead from aqueous solutions using three biosorbents of aquatic origin with the emphasis on the affective factors. *Scientific Reports*, *12*(1).

Ribeiro, L. A. de S., Rodrigues, L. A., & Thim, G. P. (2017). Preparation of activated carbon from orange peel and its application for phenol removal. *International Journal of Engineering Research & Science* , *3*(3), 122–129.

Rifler, J. P. (2018). Is a meal without wine good for health? *Diseases*, *6*(4), 105.

Rohit, Y., Saurabh , R., & Ajay, S. (2012). Review On Antioxidants Activity And Its Evaluation. *J Pharma Res*, *1*(2), 41–58.

Rudrapal, M., Khairnar, S. J., Khan, J., Dukhyil, A. B., Ansari, M. A., Alomary, M. N., Alshabrmi, F. M., Palai, S., Deb, P. K., & Devi, R. (2022). Dietary polyphenols and their role in oxidative stress-induced human diseases: Insights into protective effects, antioxidant potentials and mechanism(s) of action. *Frontiers in Pharmacology*, *13*.

Saad, H., Charrier-El Bouhtoury, F., Pizzi, A., Rode, K., Charrier, B., & Ayed, N. (2012). Characterization of pomegranate peels tannin extractives. *Industrial Crops and Products*, *40*, 239–246.

Sabraoui, T., Khider, T., Nasser, B., Eddoha, R., Moujahid, A., Benbachir, M., & Essamadi, A. (2020). Determination of punicalagins content, metal chelating, and antioxidant properties of edible pomegranate (*Punica granatum* L) peels and seeds grown in Morocco. *International Journal of Food Science*, *2020*, 1–8.

Sadeer, B. N., Montesano, D., Albrizio, S., Zengin, G., & Mahomoodally, M. F. (2020). The versatility of antioxidant assays in food science and safety—chemistry, applications, strengths, and limitations. *Antioxidants*, *9*(8), 709.

Sankhla, M. S., Kumari, M., Nandan, M., Kumar, R., & Agrawal, P. (2016). Heavy metals contamination in water and their hazardous effect on human health-A Review. *International Journal of Current Microbiology and Applied Sciences, 5*(10), 759–766.

Sellal, A., Belattar, R., & Bouzidi, A. (2019). Heavy metals chelating ability and antioxidant activity of Phragmites australis stems extracts. *Journal of Ecological Engineering, 20*(2), 116–123.

Senoner, T., & Dichtl, W. (2019). Oxidative stress in cardiovascular diseases: Still a therapeutic target? *Nutrients, 11*(9), 2090.

Shiban, M. S., Al-Otaibi, M. M., & Al-zoreky, N. S. (2012). Antioxidant activity of Pomegranate (*Punica granatum* L.) fruit peels. *Food and Nutrition Sciences, 03*(07), 991–996.

Shukla, S., Raman, T., & Shukla, S. (2016). A review on the scope for increasing in vitro production of pomegranate (*Punica granatum* L.) cultivars and its application in the human health sector with emphasis on the indian industry. *Plant Cell Biotechnology and Molecular Biology*, *16*(1&2), 60–73.

Sies, H. (1985). Oxidative Stress: Introductory Remarks . In *Introductory Remarks*. essay, Academic Press.

Sihag, S., Pal, A., Ravikant, & Saharan, V. (2022). Antioxidant properties and free radicals scavenging activities of pomegranate (*Punica granatum* L.) peels: An in-vitro study. *Biocatalysis and Agricultural Biotechnology, 42*, 102368.

Silveira, M. B., Pavan, F. A., Gelos, N. F., Lima, E. C., & Dias, S. L. (2014). *Punica granatum* shell preparation, characterization, and use for Crystal Violet Removal from aqueous solution. *CLEAN - Soil, Air, Water, 42*(7), 939–946.

Simeonidis, K., & Mitrakas, M. (2021). Technologies developing in heavy metals' removal from water. *Water, 13*(6), 860.

Sips, R. (1948). On the structure of a catalyst surface. *The Journal of Chemical Physics*, *16*(5), 490–495.

Sivaraj, C., Saraswathi, K., Sindhu, R., Subasree, S., Sangeetha, S. T., & Arumugam, P. (2018). Phytochemical investigation and antioxidant activities of methanol peel extract of *Punica granatum* L. *International Journal of Pharmacy and Biological Sciences*, *8*(4), 445–454.

Soliman, N. K., & Moustafa, A. F. (2020). Industrial solid waste for heavy metals adsorption features and challenges; a review. *Journal of Materials Research and Technology*, *9*(5), 10235–10253.

Stahl, W., & Sies, H. (2003). Antioxidant activity of carotenoids. *Molecular Aspects of Medicine, 24*(6), 345–351.

Stefanou, D. T., Kouvela, M., Stellas, D., Voutetakis, K., Papadodima, O., Syrigos, K., & Souliotis, V. L. (2022). Oxidative stress and deregulated DNA damage response network in lung cancer patients. *Biomedicines*, *10*(6), 1248.

Sukmana, H., Bellahsen, N., Pantoja, F., & Hodur, C. (2021). Adsorption and coagulation in wastewater treatment – review. *Progress in Agricultural Engineering Sciences*, *17*(1), 49–68.

Syed, Q. A., Zahoor, T., Shukat, R., & Batool, Z. (2018). Nutritional and therapeutic properties of pomegranate. *Scholarly Journal of Food and Nutrition*, *1*(4).

Tarbaoui, M., Oumam, M., Fourmentin, S., Benzina, M., Bennamara, A., & Abourriche , A. (2016). Development of a new biosorbent based on the extract residue of marine alga sargassum vulgare: application in biosorption of heavy metals. *World Journal of Innovative Research*, *1*(4), 1–5.

Teka, T., & Kassahun, H. (2020). characterization and evaluation of antioxidant activity of *aloe schelpei* reynolds. *Drug Design, Development and Therapy*, *Volume 14*, 1003–1008.

Tekin, Z., & Küçükbay, F. Z. (2019). Evaluation of phytochemical contents and antioxidant activity of Pomegranate Flower. *Journal of the Turkish Chemical Society Section A: Chemistry*, 37–42.

Tena, N., Martín, J., & Asuero, A. G. (2020). State of the art of anthocyanins: Antioxidant activity, sources, bioavailability, and therapeutic effect in human health. *Antioxidants*, *9*(5), 451.

Tien, T. T., & Luu, T. L. (2019). Electrooxidation of tannery wastewater with continuous flow system: Role of Electrode Materials. *Environmental Engineering Research*, *25*(3), 324–334.

Traber, M. G., & Bruno, R. S. (2020). Vitamin E. In B. P. Marriott, D. F. Birt, V. A. Stallings, & A. A. Yates (Eds.), *Present Knowledge in Nutrition: Basic Nutrition and Metabolism* (Vol. 1, pp. 115–136). essay, Academic Press.

Trishitman, D., Cassano, A., Basile, A., & Rastogi, N. K. (2020). Reverse osmosis for industrial wastewater treatment. In A. Basile, A. Cassano , & N. K. Rastogi (Eds.), *Current Trends and Future Developments on (Bio-) Membranes* (pp. 207–228). essay, Elsevier.

Turkoglu, A., Duru, M. E., Mercan, N., Kivrak, I., & Gezer, K. (2007). Antioxidant and antimicrobial activities of laetiporus sulphureus (bull.) Murrill. *Food Chemistry*, *101*(1), 267–273.

Turkoglu, A., Duru, M. E., Mercan, N., Kivrak, I., & Gezer, K. (2007). Antioxidant and antimicrobial activities of laetiporus sulphureus (bull.) Murrill. *Food Chemistry*, *101*(1), 267–273.

Ungureanu, E. L. , & Mustatea, G. (2022). Toxicity of Heavy Metals. In H. M. Saleh, & A. I. Hassan (Eds.), Environmental Impact and Remediation of Heavy Metals. essay, IntechOpen.

Vardhan, K. H., Kumar, P. S., & Panda, R. C. (2019). A review on heavy metal pollution, toxicity and remedial measures: Current trends and future perspectives. *Journal of Molecular Liquids*, *290*, 111197.

Vera, L. M., Bermejo, D., Uguña, M. F., Garcia, N., Flores, M., & González, E. (2018). Fixed bed column modeling of lead(II) and cadmium(II) ions biosorption on sugarcane bagasse. *Environmental Engineering Research*, *24*(1), 31–37.

Verma, J., Kumari, S., & Dhasmana, A. (2020). Toxic effect of Lead on earth's life. *INTERNATIONAL JOURNAL OF INNOVATIVE RESEARCH IN TECHNOLOGY* , *7*(1), 673–676.

Villabona-Ortíz, Á., Figueroa-Lopez, K. J., & Ortega-Toro, R. (2022). Kinetics and adsorption equilibrium in the removal of azo-anionic dyes by modified cellulose. *Sustainability*, *14*(6), 3640.

Wang, J., & Guo, X. (2020). Adsorption isotherm models: Classification, physical meaning, application and solving method. *Chemosphere*, *258*, 127279.

Wang, L., Shi, C., Wang, L., Pan, L., Zhang, X., & Zou, J.-J. (2020). Rational design, synthesis, adsorption principles and applications of Metal Oxide Adsorbents: A Review. *Nanoscale*, *12*(8), 4790–4815.

Wang, S., Li, Q., Gao, Y., Zhou, Z., & Li, Z. (2021). Influences of lead exposure on its accumulation in organs, meat, eggs and bone during laying period of hens. *Poultry Science*, *100*(8), 101249.

Wear, S. L., Acuña, V., McDonald, R., & Font, C. (2021). Sewage pollution, declining ecosystem health, and cross-sector collaboration. *Biological Conservation*, *255*, 109010.

Weber, W. J., & Morris, J. C. (1963). Kinetics of Adsorption on Carbon from Solutions. *Journal of the Sanitary Engineering Division*, *89*, 31–60.

WHO. (2002). Water Pollutants: Biological agents, dissolved chemicals, non-dissolved chemicals and sediments. *WHO CEHA*, Amman, Jordan.

WHO. (2003). The World Health Report 2003: Shaping the future. *World Health Organization*, 1211 Geneva 27, Switzerland.

Worch, E. (2021). Adsorption kinetics. In Adsorption Technology in Water Treatment: Fundamentals, Processes, and Modeling (pp. 140-186). essay, De Gruyter.

Wu, H., Liu, Y., Zhang, X., Zhang, J., & Ma, E. (2019). Antioxidant defenses at enzymatic and transcriptional levels in response to acute lead administration in Oxya chinensis. *Ecotoxicology and Environmental Safety*, *168*, 27–34.

Yan, L. J. (2014). Protein redox modification as a cellular defense mechanism against tissue ischemic injury. *Oxidative Medicine and Cellular Longevity*, *2014*, 1–12.

Yan-hui, C., Hui-fang, G., Sa, W., Xian-yan, L., Qing-xia, H., Zai-hai, J., Ran, W., Jin-hui, S.., & Jiang-li, S. (2022). Comprehensive evaluation of 20 pomegranate (L.) cultivars in China. *Journal of Integrative Agriculture*, *21*(2), 434–445.

Yaribeygi, H., Sathyapalan, T., Atkin, S. L., & Sahebkar, A. (2020). Molecular mechanisms linking oxidative stress and diabetes mellitus. *Oxidative Medicine and Cellular Longevity*, *2020*, 1–13.

Yokozawa, T., Chen, C. P., Dong, E., Tanaka, T., Nonaka, G.-I., & Nishioka, I. (1998). Study on the inhibitory effect of tannins and flavonoids against the 1,1-diphenyl-2-picrylhydrazyl radical. *Biochemical Pharmacology*, *56*(2), 213–222.

Youcai, Z. (2019). Physical and Chemical Treatment Processes for Leachate. In *Pollution Control Technology for Leachate from Municipal Solid Waste* (pp. 31–183). essay, Butterworth-Heinemann.

Younas, F., Mustafa, A., Farooqi, Z. U., Wang, X., Younas, S., Mohy-Ud-Din, W., Ashir Hameed, M., Mohsin Abrar, M., Maitlo, A. A., Noreen, S., & Hussain, M. M. (2021). Current and emerging adsorbent technologies for wastewater treatment: Trends, Limitations, and environmental implications. *Water*, *13*(2), 215.

Yousef, R., Qiblawey, H., & El-Naas, M. H. (2020). Adsorption as a process for produced water treatment: A Review. *Processes*, *8*(12), 1657.

Zaki, S. A., Abdelatif, S. H., Abdelmohsen, N. R., & Ismail, F. A. (2015). Phenolic compounds and antioxidant activities of pomegranate peels. *ETP International Journal of Food Engineering*, *1*(2).

Zhang, P., Li, T., Wu, X., Nice, E. C., Huang, C., & Zhang, Y. (2020). Oxidative stress and diabetes: Antioxidative strategies. *Frontiers of Medicine*, *14*(5), 583–600.

Zhang, W., Xiao, S., & Ahn, D. U. (2013). Protein oxidation: Basic principles and implications for Meat Quality. *Critical Reviews in Food Science and Nutrition*, *53*(11), 1191–1201.

Zhong, Y., & Shahidi, F. (2015). Methods for the assessment of antioxidant activity in foods. In F. Shahidi (Ed.), *Handbook of Antioxidants for Food Preservation* (pp. 287–333). essay, Woodhead Publishing.

Zhu, F., Yuan, Z., Zhao, X., Yin, Y., & Feng, L. (2015). Composition and contents of anthocyanins in different pomegranate cultivars. *Acta Horticulturae*, (1089), 35–41.

ملخص

أصبحت المعادن الثقيلة التي تنتجها مياه الصرف الصناعي مشكلة عالمية بسبب آثارها السلبية على البيئة وعلى صحة الإنسان لأنها تسبب الإجهاد التأكسدي المرتبط بالعديد من الأمراض (القلب والأوعية الدموية ، التنكس العصبي ، الالتهابات ، السرطان وغيرها). تشتهر فاكهة الرمان *Punica granatum* L. و أجزائها المختلفة بفوائدها الصحية وقد استخدمو منذ القدم في التغذية والطب التقليدي. يهدف الجزء الأول من هذه الدراسة إلى توصيف مسحوق قشر الرمان من الصنفين عن طريق التحليل بواسطة FT-IR ونقطة الشحن صفر والمجموعات الوظيفية السطحية وتقييم قدرات الادمصاص لهذه الكتل الحيوية مقابل أيونات الرصاص باستخدام طريقة الدُفعات وإمكانية استخدامها في معالجة مياه الصرف الصناعي الملوثة بالرصاص. تمت دراسة تأثير بعض المتغيرات التجريبية على قدرات الادمصاص. تمت أيضا دراسة حرارة وحركية الادمصاص ومعالجتها بنماذج رياضية مختلفة. كما تم تقييم تجديد مسحوق قشر الرمان الأحمر والأصفر بعد الادمصاص. يهدف الجزء الثاني من هذا العمل إلى تحديد محتوى البوليفينول الكلي والفلافونويد والعفص المكثف والأنثوسيانين في المستخلصات المائية والميثانولية والإيثانولية لقشرة الأصناف الحمراء والصفراء من *Punica granatum* L. وتقييم نشاطها المضاد للأكسدة في المختبر. أظهرت النتائج ثراء الكتلتين الحيويتين بالمجموعات الوظيفية الحمضية السطحية. أظهرت دراسة العوامل المختلفة على عملية الادمصاص أن قدرة الادمصاص تزداد مع الأس الهيدروجيني حتى الرقم الهيدروجيني 6 ووقت التجربة وتركيز المعدن الأولي وتتناقص مع زيادة جرعة المدمص الحيوي. بالنسبة لحرارة ادمصاص الرصاص على مسحوق قشر الرمان الأحمر والأصفر ، كان نموذج Langmuir أكثر ملائمة مع قدرة ادمصاص (Q_{max}) تبلغ 90 و 25.89 مجم / جرام على التوالي. تلائم البيانات الحركية نموذج الدرجة الثانية بشكل أفضل. كان اندصاص الرصاص الحمضي فعالاً مع نسبة عالية من الاسترجاع. تشير النتائج إلى أنه يمكن استخدام هذه الكتل الحيوية كمواد مدمصة حيوية لإزالة الرصاص من المحاليل المائية مع إمكانية إعادة استخدامها. أظهرت النتائج ايضا أن مستخلصات القشور الميثانولية والإيثانولية للأصناف الحمراء والصفراء أكثر ثراءً في البوليفينول والفلافونويد والعفص المكثف والأنثوسيانين من المستخلصات المائية. أظهرت جميع المستخلصات التي تم اختبارها أنشطة استخلاب قوية للجذور الحرة DPPH و ABTS وتأثير مضاد للأكسدة مع اختبار ارجاع الطاقة ، واستخلاب الحديد واختبارات بيتا كاروتين.

.

الكلمات المفتاحية: *Punica granatum* L. ، قشر الرمان ، مركبات الفينول ، نشاط مضاد الأكسدة ، الادمصاص الحيوي ، حرارة الادمصاص ، حركيات الادمصاص ، معالجة مياه الصرف الصحي الصناعية ، المعادن الثقيلة ، الرصاص.

Abstract

Heavy metals produced by industrial wastewaters have become a global problem due to their negative effects on the environment and on human health as they induce oxidative stress which has been linked to several diseases (cardiovascular, neurodegenerative, inflammatory, cancer and others). Pomegranate fruit *Punica granatum* L. and its diffrent parts are known for their health benefits and have been used since ancient times in nutrition and in traditional medicine. The first part of this study aimed to characterize the pomegranate peels powder of both varieties via FT-IR, point of zero charge and surface functional groups analysis and to evaluate the adsorption capacities of these biomasses towards leads ions using batch method and the potential of using them for the treatment of industrial wastewater polluted with lead. The effect of some experimental parameters on the adsorption capacities was studied. Isotherms and adsorption kinetics have also been studied and treated with different mathematical models. The regeneration of the red and yellow pomegranate peels powder after adsorption was also assessed. The second part of this work aimed to determine the total polyphenols, flavonoids, condensed tannins and anthocyanins content in the aqueous, methanolic and ethanolic peels extracts of the red and yellow *Punica granatum* L. varieties and to evaluate their antioxidant activity *in vitro*. Results showed the richness of both biomasses with acidic functional surface groups. The study of different factors on the adsorption process showed that the adsorption capacity increases with pH until pH 6, contact time and initial metal concentration and it decreases with increasing the biosorbent dose. For the adsorption isotherms of lead onto the red and yellow pomegranate peels powder, the Langmuir model was more fitting with an adsorption capacity (Q_{max}) of 90 and 89.25 $mg.g^{-1}$, respectively. The kinetic data suited better with the pseudo-second order model. Lead acidic desorption was efficient, with a high percentage of recovery. The findings indicate that these biomasses can be utilized as biosorbents for lead removal from aqueous solutions with the possibility of their reuse. The results also showed that the methanolic and ethanolic peels extracts of red and yellow varieties are richer in polyphenols, flavonoids, condensed tannins and anthocyanins than the aqueous ones. All the tested extracts have shown powerful scavenging activities towards DPPH and ABTS radicals and an appreciable antioxidant inhibiting effects with the reducing power, iron chelation and β-carotene tests.

Keywords: *Punica granatum* L., Pomegranate peels, Phenolic compounds, Antioxidant activity, Biosorption, Adsorption isotherms, Adsorption kinetics, wastewater treatment, Heavy metals, Lead.

Résumé

Les métaux lourds produits par les eaux usées industrielles sont devenus un problème mondial à cause de leurs effets négatifs sur l'environnement et sur la santé humaine car ils induisent le stress oxydant qui a été lié avec plusieurs maladies (cardiovasculaires, neurodégénératives, inflammatoires, cancéreuses et autres). Le fruit de la grenade *Punica granatum* L. et ses différentes parties sont connues pour leurs bienfaits pour la santé et sont utilisées depuis l'Antiquité en nutrition et en médecine traditionnelle. La première partie de cette étude visait à caractériser la poudre des écorces de grenade des deux variétés via l'analyse par IR-TF, point de charge nulle et des groupes fonctionnels de surface et à évaluer les capacités d'adsorption de ces biomasses vis-à-vis des ions plomb en utilisant la méthode batch et le potentiel de leur utilisation pour le traitement des eaux usées industrielles polluées par le plomb. L'effet de certains paramètres expérimentaux sur les capacités d'adsorption a été étudié. Les isothermes et la cinétique d'adsorption ont également été étudiées et traitées avec différents modèles mathématiques. La régénération de la poudre des écorces de grenade rouge et jaune après adsorption a également été évaluée. La deuxième partie de ce travail visait à déterminer la teneur en polyphénols totaux, flavonoïdes, tanins condensés et anthocyanes dans les extraits aqueux, méthanoliques et éthanoliques des écorces des variétés rouges et jaunes de *Punica granatum* L. et à évaluer leur activité antioxydante *in vitro*. Les résultats ont montré la richesse du deux biomasses en groupements fonctionnels acides de surface. L'étude de différents facteurs sur le processus d'adsorption a montré que la capacité d'adsorption augmente avec le pH jusqu'à pH 6, le temps de contact et la concentration initiale en métal et qu'elle diminue avec l'augmentation de la dose de biosorbant. Pour les isothermes d'adsorption du plomb sur la poudre des écorces de grenade rouge et jaune, le modèle de Langmuir était plus adapté avec une capacité d'adsorption (Q_{max}) de 90 et 89,25 $mg.g^{-1}$, respectivement. Les données cinétiques convenaient mieux au modèle de pseudo-second ordre. La désorption acide du plomb a été efficace, avec un pourcentage élevé de récupération. Les résultats indiquent que ces biomasses peuvent être utilisées comme biosorbants pour l'élimination du plomb des solutions aqueuses avec la possibilité de leur réutilisation. Les résultats ont également montré que les extraits méthanoliques et éthanoliques des écorces des variétés rouges et jaunes sont plus riches en polyphénols, flavonoïdes, tanins condensés et anthocyanes que les extraits aqueux. Tous les extraits testés ont montré de puissantes activités de piégeage des radicaux DPPH et ABTS et un effet antioxydant appréciable avec les tests de pouvoir réducteur, chélation du fer et β-carotène.

Mots-clés : *Punica granatum* L., Ecorces de grenade, Composés phénoliques, Activité antioxydante, Biosorption, Isothermes d'adsorption, Cinétique d'adsorption, Traitement des eaux usées, Métaux lourds, Plomb.